Electronic Thesis and Dissertation Repository

August 2011

# Representation of Somatosensory Afferents in the Cortical Autonomic Network

Ruma Goswami, *The University of Western Ontario*

Supervisor: Dr. J. Kevin Shoemaker, *The University of Western Ontario*
A thesis submitted in partial fulfillment of the requirements for the Doctor of Philosophy degree in Kinesiology
© Ruma Goswami 2011

## Recommended Citation

REPRESENTATION OF SOMATOSENSORY AFFERENTS IN THE CORTICAL
AUTONOMIC NETWORK

(Spine title: Somatosensory Afferents in the Cortical Autonomic Network)

(Thesis format: Integrated-Article)

by

Ruma <u>Goswami</u>

Graduate Program in Kinesiology

A thesis submitted in partial fulfillment
of the requirements for the degree of
Doctor of Philosophy

The School of Graduate and Postdoctoral Studies
The University of Western Ontario
London, Ontario, Canada

# CERTIFICATE OF EXAMINATION

Supervisor

_____
Dr. J. Kevin Shoemaker

Supervisory Committee

_____
Dr. Matthew Heath

_____
Dr. Greg Marsh

Examiners

_____
Dr. Matthew Heath

_____
Dr. Timothy Doherty

_____
Dr. Ruth Martin

_____
Dr. Bradley MacIntosh

The thesis by

## Ruma Goswami

entitled:

**Representation of Somatosensory Afferents in the Cortical Autonomic Network**

is accepted in partial fulfillment of the
requirements for the degree of
Doctor of Philosophy

Date_____          _____
                                             Chair of the Thesis Examination Board

# ABSTRACT

The relationship between somatosensory stimulation and the autonomic nervous system has been established with effects on heart rate (HR) and sympathetic tone. However, the involvement of the cortical autonomic network (CAN) during muscle sensory afferent stimulation has not been identified. The main objective of the research in this dissertation was to determine the representation of somatosensory afferents in the CAN and their physiologic impact on cardiovascular control. Somatosensory afferent activation was elicited by electrical stimulation of type I and II afferents (sub-motor threshold) and type III and IV afferents (motor threshold), and CAN patterns were assessed using blood-oxygenation level-dependent functional magnetic resonance imaging. Study 1 (Chapter 2) established CAN regions associated with sub-motor stimulation including the ventral medial prefrontal cortex (vMPFC), subgenual anterior cingulate cortex (sACC), and posterior insula, along with a trend towards increased heart rate variability (HRV). Motor threshold stimulation was associated with activation in the posterior insula. Having established the CAN regions affected by sensory afferent input, diffusion tensor imaging was used (Chapter 3) to establish structural connections between the cortical regions associated with functional cardiovascular control. We identified two discrete patterns of white matter connectivity between the anterior insula-sACC and posterior insula-posterior cingulate cortex, suggesting that a structural network may underlie functional roles in autonomic regulation and sensory processing. As somatosensory stimulation had modest impact on cardiovascular control under baseline conditions, Study 3 (Chapter 4) aimed to establish the effects of somatosensory stimulation during baroreceptor unloading

(lower-body negative pressure, LBNP) on muscle sympathetic nerve activity (MSNA) and cortical activity. Sensory stimulation during LBNP led to an attenuated increase in MSNA burst frequency, as well as absent activity in the right insula and dorsal ACC, supporting the sympatho-excitatory role of these regions. No effect of somatosensory stimulation during chemoreflex-mediated sympatho-excitation was observed on MSNA, while right insular and dorsal ACC activities were maintained. Overall, the results of these studies provide evidence of somatosensory representation within the CAN regions that are anatomically linked, and highlight a role for type I and II sensory afferents in modulating autonomic outflow in a manner that depends upon baroreceptor loading.

**Keywords**: cortical autonomic network, muscle sensory afferents, autonomic nervous system, functional MRI, diffusion tensor imaging, heart rate variability, muscle sympathetic nerve activity, baroreflex activity

# ACKNOWLEDGEMENTS

Over the course of my graduate career, I have been privileged to work with many talented people that have aided in my academic and personal development. Firstly, to Dr. Kevin Shoemaker, you have been a wonderful mentor and helped me build a foundation upon which to successfully move forward. The opportunities you have provided me with in the lab and in other academic realms have been exceptional and have aided in furthering my growth and development. I would like to thank my committee Dr. Matthew Heath and Dr. Greg Marsh for the wide ranging perspectives on my work, which has been extremely valuable. I express sincere gratitude to Savio Wong and Harish Sharma for taking time out to impart MRI wisdom and for teaching me various aspects of data analysis. Many thanks to Joy Williams and Kim Kreuger for assistance with MRI set-up and acquisition, as well as to Craig Steinback for data collection in the lab sessions. To past and present NVRL members, it has been a great ride. I have learned a lot from you and I wish you the best in future endeavours. All Kinesiology friends, you made going to school everyday enjoyable, and provided the perfect work-life balance. I sincerely thank Maria Frances for the tireless help in the lab with running the studies and for enabling me to complete all of the experiments. You are a most genuine friend and I have treasured the years spent together. You are always by my side and drive me toward success and I thank you for your endless support in the whole process. To my loving Mom, Dad, Rinku and Shreyas, words cannot suffice what your boundless love and encouragement mean to me. You are my backbone and role models in life, and I am truly blessed to have you. You have motivated me to achieve my aspirations, and exceeded every need of mine and I dedicate this to you.

# TABLE OF CONTENTS

# LIST OF TABLES

# LIST OF FIGURES

# LIST OF ABBREVIATIONS

| | |
|---|---|
| ACC | anterior cingulate cortex |
| ANOVA | analysis of variance |
| ADC | apparent diffusion coefficient |
| ATP | adenosine triphosphate |
| b | diffusion weighting factor |
| BOLD | blood-oxygenation level-dependent |
| BP | blood pressure |
| CAN | cortical autonomic network |
| CVLM | caudal ventrolateral medulla |
| D | diffusion coefficient |
| dACC | dorsal anterior cingulate cortex |
| dHb | deoxygenated hemoglobin |
| DBP | diastolic blood pressure |
| DTI | diffusion tensor imaging |
| ECG | electrocardiogram |
| EPI | echo planar imaging |
| FA | fractional anisotropy |
| FACT | fibre assignment by continuous tracking |
| FDR | false discovery rate |
| fMRI | functional magnetic resonance imaging |
| FOV | field of view |
| FWHM | full width at half maximum |
| GLM | general linear model |
| Hb | oxygenated hemoglobin |
| HFP | high frequency power |
| HG | handgrip |
| HR | heart rate |
| HRF | hemodynamic response function |
| HRV | heart rate variability |
| IC | insular cortex |
| LBNP | lower-body negative pressure |
| MD | mean diffusivity |
| MI | motor cortex |
| MAP | mean arterial pressure |
| MCC | middle cingulate cortex |
| MNI | Montreal Neurological Institute |
| MOT | motor |
| MPFC | medial prefrontal cortex |
| MSNA | muscle sympathetic nerve activity |
| MVC | maximal voluntary contraction |
| NPY | neuropeptide-Y |
| NTS | nucleus tractus solitarius |
| PAG | periaqueductal gray matter |
| PCC | posterior cingulate cortex |

| | |
|---|---|
| PECO | post-exercise circulatory occlusion |
| PNS | parasympathetic nervous system |
| Q | cardiac output |
| RF | radiofrequency |
| ROI | region of interest |
| RVLM | rostral ventrolateral medulla |
| sACC | subgenual anterior cingulate cortex |
| SI | somatotsensory cortex |
| SBP | systolic blood pressure |
| SNA | sympathetic nerve activity |
| SPM | statistical parametric mapping |
| SUB | sub-motor |
| TE | echo time |
| TENS | transcutaneous electrical nerve stimulation |
| TR | time to repetition |
| vMPFC | ventral medial prefrontal cortex |
| VOL | volitional |

## Chapter 1 Introduction

### 1.1    General Background

Historically, control over the autonomic nervous system has focused on the sub-cortical regions, specifically within the medulla.  Over a century ago, observations of autonomic changes during motor seizures in epileptic patients by the neurologist J.H. Jackson gave rise to the idea of the representation of involuntary movements of the blood vessels and viscera within the cerebral cortex (54).  Associations between stroke lesions in the cortex and cardiovascular dysregulation have lent further support to the role of the cerebral cortex in autonomic regulation (23).  Electrical stimulation and neuroanatomical techniques in animals have characterized a cortical autonomic network (CAN) comprising cortical and sub-cortical regions involved in the modulation of respiration, heart rate (HR), blood pressure (BP), sympathetic activity, parasympathetic activity, and gastrointestinal motility.  The primary regions include the insular cortex, prefrontal cortex (MPFC), anterior cingulate cortex (ACC), and amygdala (11; 18).

The advent of functional magnetic resonance imaging (fMRI) has revealed a similar network of autonomic regions in conscious humans during various physiological and behavioural stressors, such as exercise (67;151); mental stress (28), and baroreflex function (52; 66).  However, most studies have utilized volitional procedures (i.e., exercise, breath holds) that often simultaneously engage neural pathways including central command, baroreceptor activation and afferent information from skeletal muscle in the control of autonomic function.  Thus, it is difficult to discern from neuroimaging data whether activated regions are representing a feed-forward modulation of cardiovascular responses from central command or whether the activity reflects

processing of afferent signals from the peripheral baroreceptor and activated muscle sites. While previous stimulation studies in animals have enhanced our understanding of the viscerosensory and visceromotor regions of the CAN, less is known regarding the representation of somatosensory information in human CAN regions.

In humans, post-exercise circulatory occlusion (PECO) of exercising limbs has been used to investigate the effects of muscle afferent metaboreceptor activation on cortical regions (148). Cuff inflation is used to trap the accumulated metabolites due to muscle contraction but also keeps BP elevated at exercise levels. The PECO was associated with activation in the insula; however, the authors were unable to confirm whether the activity was due to the effects of metaboreceptors or BP (148). Gray and colleagues (2009) have also implicated the insula as well as the amygdala and brainstem nuclei in the integration of somatosensory stimuli using electrical shocks delivered at different phases of the cardiac cycle (48). The study by Williamson and colleagues (1999) selectively activated type IV metaboreceptors with PECO but also elicited concomitant increases in BP and potentially pain (148). Gray et al. (2009) utilized strong electrical shocks that induced arousal responses with BP (48). Thus, the aforementioned studies did not differentiate between the four types of muscle afferents (types I-IV), nor could they distinguish whether the cortical activity was due to somatosensory processing or an arousal response.

Electrical stimulation is a useful modality to selectively activate somatosensory afferents and can readily be implemented in fMRI experiments. Past fMRI experiments have utilized this technique to study the sensori-motor and cognitive effects of somatosensory stimulation (5; 22; 38), as well as in the context of touch and pain (32;

154). However, no studies have solely examined the representation of somatosensory inputs within the CAN regions, with specific emphasis on the effects of the four afferent types on cortical activity and efferent autonomic cardiovascular control.

Therefore, the **overall purpose** of this research was to investigate the association between somatosensory stimulation and patterns of activity within the autonomic regions of the brain. This thesis aims to address the **working hypothesis** that somatosensory inputs are represented within the CAN and that discrete CAN regions will be associated with changes in autonomic function. Using varying intensities of electrical stimulation, we were able to associate different groups of muscle afferents with CAN regions of activation in the studies of this dissertation. As well, isometric handgrip exercise was used to compare passive electrically stimulated conditions to an active task that raised HR. Finally, in order to study the interactive effects of somatosensory afferents and baroreceptors, we used lower-body negative pressure (LBNP) as a technique to activate the baroreflex. By combining neuroimaging data with laboratory physiological recording sessions, we were able to investigate both the cortical responses to somatosensory input as well as peripheral autonomic outcomes. Using these approaches, the working hypothesis was addressed by the following three studies:

**Study 1** entitled 'Representation of somatosensory inputs within the cortical autonomic network', tested the hypothesis that CAN regions integrate muscle sensory afferents, with differential activation patterns observed between passive and active tasks. It was also hypothesized that regions implicated with parasympathetic activity (i.e, ventral medial prefrontal cortex) will be differentially activated during electrical

stimulation and handgrip exercise, and would reflect efferent measures of parasympathetic activity.

**Study 2** entitled 'Anatomical connections between autonomic regions of the brain', aimed to determine whether function is linked to structure. Specifically, it was hypothesized that the functional responses within the CAN regions associated with somatosensory stimulation and isometric handgrip exercise are reflective of structural connections between the regions, providing the anatomical basis for the CAN to act as a functional network.

**Study 3** entitled 'Forebrain organization representing integration of baroreceptor and somatosensory afferents within the cortical autonomic network', aimed to establish the effects of muscle sensory afferents on CAN activation patterns during conditions of baroreceptor unloading. It was hypothesized that muscle sensory afferent stimulation differentially impacts CAN regions involved in sympathetic activity (i.e., insular cortex) during baroreceptor loading (supine rest) and unloading (LBNP), which will be associated with changes in muscle sympathetic nerve activity.

## 1.2 Autonomic Nervous System

Regulation of the circulation directs appropriate delivery of oxygen to organs and tissues depending on their metabolic demands while ensuring maintenance of arterial BP. Local factors produce mechanical adjustments of blood vessels to enable regional changes in blood flow, whereas central neural activity is necessary to govern cardiovascular function to meet the body's needs at the global level. For instance, movement from a supine to standing position initiates a complex series of adjustments in BP and blood volume redistribution to maintain arterial pressure in order to preserve

cerebral blood flow within its autoregulatory limits. Such cardiovascular adjustments are achieved by concerted action of central neural outflow directed towards the heart and vasculature.

The autonomic nervous system regulates involuntary control of nearly all organ systems, including the heart and blood vessels, and is divided into the sympathetic and parasympathetic divisions (119). The cell bodies of preganglionic fibres are located in the thoracic and lumbar sections of the spinal cord for the sympathetic division, and in the brainstem or sacral spinal cord for the parasympathetic division (133). The axons of the preganglionic fibres exit the central nervous system in cranial nerves or ventral roots to synapse on second-order neurons in autonomic ganglia. This gives rise to postganglionic fibres which directly innervate effector tissues including smooth and cardiac muscle (119). Both the sympathetic and parasympathetic branches have preganglionic and postganglionic fibres with the differences lying in the fact that the parasympathetic side has short postganglionic fibres and the sympathetic side has long postganglionic fibres arising from a paravertebral chain (133).

Both sympathetic and parasympathetic preganglionic fibres are cholinergic and release the neurotransmitter acetylcholine which binds to nicotinic acetylcholine receptors on postganglionic fibres. Muscarinic receptors are used for postganglionic parasympathetic fibres whose principal neurotransmitter is acetylcholine, which does survive long in the bloodstream due to rapid actions of the enzyme acetylcholinesterase (109). The classical neurotransmitter derived from sympathetic postganglionic fibres is norepinephrine, which acts on alpha and beta adrenergic receptors (46). Norepinephrine can undergo several changes including reuptake into the nerve terminal to be

repackaged in vesicles and released again, metabolism, or diffusion into the bloodstream (133). Sympathetic neurons also synthesize and release other neurotransmitters including adenosine triphosphate (ATP) and neuropeptide Y (NPY) which all produce vasoconstriction of vascular smooth muscle cells (15).

### 1.2.1 Direct Measurement of Sympathetic Nerve Activity

Sympathetic postganglionic neurons are small diameter unmyelinated C fibres from which direct neural measurements of sympathetic nerve activity can be made using the technique of microneurography (136; 137). This technique permits measurement from sympathetic axons contained within a fascicle that innervate skin or skeletal muscle (136), with the common measurement being muscle sympathetic nerve activity (MSNA). Multiunit recordings of multiple neurons are made with percutaneous insertion of a tungsten microelectrode into the nerve fascicle of a peripheral nerve, commonly the peroneal nerve. Confirmation of a suitable MSNA site is observed by changes in burst frequency and amplitude during events in response to known sympathetic reflexes such as changes in BP (i.e., Valsalva maneuvre) or chemoreflex (i.e., apnea). As well, a defining characteristic of a MSNA signal containing solely sympathetic vasconstrictor nerves is a 'burst' pattern that is pulse synchronous as regulated by the arterial baroreflex (146). For example, a decrease in BP leads to a reflex increase in MSNA, causing vasoconstriction and a subsequent increase in BP, which in turn reflexively decreases MSNA. These constant fluctuations are observable at rest and constitute normal variations in most healthy individuals (21). Another characteristic of a MSNA signal is a lack of bursting activity during arousal (i.e., loud clap), which on the other hand is associated with nerve activity to the skin (146). It is

also important to note that MSNA recorded from the leg and arm is similar at rest (127),

and also during baroreflex-mediated increases in MSNA (107).

### 1.2.2 Neural Control of the Heart

Autonomic control of the heart including cardiac rate and conduction velocity

involves both parasympathetic and sympathetic fibres which innervate the sinoatrial and

atrioventricular modes.  Sympathetic fibres also innervate atrial and ventricular

myocytes to mediate contraction and relaxation processes of the heart (133).  The

parasympathetic neurons in the vagus nerve release acetylcholine which acts on $M_2$

muscarinic acetylcholine receptors, resulting in hyperpolarization of the membrane due

to increased potassium conductance.  This leads to decreased firing and conduction in

the sinoatrial and atrioventricular nodes, respectively, and a subsequent reduction in HR

(133).  Norepinephrine from sympathetic fibres act on beta adrenergic receptors which

increases diastolic depolarization in the sinoatrial node and conduction in the

atrioventricular node, leading to an increase in HR (133).  In addition to this, stroke

volume is higher due to increased membrane calcium currents in myocytes which

augment calcium release and reuptake via the sarcoplasmic reticulum to effectively

increase contraction and relaxation of the heart (133).

### 1.2.3 Neural Control of the Vasculature

The sympathetic postganglionic nerves innervate the arterial tree of most

arteries, arterioles, and veins, though innervations of skeletal muscle veins and venules

are questionable (109).  Norepinephrine release from nerve varicosities produces

vascoconstriction of vascular smooth muscle cells by activating alpha-1 and alpha-2

receptors (109).  Calcium levels rise due to release from the sarcoplasmic reticulum or

plasmalemmal calcium channels, which ultimately leads to activation of myosin ATPase and binding of myosin and actin filaments to produce contraction (133). Co-transmission of norepinephrine often occurs alongside NPY which exerts powerful and long-lasting vasoconstrictor effects through $Y_1$ receptors (50). As well, ATP is released from synaptic vesicles with norepinephrine and NPY and acts through $P_2X$ receptors (133). The type of neurotransmitter released for vasoconstriction often depends on the vascular bed and the rate of nerve firing (109). The vasculature is under tonic control of the sympathetic nervous system and remains in a partly constricted state; this overall vasoconstrictor activity of arterial and venous vessels constitutes a measure of total peripheral resistance.

### 1.2.4 Cardiovascular Responses to Isometric Exercise

At the onset of isometric exercise, characteristic increases in HR, cardiac output and BP occur (109). A study of graded isometric handgrip exercise showed very large increases in BP that was associated with the intensity of the contraction, expressed as a percentage of the maximum voluntary contraction (MVC) (41). Similarly, the increases in HR and cardiac output are a function of the degree of exertion (85). The rapid onset of HR change implies a neurogenic mechanism whereby the initial increase in HR occurs via parasympathetic withdrawal, since the response is blocked by the parasympathetic blocker atropine (41) but not by the sympathetic blocker propranolol (142). Furthermore, during the first minute of moderate intensity handgrip there is no change in MSNA (77; 116). An increase in MSNA is associated with metabolite accumulation and with fatigue, and it has been demonstrated that non-fatiguing contractions (i.e., 15% MVC) do not elicit a rise in MSNA (117). Thus the increase in

BP during a short bout of moderate intensity isometric contraction is due to an increase in cardiac output (not an increase in vascular resistance), which in turn is elevated by the rise in HR via parasympathetic withdrawal. Contractions at stronger intensities (50-95% MVC) still induce a HR response via parasympathetic withdrawal but also involve a sympathetic response that arises earlier on 10 seconds after the contraction (76). Thus, based on a study of HR responses to 30 second isometric contractions at 30% MVC showing that the inhibition of parasympathetic activity predominates in the first 30 seconds of activity (78), we utilized this model for isometric handgrip exercise to isolate the effects of parasympathetic withdrawal on cortical activation patterns.

Homeostasis of the internal environment during exercise and rest is achieved by sympathetic-parasympathetic balance, which in turn is maintained by integration of autonomic reflexes including the arterial baroreflex, chemoreflex, descending signals from higher central nervous system centers ('central command'), and the skeletal muscle reflex (110).

### 1.2.5 Arterial Baroreflex

The arterial baroreflex functions as a critical feedback control system to buffer or oppose beat-to-beat fluctuations in BP to maintain circulation to the brain and other organs. The baroreflex senses changes in BP indirectly via the extent of stretch of baroreceptors, which are sensory afferent nerve endings located in walls of the carotid sinus and aortic arch (37). As detailed below, an increase in BP and stretching of the baroreceptors will increase afferent discharge into the central nervous system, which elicits a reflex decrease in sympathetic outflow and parasympathetic activation, which in turn decreases HR, cardiac contractility, vascular resistance and venous return (71).

Together, this restores BP to its previous level.  The opposite occurs when BP

decreases, whereby reflex increases in sympathetic outflow in response to baroreceptor

unloading act to increase HR, stroke volume and vascular resistance in order to increase

BP.

At resting levels of BP, baroreceptors send tonic, excitatory signals to neurons in

the nucleus tractus solitarius (NTS) (123).  In response to increased BP, baroreceptor

afferents travel in the glossopharyngeal nerve (cranial nerve IX) and synapse in the NTS

in the medulla of the brainstem (133).  The baroreceptor signals are relayed from the

NTS to the caudal ventrolateral medulla (CVLM) which is a rich source of GABAergic

neurons (115).  Glutamatergic excitation of the CVLM GABAergic neurons produces

an inhibitory influence on the presympathetic neurons in the rostral ventrolateral

medulla (RVLM).  The RVLM is the major center which sends excitatory signals to

sympathetic vasomotor neurons.  Inhibition of the RVLM has been shown to nearly

abolish sympathetic outflow and decrease arterial pressure (126), highlighting the

importance of RVLM neurons in maintaining pressure.  Neurons in the NTS have been

shown to project directly to the RVLM; however, neuroanatomical and tracing

experiments emphasize the CVLM as the major source of baroreflex-mediated

inhibition of RVLM sympathetic pre-motor neurons (115).  The RVLM neurons project

to sympathetic pre-ganglionic neurons on the intermediolateral (IML) horn of the

thoracic and lumbar segments of the spinal cord (11).  These pre-ganglionic neurons

then synapse with sympathetic ganglia in the paravertebral chain, which project to the

heart and vasculature.  Thus, with the inhibitory effect of the CVLM on the RVLM

sympathetic neurons, there is lower sympathetic nerve firing through the sympathetic

ganglia, thereby reducing vascular resistance and arterial pressure. On the other hand, in response to a decrease in BP, there is reduced baroreceptor afferent signaling to the NTS, leading to decreased stimulation of the GABAergic CVLM neurons, thereby removing the inhibitory effect on the RVLM neurons. Thus the firing rate of presympathetic RVLM neurons increases and elevates sympathetic nerve activity, ultimately restoring BP back to baseline levels (115).

The baroreflex also acts on the heart by elevated parasympathetic activity to combat increases in arterial pressure. The NTS sends excitatory signals to the nucleus ambiguus and dorsal motor nuclei of the vagus, sites of parasympathetic motor nuclei to decrease the force and rate of contraction of the heart (37).

Lower-body negative pressure (LBNP) is a commonly used technique to elicit baroreflex-mediated increases in MSNA (128). Since the invention of LBNP in the 1960's, it has been commonly used to study the cardiovascular effects to changes in blood volume displacement (49). During LBNP, individuals are sealed in an air-tight box at the level of the iliac crest, which induces sub-atmospheric pressure around the lower portion of the body. Various levels of negative pressure can be used to prompt a diversion of blood from the central intra-thoracic to the lower leg venous compartments. Such an episode triggers an integrated systemic-wide response to the sudden removal of blood from the coronary/pulmonary circulation necessitating autonomic cardiovascular adjustments to maintain arterial BP (131). Thus, LBNP provides a simulated orthostatic stress and a means to examine neuro-circulatory reflexive responses to decreases in venous return to the heart (57). Cardiopulmonary baroreceptors, which are low-threshold receptors located in the atria, ventricles and pulmonary vessels are selectively

unloaded when LBNP is less than 20 mmHg, whereas the arterial baroreflex becomes
engaged when LBNP is greater than 20 mmHg (57). Generally, LBNP elicits increases
in HR at levels of 30 mmHg and above (57; 64). However, increases in MSNA are
observed from levels of LBNP as low as 5 mmHg, and MSNA progressively rises in
frequency and amplitude over larger levels of suction (141).

### 1.2.6 Chemoreflex

The chemoreflex has an established role in the control of respiration and also on
cardiac and vascular function (17). The anatomical structure of the chemoreflex
consists of peripheral chemoreceptors located in the carotid bodies of the internal
carotid artery, and central chemoreceptors situated in the brainstem (61). Generally, the
peripheral chemoreceptors are sensitive to decreases in oxygen (hypoxia), whereas
central chemoreceptors are more responsive to elevations in carbon dioxide
(hypercapnia) (61). The act of breathing has a negative feedback on cardiovascular
responses whereby stretch of lung receptors by ventilation attenuates chemoreflex-
mediated sympathetic activation (122). However, during apnea when there is no
activation of lung receptors, hypoxia and hypercapnia augment the effect of
chemoreceptors resulting in increased sympathetic vasoconstrictor activity to the blood
vessels (61). The impact of chemoreflex activation on regulating vascular resistance is
modulated through afferent signals to vasomotor centers in the medulla, including the
NTS. The NTS may be the first synapse for carotid chemoreceptor afferents (101). The
RVLM is suggested to be the final brainstem structure for sympathetic outflow and
evidence suggests that the influence of chemoreflex activation on RVLM neurons may
come via direct connections with the NTS (1).

### 1.2.7 Descending Neural Control to Brainstem Cardiovascular Centers

Autonomic function is also dependent upon top-down signals ("central command"), which involves a diffuse irradiation of neural motor signals to cardiovascular control centers in a feed-forward manner (109). This system is linked to the coupling between blood flow and oxygen demands and has been suggested that as muscle fatigues and motor unit recruitment increases, there is an equivalent increase in cardiovascular responses (47). The origin of central command arose from observations of nearly instantaneous increases in HR and ventilation at the onset of voluntary exercise (68), prompting the notion that the speed of cardiovascular and respiratory responses had to be centrally generated as opposed to peripherally. Evidence from a neuromuscular blockade study showed no difference in HR and ventilation between actual and attempted exercise in which subjects used near-maximal effort (central command) to attempt sustained handgrip without producing force (142). Another study altered the levels of central command by applying vibration to muscle spindles of agonist muscles to decrease central command, or to the antagonist muscles to increase central command to maintain a constant level of isometric contraction (47). At the same level of muscle tension, HR and BP decreased when central command decreased, and cardio-respiratory measures increased when central command increased.

Lastly, the increase in HR with exercise appears to be mediated primarily by central command, whereas mechanically and metabolically sensitive muscle afferents are suggested to stimulate the increases in BP and muscle sympathetic outflow (77; 83; 142). Further, central command governs the immediate increase in HR at the onset of exercise via parasympathetic withdrawal as opposed to sympathetic activation (109). A

latency period of 0.5 seconds occurs between the onset of a muscle contraction and the increase in HR, and given that parasympathetic responses to the heart occur in less than 1 second and sympathetic responses come into effect 10 to 15 seconds later (109), it strongly points to a parasympathetically-mediated increase in HR.

### 1.2.8 Exercise Pressor Reflex (Muscle Afferents)

Afferent fibres from skeletal muscle receptors also contribute significantly to the reflex regulation of the cardiovascular system (84). The "exercise pressor reflex" states that exercise-induced signals which comprise the afferent arm of the reflex provide feedback to brainstem cardiovascular centres regarding the mechanical and metabolic conditions within the muscles (25; 80). During muscle contraction, there is an increase in the concentration of various chemicals including lactic acid, $H^+$, bradykinin, $K^+$ and adenosine in the interstitial space, which stimulates the free nerve endings of the muscle afferents (120; 121). Contraction also causes an increase in the discharge of mechanically sensitive muscle afferents. Upon stimulation of these fibres, a central neural signal is generated that contributes to the increase in HR, BP and sympathetic outflow that occurs with exercise.

Alam and Smirk (1937) were the first to show evidence that a reflex originating in contracting skeletal muscle was involved in the cardiovascular and ventilatory responses to exercise (2). They reported that BP remained elevated above baseline values when the circulation to the exercising muscles was occluded at the end of the exercise period. Support for the exercise pressor reflex during muscle contraction was given by Coote et al. (1971). In anaesthized rats, electrical stimulation of the ventral roots increased arterial BP and HR. Cutting the dorsal roots receiving afferents from

the muscle abolished the pressor response, providing further evidence that the response originated in the exercising limb (25). In humans, during neuromuscular blockade (termed curare), the intent to exercise (central command) without any sustained contraction caused pressor and sympathetic responses that were half as large as that to normal handgrip exercise (142), confirming the role of the muscle reflex. Activation of this reflex involves stimulation of the group III and IV muscle afferents (80). Nerve block of only the large myelinated type I and II fibres, which include afferents from muscle spindles and Golgi tendon organs, did not alter the cardiorespiratory responses. Whereas blockade of the dorsal roots preferentially blocking the unmyelinated and smaller myelinated fibres (type III and IV) did abolish the cardiovascular and respiratory responses. In addition, group III fibres are predominantly mechanically sensitive while the group IV muscle afferents are activated primarily by metabolites (63), though the fibres do exhibit polymorphism. It has been further evidenced that preferential activation of group I and II afferents appears to have no reflex effect on BP, HR or respiration. Succinylcholine administered to cats before and after muscular paralysis to activate group I and II afferents in the hindlimb did not change respiratory or cardiovascular function (145). In addition, vibration is a powerful stimulus to the primary endings of muscle spindles; this has not been shown to produce any appreciable increase in BP, HR, or ventilation in the decerebrate or anesthetized cat (79).

Activation of the skeletal muscle receptors reflexively increases HR and BP mainly through an increase in sympathetic activity and decrease in parasympathetic activity (62). Though the exact central integration of muscle afferents is not known, type III and IV afferent neurons project to the dorsal horn of the spinal cord in Rexed's

laminae I, II, V and X (121). The mapping of sensory afferents between the spinal cord and brainstem is not fully known, but tracing techniques in rodents reveal projections to the NTS, CVLM and RVLM (121). Skeletal muscle inputs produce excitatory responses in NTS neurons, and muscle contraction elicits activity in neurons within the CVLM and RVLM implicating these regions as an important integration centers for the exercise pressor reflex (73). Central processing of the type III and IV afferents in the brainstem is followed by transmission of inputs through the parasympathetic and sympathetic arcs through the respective pathways to innervate the heart and vasculature in order to regulate perfusion pressure during exercise (121).

## 1.3    The Somatosensory System

### 1.3.1    Characteristics of Muscle Sensory Afferents

Within the somatosensory system, specialized receptors located in skin, hair follicles, joints and muscle transduce mechanical and thermal energy (4). A receptor consists of a peripheral axon terminal of one primary afferent neuron, whose cell body resides in the dorsal root ganglion (4). Skeletal muscle sensory afferent fibres can be classified according to their diameter or conduction velocity, and are labelled as types I-IV in order of decreasing fibre diameter (84). Each type of receptor gives rise to fibres within a particular diameter range, whereby the rate of impulse conduction varies directly with diameter (i.e., large diameter axons conduct action potentials more rapidly than thinner axons) (4). Each muscle nerve contains four types of afferent fibres (Table 1.1). The characteristics of these fibres have been classified in stimulation studies performed in anaesthetized cats from the impulses arising from hindlimb skeletal muscle (80), which will reflect higher conduction velocities compared to human data.

Types I, II, and III are myelinated whereas type IV afferents have no myelin sheath (84). The largest diameter type I fibres innervate muscle spindles as annulospiral endings (Ia) and the Golgi tendon organs (Ib). The type II afferents are slightly thinner and slower than type I and originate in muscle spindles to form secondary sensory endings on the intrafusal fibres. The thinly myelinated type III nerve fibres and unmyelinated type IV afferents terminate as "free nerve endings" in the skin and musculature (84).

The cable properties of axons characterize the largest diameter, fast conducting fibres as having the lowest threshold for electrical stimulation (129). This exists due to the fact that longitudinal current flow is proportional to the square of the fibre diameter, and large fibres exhibit less input resistance to current flow (129). Thus, graded levels of electrical stimulation can be used to selectively activate large diameter fibres at the weakest effective stimulus intensity, and subsequently recruit smaller diameter fibres with increasing stimulus intensity. At the median nerve, the response to Type I fibres can be recorded at threshold for perception of the stimulus (136). Accordingly, sub-motor threshold stimulation has been used in humans to stimulate the large diameter Type I/II afferents (55; 118). In the current thesis, sub-motor threshold stimulation was used to recruit the Type I and II afferents, while higher intensity motor threshold stimulation to elicit wrist flexion aimed to further recruit the Type III and possibly Type IV mechanoreceptors and metaboreceptors.

**Table 1.1 Classification of Afferent Nerve Fibres**

| Type | Myelination | Conduction Velocity, m/s | Target/Receptor | Sensitive To |
|---|---|---|---|---|
| I | Thick | 72-120 | Ia, primary ending of muscle spindle<br><br>Ib, Golgi tendon organ | Ia – muscle length and rate of change of length<br><br>Ib – muscle tension |
| II | Thick | 31-71 | Secondary spindle ending | Muscle length |
| III | Moderate | 2.5-30 | Mainly "free nerve endings" | Pain, touch, chemical stimuli, and temperature |
| IV | None | Less than 2.5 | "Free nerve endings" | Pain, chemical stimuli, and temperature |

(Source:  Adapted from Kaufman, M.P. and Hayes, S.G.  The Exercise Pressor Reflex, *Clinical Autonomic Research* 12: 429-439, 2002)

**1.3.2    Ascending Central Pathways**

The dorsal column medial lemniscus pathway carries information from sensory

receptors that mediate discriminate touch, vibration and kinesthesia from group I and II

fibres originating from muscle spindle and Golgi tendon organs.  Fibres originating

from below the mid-thoracic region become medially located in the dorsal column to

form the *fasciculus gracilis*, while those originating from upper thoracic and cervical

segments form the *fasciculus cuneatus* of the ipsilateral dorsal column (150).  Axons

from the gracile and cuneate fasciculi terminate in the ipsilateral dorsal column nuclei

of the medulla oblongata (4).  Axons of second order neurons in the gracile and cuneate

nuclei cross the midline of the medulla as internal arcuate fibres and continue to the

thalamus as the medial leminscus (65).  The medial lemniscus enters the lateral division

of the ventral posterior nucleus of the thalamus, which is the primary somatosensory

relay and the source of most thalamo-cortical projections (4).  The pathway is

completed by the relay from the thalamus nuclei to the primary somesthetic area (SI) in

the parietal lobe in the cerebral cortex (65).  Representations of the body surface occur

on the SI termed the sensory homunculus, in which the magnitude of the cortical

representation of a body region is proportional to the use of the region and not its size

(4).

The small diameter sensory fibres which convey pain, temperature and crude

touch ascend in the spinothalamic tract (150).  These axons enter the spinal cord via the

dorsal root and travel for one to two segments as Lissauer's tract before synapsing in the

nucleus proprius at the base of the dorsal horn (65).  The fibres cross the midline in the

ventral white commissure to the opposite side of the spinal cord and course upward as

the spinothalamic tract, in one of two pathways, the anterior spinothalamic tract which carries touch information, and the lateral spinothalamic tract, which contains pain and temperature axons (65). The spinothalamic fibres ascend to the medulla and above this level the fibres constitute the spinal lemniscus, which then terminate in the ventral posterolateral division of the thalamus (4). The axons from the thalamus cross the internal capsule to reach SI (65).

### 1.3.3 Effect of Somatosensory Stimulation on Autonomic Tone

Somatosensory information from skin, joints and muscle is transmitted by afferent fibres to the central nervous system and has been shown to evoke autonomic responses (114). Both pressor and depressor responses in terms of sympathetic activity are observed during somatosensory input, and spinal, medullary and supra-spinal components have been identified in the somato-sympathetic reflex (114). Transcutaneous electrical nerve stimulation (TENS) is a commonly used modality to study the peripheral circulatory effects of somatosensory stimulation.

Low-frequency electrical stimulation of the sciatic nerve in rats has been shown to cause peripheral vasodilation and decreased systemic BP, pointing to sympatho-inhibition (153). Kaada et al. (1990) used low-frequency (2 Hz) TENS at the web between the first and second metacarpal bones at an intensity that caused non-painful, local, rhythmic contractions of the finger. They observed a reduction in mean femoral arterial BP and systemic vascular resistance in normotensive patients undergoing cardiac catheterization (60). The authors attributed the mechanism most likely to be sympatho-inhibition, due to central activation of a serotonergic system leading to peripheral 'passive' withdrawal of sympathetic activity. Jacobsson et al. (2000)

investigated the effects of low frequency (1.7 Hz) TENS below the pain threshold

applied between the first and second metacarpal bones in patients with therapy-resistant

hypertension (58). After four weeks of treatment, 24-hour ambulatory BP recordings

showed decreased systolic and diastolic BPs that continued to stay reduced one week

after the stimulation period. The effects of TENS were suggested to occur through

central inhibition of sympathetic activity, involving an endorphinergic mechanism

leading to an increase in opioid peptide content (58). Kaada et al. (1991) similarly

noted lowered systolic, diastolic and mean BPs in response to low frequency (2 Hz)

TENS applied at non-painful motor threshold of the fingers in individuals with

mild/moderate hypertension (59). In addition, they noted a continued lowering of BPs

after two weeks of daily TENS therapy. High-frequency TENS (75 Hz) on the ulnar

nerve in healthy individuals has also been shown to decrease sympathetic tone (100).

The authors used infrared thermography and demonstrated increased infrared emission

and increased skin temperature, providing indirect evidence of skin vasodilation and a

decrease in sympathetic tone. Direct measures of MSNA were obtained by Hollman

and Morgan (1997) to study the effects of TENS during handgrip exercise in healthy

volunteers. Sub-motor threshold TENS (60 Hz) to active type I and II afferents was

applied to the ipsilateral forearm alone and during 2 min of 25% MVC handgrip

exercise (55). The sympathetically-mediated pressor responses to handgrip exercise,

including MSNA burst frequency and systolic BP, were attenuated with concurrent

TENS delivered over the forearm. The blunted sympathetic response was attributed to a

modulation of III and IV afferents activated with handgrip exercise by type I and II

afferents at the spinal level. Sanderson et al. (1995) also examined the effects of high

frequency (150 Hz) TENS on the chest and back during sustained handgrip exercise, observing a reduction in the rise of DBP (113).  Lastly, sensory stimulation in the form of electric shock to the finger at an intensity as high as possible without causing pain has been shown to attenuate the amplitude of one to two subsequent MSNA bursts.  The shocks were delivered 200-400 ms after the R wave of the electrocardiogram (ECG), suggesting that the inhibitory effect was due to the level of afferent baroreceptor discharge (35).

However, sub-motor and mild motor threshold electrical stimulation do not always produce depressor effects.  Sherry et al. (2001) observed no changes in arterial BP or foot temperature, nor in calf blood flow or vascular resistance in response to sub-motor and motor threshold TENS (85 Hz) of the tibial and peroneal nerves (118).  In addition, Indergand and Morgan (1994) studied the effects of high-frequency TENS (110 Hz) of the peroneal and tibial nerves at sub-motor and motor threshold intensities in healthy subjects.  Neither intensity influenced calf blood flow, mean arterial pressure nor calf vascular resistance.

Thus, stimulation of peripheral afferent nerves has been shown to produce depressor effects on MSNA and BP and other indices that indicate sympatho-inhibition.  However, the studies vary in terms of stimulation parameters (high versus low frequency) and stimulation intensity, including sub-motor threshold, motor threshold, or simply non-painful.  These varying levels of intensity activate different groups of afferents, thus, it is important to separately study the intensity levels further.  In addition, the inclusion of other measures including heart rate variability and MSNA are lacking to elucidate whether parasympathetic versus sympathetic activity is altered with

somatosensory stimulation. Lastly, central mechanisms within the spinal cord and medulla have been suggested to modulate somato-autonomic regulation; however, the involvement of higher cortical centers has not been investigated. While the neural pathway from somatosensory receptors to the spinal cord, brainstem and to the somatosensory cortex is well known, the representation of sensory inputs within other cortical regions including autonomic areas requires investigation. Thus, this thesis aims to further examine the effects of somatosensory stimulation, particularly sub-motor threshold electrical stimulation to activate the Type I and II afferents, on indices of heart rate variability and MSNA, as well as on cortical patterns of activity.

## 1.4     Central Modulation of Cardiovascular Control

Past stimulation and neuroanatomical studies have established a role for the cerebral cortex in autonomic cardiovascular control. Regions implicated in the modulation of cardiovascular control mechanisms include the insular cortex, medial prefrontal cortex (MFPC), anterior cingulate cortex (ACC), amygdala and cerebellum (18; 31; 140). This thesis will focus specifically on the roles of the insula, MPFC and ACC as these forebrain regions are better described in terms of their currently accepted roles in autonomic function as compared to the amygdala and cerebellum.  .

### 1.4.1   Insular Cortex

The insula lies buried within the lateral sulcus covered by the operculum, consisting of the inferior frontal gyrus, inferior parietal lobule, and the superior temporal gyrus (7) (Figure1.1). The insula has been classified into three distinct subdivisions: ventral anterior insula, dorsal anterior to middle insula, and middle to posterior insula (81) (Figure1.2). Insular pathways project to various subcortical

regions known to be involved in autonomic function, such as the nucleus tractus solitarius (NTS), the lateral hypothalamus, the parabrachial nucleus, and the central nucleus of the amygdala (18).
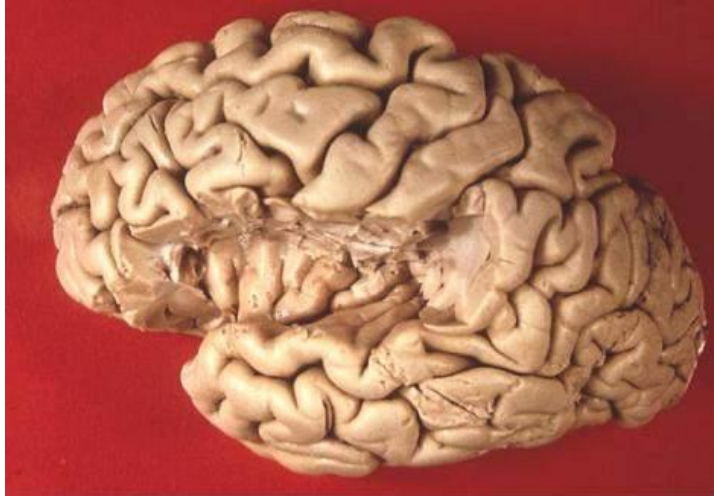
**Figure 1.1 -- Histologic view of the insula buried under the operculum.**

(Source: http://www.healcentral.org/healapp/showMetadata?metadataid=40566. By John A. Beal, Ph.D., Department of Cellular Biology & Anatomy, Louisiana State University Health Sciences Center Shreveport)
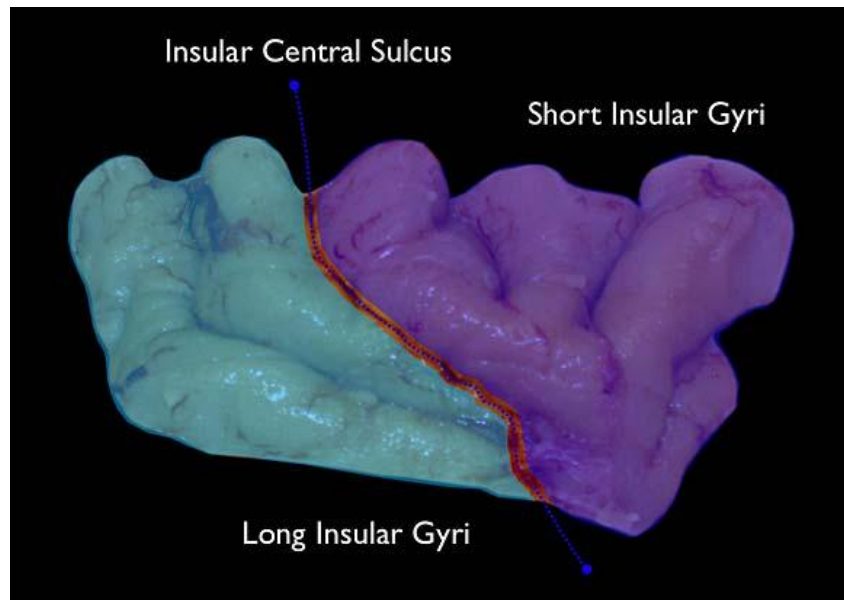
**Figure 1.2 -- Cytoarchitectonic delineation of the anterior insula consisting of three short gyri and the posterior insula consisting of two long gyri, separated by the central sulcus.**

(Source:  Used with permission by Prefrontal.org, Brain Dissection Insula Anatomy)

Stimulation of the insular cortex has been shown to elicit changes in HR and BP in both rats (94) and humans (95). In rats, the rostral posterior insula produces tachycardia, whereas bradycardia is produced by stimulation of the caudal posterior insula. Furthermore, in humans, lateralization has been observed with direct cortical stimulation of the left insula producing bradycardia, and right insular stimulation producing tachycardia and a pressor response (95). Lateralization of insula-induced cardiovascular control has also been demonstrated by a lesion study showing damage to the left insula shifts cardiovascular function towards higher sympathetic outflow (96).

The insulae also feature prominently in non-invasive neuroimaging studies in conscious humans. In these studies, several manoeuvres have been employed to understand the patterns of activation within this region that are associated with cardiovascular arousal. For example, a functional neuroimaging study has also reported right posterior insular activation during handgrip and mental stress (28). Although the posterior region of the right insula contains a high percentage of sympatho-excitatory neurons which are stimulated during pharmacologically-induced BP challenges (94; 155), neuroimaging studies show the anterior-mid insula also responds to sympatho-excitatory tasks. Gianaros et al. (2007) observed activation in the anterior insula during a mental stressor (colour-word Stroop task) that elevated BP (44), and Macefield and colleagues (2006) showed anterior insula involvement during increased MSNA with inspiratory apnea (75). In addition, the bilateral anterior-mid insula modulates the HR increase during moderate intensity isometric handgrip exercise (151). In addition, the effect of central command or increased sense of effort on HR has been attributed to right posterior and left anterior insular activation during static handgrip exercise (148).

These authors also employed an "imagined" exercise task to test the idea that the observed patterns of cortical activation during handgrip were induced by "top-down" central command phenomena rather than "bottom-up" sensory inputs. In the imagined exercise cardiovascular responses were elicited and these were associated with insular activation (149).

The above evidence has largely focused on the association of insular activation patterns and HR regulation by the reflexive manoeuvres. Such changes in HR can be induced by alterations in parasympathetic and/or sympathetic neural changes. In this regard the insula plays a role in sympathovagal balance in a manner that largely reflects parasympathetic modulation. In particular, the posterior insula is associated with the high frequency component of heart rate variability (HRV), an index of parasympathetic activity (89). Similar to aforementioned stimulation studies, the left insula is correlated with high frequency power during emotion (70) and working memory (45) tasks, suggesting an association of the left insula with parasympathetic activity.

In addition to these cardiovascular "motor" effects of the insulae, these cortical regions also receive sensory inputs related to somatosensory processing and cardiovascular function. The posterior insula plays an important role as a somatosensory association area (42; 69; 82), in which the 'sensory' posterior insula integrates vibrotactile stimuli (24) and touch (12). Regarding cardiovascular function, neurons in the right posterior insula are responsive to baroreceptive inputs and to changes in BP (155). This issue of sensory signals being represented in the CAN is particularly pertinent to the study of the cortical modulation of cardiovascular arousal during exercise. In particular, representation of skeletal muscle afferent

metaboreceptors has been shown in the insula during PECO of the exercising forearm to trap circulating metabolites (148). This likely involved the type III/IV afferents because they are stimulated by the trapped metabolites and there was no movement of the forearm. However, this study could not differentiate sensory signals arising from type III/IV muscle afferents from baroreflex sensors that would be activated during PECO. Thus, a passive technique that stimulates somatosensory afferents without engaging central command or afferent BP or cardiac input to the central nervous system would aid in revealing the effects of type I and II somatosensory inputs to the CAN. Electrical stimulation affords the opportunity to study this and can be used to activate different groups of somatosensory afferents. Median nerve electrical stimulation at motor threshold activates the bilateral insula (5; 38). Tingling level electrical stimulation has been associated with posterior insula activation (32). However, these studies did not study cardiovascular responses to the stimuli nor relate the activity to other CAN regions.

Overall, the above text indicates that the insula has established roles in autonomic function as well as in sensory integration. These are not likely mutually exclusive roles and it remains to be determined how sensory signals represented in this region affect cardiovascular control in conscious humans, independent of other perceptual or emotive features such as pain, which will also induce cortical activation patterns. For example, the anterior insula is involved with awareness and emotion (26; 30) as well as with autonomic function, whereas the posterior insula contains sympatho-excitatory neurons and integrates sensory information. Thus, this thesis aims to address the role of the insula in the integration of Type I/II afferents versus III/IV afferents

during volitional and electrically-stimulated procedures that do not increase HR and BP in order to control for afferent cardiac and baroreceptor inputs to the brain.

### 1.4.2 Ventral Medial Prefrontal Cortex

The vMPFC is an established visceromotor region in the modulation of autonomic nervous activity (90) (Figure 1.3). Stimulation of the vMPFC in rats leads to decreased mean arterial pressure and inhibition of sympathetic tone (98; 99), suggesting that the vMPFC is involved as a central sympatho-inhibitory pathway. Broadly ranging anatomical connections from the vMPFC to central regions involved in cardiovascular regulation include the amygdala, the lateral hypothalamus, the periaqueductal gray (PAG), the NTS, the CVLM and RVLM (56; 90). The lateral hypothalamus, PAG, NTS, CVLM and RVLM appear to be the main nuclei within the neural pathway for producing hypotension during electrical stimulation of the vMPFC in the anaesthetized rat (39; 97). For instance, the depressor responses to electrical stimulation of the vMPFC are attenuated during NTS inhibition by GABA agonists (97).

The importance of the vMPFC in autonomic cardiovascular arousal is also evident in neuroimaging studies of conscious humans and monkeys. First, this region is active in humans during rest (106) and during sleep in monkeys (108). This concept is important when it is considered that, at rest, sympathetic levels are low and parasympathetic outflow is high. From this position, the vMPFC adjustments would be important in exercise whereby autonomic balance is adjusted. In support of this view, Wong et al. (2007) showed that vMPFC deactivation during bouts of short-term (i.e., 30-sec) moderate intensity handgrip exercise is associated with the parasympathetically-mediated rise in HR response (151). It is noteworthy that this exercise task emphasizes

PNS withdrawal in the absence of sympathetic activation. Thus, in this model, the

vMPFC appears to be involved with the modulation of parasympathetic activity.

However, it remains uncertain whether the levels of vMPFC activation at rest or during

exercise are directly related to PNS levels and whether the deactivation in this region

with volitional handgrip is due specifically to an active "motor" role of the cortex or the

representation of a sensory signal from the activated muscle or the heart that are

concurrently elicited during the handgrip exercise.
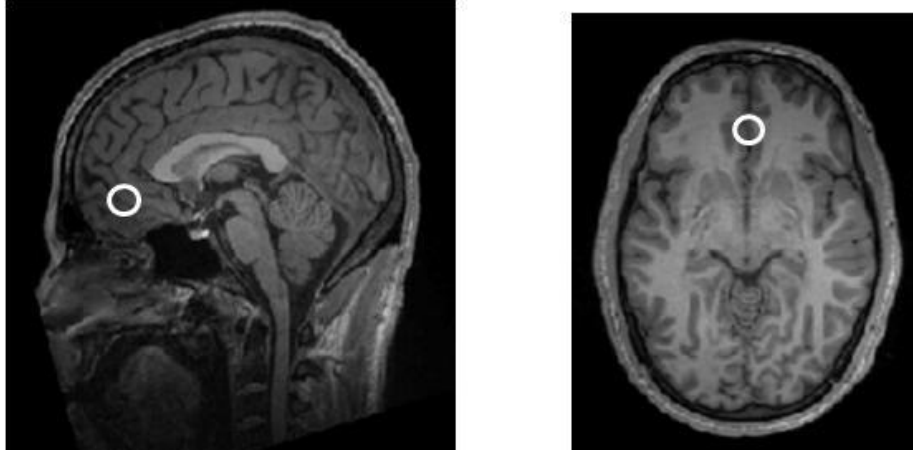
**Figure 1.3 -- Sagittal (left) and axial (right) view of the vMPFC.**

### 1.4.3 Anterior Cingulate Cortex (Subgenual and Dorsal)

The anterior cingulate cortex (ACC) lies ventral, rostral and dorsal to the corpus callosum and belongs to the limbic lobe (16; 33). In addition to playing a role in motor function as well as processing cognitive and emotional function, the ACC has a significant role in modulating autonomic function (14; 33; 143). The ACC displays interconnections with autonomic nuclei in the hypothalamus, amygdala, insula and orbitofrontal regions (3; 140).

The two major subdivisions of the ACC include the dorsal and rostral-ventral regions. The psychology literature points to these regions as being related to cognitive and affective roles, respectively (16). In addition to roles in cognition and emotion, electrical stimulation studies of the ACC in animals have revealed significant autonomic responses, yielding changes in sympathetic activity and respiration (91). The subgenual ACC (Brodmann area 25, Figure 1.4) contains extensive connections with autonomic centres including the parasympathetic nucleus of the solitary tract (132) and the dorsal motor nucleus of the vagus (56), supporting the involvement of the subgenual ACC in parasympathetic activity. On the other hand, the dorsal ACC (Brodmann area 32 and 24, Figure 1.5) is tightly linked with sympathetic nervous system control. Human neuroimaging studies have revealed an association between the dorsal ACC and sympathetic control of HR during cognitive and motor tasks (29). Working memory tasks that decrease HRV (decreased cardiac parasympathetic activity) (45), as well as baroreflex-mediated increases in MSNA via an orthostatic stressor (66), are associated with activity in the dorsal ACC, supporting its role in sympathetic regulation of cardiac function. Though the middle cingulate region is implicated with sensori-motor control

(27) and is activated with electrical stimulation (5), the involvement of the ACC

subdivisions with somatosensory processing requires further investigation.
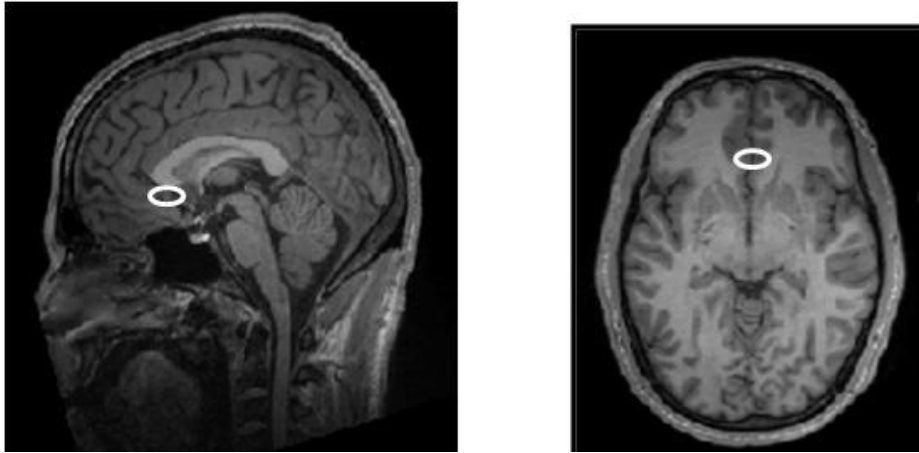
**Figure 1.4 -- Sagittal (left) and axial (right) view of the subgenual ACC.**
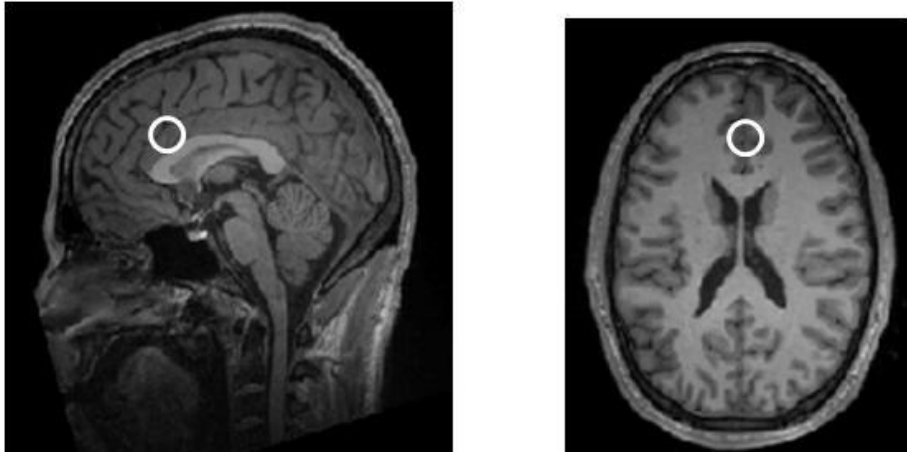
**Figure 1.5 -- Sagittal (left) and axial (right) view of the dorsal ACC.**

**1.5      Anatomical Connectivity between CAN Regions**

Previous animal studies have established patterns of structural connectivity between brain regions, including those implicated within the CAN.  These axonal projections physically linking cortical regions are suggested to subserve their functional roles (8).  In this regard, the anterior insula is connected to the ACC, while the posterior insula is connected with the middle cingulate and posterior cingulate (81; 144). Specifically, axonal tracer studies in rhesus monkeys show the anterior insula is connected to Brodmann areas 24 of the perigenual ACC, while the mid and posterior insula has connections with the mid and posterior cingulate areas 24' and 23 (Figure 1.6) (7; 36; 81).  Histochemical and radiographical experiments show that the insula forms a functional unit with orbital and frontal opercular areas, with reciprocal connections observed between the insula and the prefrontal cortex in non-human primates (7; 40).  Intra-insular connections are also evident in which the anterior insula receives afferents from adjacent agranular and anterior dysgranular areas, while the posterior insula receives afferents from both anterior and mid-insula (40).

The analysis of white matter axonal connections between regions implicated in autonomic function in humans has not been performed.  Given the information outlined above, it appears that the anterior insula will project toward the forebrain whereas the posterior insula will project more posteriorly.  This question was addressed in Chapter 3 in order to determine whether the underlying function of the CAN regions may be associated with their physical connectivity.
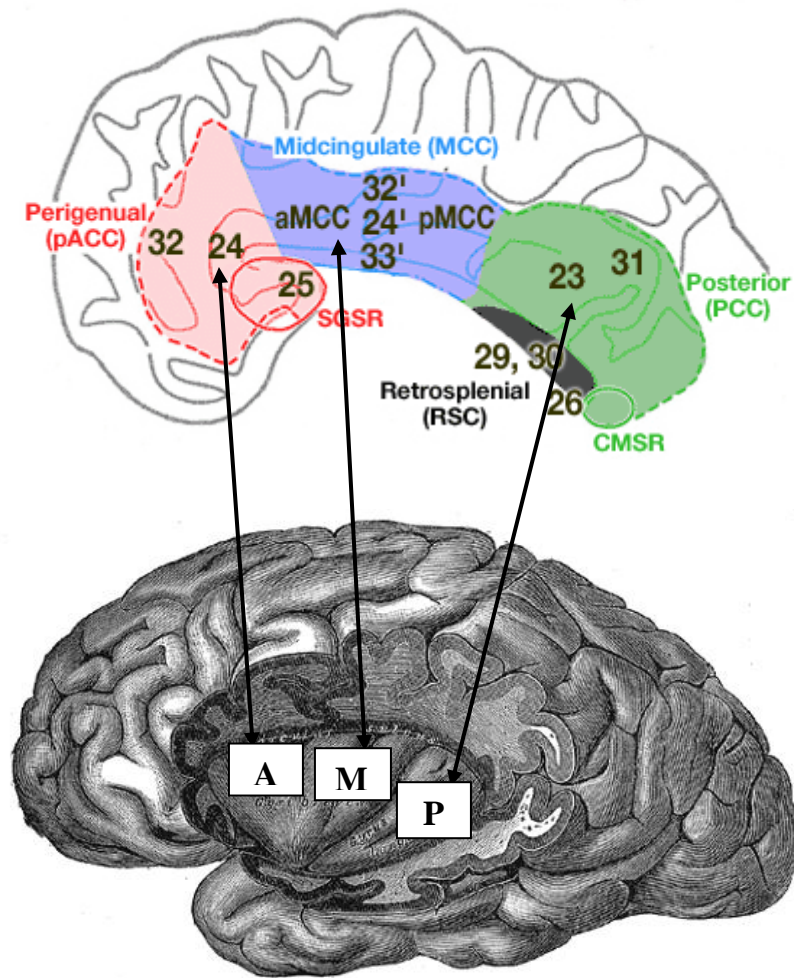
**Figure 1.6 -- Connectivity patterns between anterior (A), mid (M), posterior (P) insula (bottom) with anterior, mid and posterior cingulate areas (top).**

(Source top figure used with permission by Vogt BA, Cingulate Neurobiology and Disease, published by Oxford University Press.  Source bottom figure: 20th U.S. edition of Gray's Anatomy of the Human Body insula)

**1.6     Methods and Techniques**

**1.6.1   Functional MRI**

Functional magnetic resonance imaging (fMRI) is a sensitive, noninvasive tool used to map patterns of activation within the brain.  The relationship between neuronal activity and blood flow, termed neurovascular coupling, was first provided by Roy and Sherrington.  They observed that the byproducts of brain metabolism produced vasodilation that altered blood supply in response to changes in functional activity (74). The blood-oxygenation-level-dependent (BOLD) effect is the basis for most fMRI studies, and the level of blood oxygenation is used as an endogenous contrast (105). This BOLD effect was first reported by Ogawa and colleagues (1990) who recognized a difference in magnetic susceptibility of oxygenated haemoglobin (Hb) compared to deoxygenated haemoglobin (dHb) in the blood, due to Hb being less paramagnetic than dHb (93).  Cortical activity is thus related to an increase in Hb in the venous blood near the active site (105).

The measured MRI signal arises from hydrogen atoms which are abundant in biological tissues (13).  Hydrogen protons act as magnetic dipoles due to the odd number of protons and, thus, possess nuclear spin (74).  When exposed to an external magnetic field ($B_0$ field), hydrogen dipoles align and precess (spin) in the direction of the magnetic field, with a small number of protons aligned anti-parallel to the field, creating a weak equilibrium magnetization (13).  An additional magnetic field perpendicular to the main field and oscillating at the same resonance frequency can be used to tip the equilibrium magnetization.  A radiofrequency (RF) coil ($B_1$ field) applies a pulse to excite the nuclear spins and tip the tissue magnetization away from the main magnetic field by an angle called the flip angle (13).  This splits the equilibrium

magnetization into a residual component along the longitudinal axis defined by $B_0$, and

a precessing (spinning) component at a right angle to the main magnetic field, termed

the transverse component.  Prior to the RF pulse, the spins are randomly oriented and

sum to zero, and $B_1$ causes a coherent alignment of the spins in the transverse

component.  In turning off the RF pulse, the atoms are subjected only to the static

magnetic field, causing the atoms to return to their equilibrium state.  The longitudinal

component of magnetization returns exponentially to its equilibrium with a relaxation

time constant referred to as $T_1$ (74).  The transverse component decays exponentially

with a transverse relaxation constant termed $T_2$.  $T_2$ refers to the spin-spin relaxation in

a perfectly homogenous magnetic field; however, due to local field inhomogeneities, a

$T_2$* refers to the effective transverse relaxation time (74).  BOLD fMRI relies on the

paramagnetic properties of dHb, which enhances spin phase dispersion, and thereby

exerts its effects on $T_2$*, especially when dHb is compartmentalized in red blood cells

within blood vessels (34).

Increased neural activity leads to an increased BOLD signal as measured by

$T_2$*-weighted imaging.  The BOLD response to neural activity takes form as three

distinct phases (Figure 1.7).  After a stimulus, there is a small negative dip in the signal

2-3 sec post-stimulus, and though the initial dip remains difficult to detect, it appears to

be due to an increase in the metabolic consumption of oxygen without any change in

blood flow or blood volume (92).  This is followed by the main BOLD response which

peaks at around 5 seconds, in which blood flow increase more than the metabolic rate of

oxygen consumption, leading to decreased dHb and an increased MR signal.  The final

phase is characterized by a post-stimulus undershoot due to the delayed return of blood

volume to baseline (92).
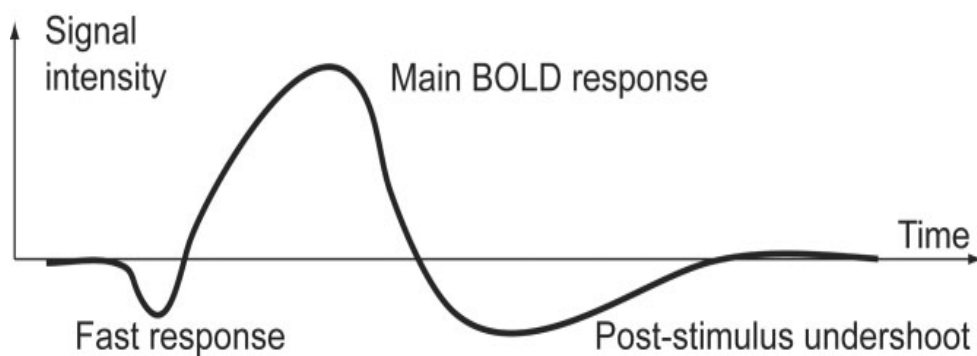
**Figure 1.7 -- Time course of the BOLD response to a short stimulus.**

(Source:  Used with permission by Norris, D.G.  Principles of Magnetic Resonance Assessment of Brain Function.  *Journal of Magnetic Resonance Imaging* 23: 794-807, 2006)

### 1.6.2    Diffusion Tensor Imaging

Diffusion tensor imaging (DTI) is one of the most innovative accomplishments in neuroimaging to surface over the last decade.  Conventional modalities of imaging cannot provide information on the structure of white matter anatomy.  However, DTI now allows macroscopic *in vivo* characterization of white matter fibre tracts which would otherwise be impossible in humans (104).  The white matter of the brain represents the axonal elements of neural tissue and reflects projections between various subcortical nuclei and connects gray matter regions.  Thus, DTI is an important tool used to perform tractography within the brain and used in conjunction with fMRI to discern connectivity pathways between gray matter regions involved in particular tasks (152).

### 1.6.2.1 General Concepts of DTI

Diffusion tensor imaging relies on the diffusion properties of water molecules, where diffusion represents translational motion and is based on thermal motion (Brownian motion) (88).  In regions with little or no physical constraints such as cerebrospinal fluid, water is free to move randomly in every direction constituting isotropic diffusion.  However, when a water molecule lies within the constraints of an axon in white matter, movement is restricted within the boundaries of the axon sheath, and is called anisotropic diffusion (103).  The diffusion of water in white matter occurs in extracellular and intracellular space (125).  The extracellular or interstitial space between fibres is conducive to water diffusion and animal studies suggest that it is in the extracellular compartment that diffusion is mainly detected by DTI (125).  Diffusion MRI is based on the translational displacement of water molecules (6).  The direction of

water diffusion within white matter is primarily dependent upon axonal alignment whereby water diffuses preferentially along the longitudinal axis of the axon and is more restricted in the perpendicular axis (9). Water diffusion along a white matter tract is faster in the longitudinal direction than perpendicular and it is the difference between these two motions (termed diffusion anisotropy) that underlies the DTI technique (6). The anisotropy is represented mathematically by a tensor (or ellipsoid), and is typically cigar shaped within white matter (152). DTI involves computation of a tensor to mathematically describe the 3D ellipsoid, which illustrates the magnitude and orientation of diffusion in each voxel (20). The tensor is assigned three orientation vectors representing the three major axes of the diffusion ellipsoid, labelled as eigenvectors $\lambda_1, \lambda_2$ and $\lambda_3$ (152).

The long eigenvalue of the tensor which is aligned in the longitudinal or axonal

direction is termed $\lambda_1$ and is named the longitudinal, axial or parallel diffusivity. The

eigenvalues $\lambda_2$ and $\lambda_3$ along the small axes represent diffusivity in the perpendicular axis

and are usually averaged together $(\lambda_2 - \lambda_3)/2$ as one average radial diffusivity measure

(152). The degree of anisotropy or orientational preference within a voxel, measured by

fractional anisotropy (FA), is determined by the extent to which the axial eigenvalue $\lambda_1$

dominates $\lambda_2$ and $\lambda_3$. The FA is the most commonly reported DTI measure and varies in

accordance with the type of tissue. The FA in ventricular cerebrospinal fluid with

isotropic diffusion of water molecules is near 0, whereas the FA of the white matter

structure the corpus callosum containing parallel fibres is 0.8 to 0.9 indicating that a

higher density of fibres are oriented along the axis (20). The apparent diffusion

coefficient (ADC) is the average eigenvalue and represents the overall mean-squared

displacements of water molecules, and is independent of anisotropic diffusion. The

ADC quantifies water motility independent of orientation in a voxel and is usually

negatively correlated with FA in white matter (102).

**1.6.2.2 Technical Principles of DTI Acquisition**

In order to measure diffusion by MRI, it is necessary to obtain two images with

different diffusion weighting factors (b) that are used to produce a diffusion coefficient

(D), which corresponds to the diffusion property of a water molecule (88). To obtain

the images, gradient pulses are applied into the main magnetic field (i.e., 3 Tesla MRI

scanner), which changes the strength of the magnetic field. MRI scanners have

magnetic field gradients in the X, Y and Z axes, and when combined with the gradient

pulses, a magnetic field gradient can be produced along any given orientation. For

example, two water molecules along the Y axis resonate at the same frequency in the

main magnetic field. When a gradient pulse is applied along the Y axis, one water

molecule along the Y axis begins to resonate at a lower frequency, thus the two

molecules are out of phase. A second Y gradient pulse 20-50 ms after the first pulse

with the opposite polarity rephases the spins if no net movement between the two water

molecules occurs (88). However, if the water molecules moved between the two

gradient pulses (i.e, diffusion occurs), refocusing does not occur and leads to signal

attenuation. Thus, the magnitude of signal loss depends on the amount of translational

motion or diffusion. The b values, defined above, which are governed by the gradients,

can be changed by altering the strength of the diffusion gradients, the duration of the

gradients and the timing of the gradient pulses, amounting to different amounts of signal

loss (88). The two b values include a nearly zero gradient (b=0) in which a non-

weighted image is obtained, and a second gradient (i.e, 700 s/mm$^2$) which produces a

diffusion-weighted image. As stated above, diffusion leads to an attenuation of the MRI

signal, which depends on the diffusion coefficient D and the gradient pulses (b) used in

the MRI sequence. When a water molecule undergoes anisotropy, diffusion cannot be

characterized by a single value, and as a result, a diffusion tensor is used to account for

the changes (10). Axonal tract orientations realistically occur across numerous axes and

are not restricted to the three X,Y and Z axes of the MRI scanner. Thus, a simplified

mathematical model to account for the different molecular movements along each

direction is fitted to the 3D tensor (72). The properties of the tensor (eigenvectors $\lambda_1$, $\lambda_2$

and $\lambda_3$) and their orientations (eigenvalues $v_1$, $v_2$, and $v_3$), can be defined by a 3x3

matrix, thus applying diffusion gradients in at least six non-collinear directions making it possible to calculate a tensor for each voxel (88).

The tensors are then reconstructed to track the 3-dimensional fibre orientation in the brain (152). The tracking is achieved by the use of algorithms which translate the longest axis of the tensor (v1) into neural trajectories.

The algorithms can be categorized into deterministic and probabilistic, with deterministic being the original and most commonly used method (152). Within the deterministic approach, the fibre assignment by continuous tracking (FACT) algorithm is widely used (86). Diffusion tractography is performed by outlining at least two regions of interest (ROI) in 3D space, and a line is propagated from the seed point with a pixel connection approach (87). The algorithms within this line propagation technique include termination criteria to stop tracking at pixels with low anisotropy such as grey matter (i.e., deviation from the 'cigar'-shaped tensor) or trajectory angles that are too large (87).

Limitations of DTI include deviation from ellipsoid/cigar-shaped anisotropy, noise, and validation. A major assumption is that the large principal eigenvalue is in one fibre orientation. However, cases arise when two large eigenvalues exist creating a pancake shaped ellipsoid rather than cigar shaped (87). A solution to this problem has been the creation of cigar and planar shaped ellipsoids with specific thresholds for termination in areas with cigar or high planar values (87). The second limitation for tractography includes noise and partial voluming within other tissues or fibre types, in which tracking may not reflect real tract pathways. One remedy for this includes the use of knowledge-based multiple region of interest (ROI) approach. For instance, by

constraining the tract reconstruction to two or more ROI's rather than one ROI reduces

the chances of tracking other tracts, some of which may be due to noise or partial

volume effects (87). On the last point concerning validation of DTI, it is a method

which has a resolution of approximately 1-5 mm and reveals bundles of fibre tracts but

cannot discern individual axons with much smaller diameters. The gold standard for

tracking is chemical tracer techniques which can resolve tracts at the cellular level;

however, chemical tracers reveal only a small portion of the actual number of axons

within the white matter bundle. The advantage of DTI is the rapid reconstruction of

large datasets of white matter structures, and validation is possible if tractography is

performed diligently and the results are compared with known anatomical connections

from previous tracing literature (87).

### 1.6.3   Assessment of Autonomic Modulation of Cardiac Function

Heart rate variability (HRV) is a measure of variations in HR and represents a

marker for autonomic control of the heart (111; 124). The measurement of HRV

provides valuable information regarding sympathetic and parasympathetic autonomic

balance, and is an independent predictor of mortality after acute myocardial infarction

(130). The concept of HRV is based on the observation that the cardiac intervals (beat)

of a healthy heart do not exhibit regularity due to the effects of respiratory rate, BP and

thermoregulatory adjustments in blood flow and peripheral vascular resistance on the

sinus node (124). Thus, HRV describes the oscillations of the intervals between

consecutive heart beats (R-R interval) that arise from the aforementioned variables

inherent to the autonomic nervous system (139). Analysis of the rhythms (respiratory

sinus arrhythmia, baroreflex) provides a noninvasive measurement of autonomic control of the heart (124).

Analysis of HRV of a series of R-R intervals can be assessed by spectral analysis in the frequency domain. Spectral analysis of R-R interval variations provides information on frequency-specific oscillations, and provides the amount of overall variability in HR resulting from periodic oscillations in HR at different frequencies (124). In spectral analysis, a Fourier transform decomposes a series of R-R intervals into a sum of sinusoidal functions consisting of different amplitudes and frequencies (138). The resultant power spectrum presents the amplitude of HR fluctuations occurring at different oscillation frequencies (138) (Figure 1.10). Heart rate is usually measured as milliseconds, and the variance referred to as 'power' is measured in milliseconds squared (124). Frequency analysis decomposes HRV into three main oscillatory components: high frequency (0.15 to 0.4 Hz), corresponding to respiratory rate and parasympathetic influence on the heart; low frequency (0.04 to 0.15 Hz), which is suggested to reflect joint activity of parasympathetic and sympathetic influences on the heart but with sympathetic predominance; and very low frequency (<0.04 Hz) (138; 139).
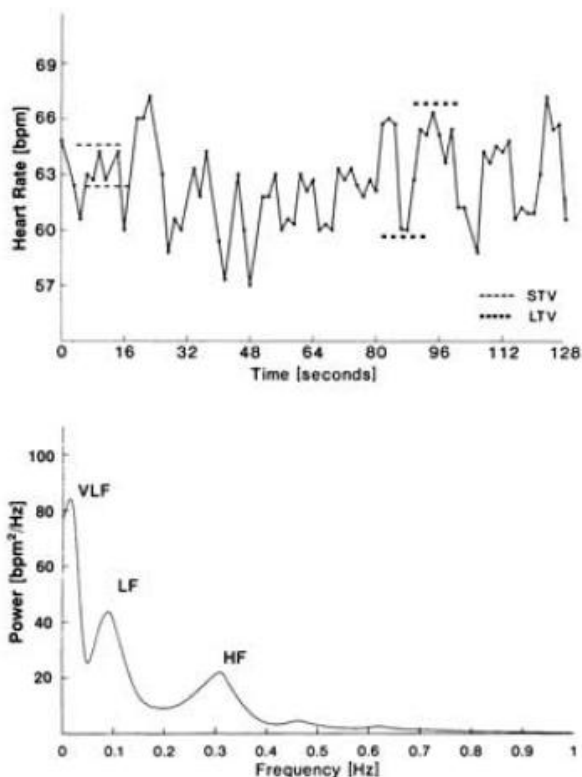
**Figure 1.8 -- The top panel represents a tachogram tracing of the instantaneous heart rate calculated from the R-R interval length. Bottom panel represents the power spectrum of the heart rate trace above and illustrates the three components corresponding to the main fluctuations in heart rate: very low frequency (VLF), low frequency (LF), and high frequency (HF)**

(Source:  Used with permission by van Ravenswaaij-Arts CMA, Kollee LAA, Hopman JCW, Stoelinga GBA and van Geijn HP. Heart rate variability. *Annals of Internal Medicine* 118: 436-447, 1993.

Conventionally, spectral analysis typically requires 5 minutes or more of continuous data (124). However, due to the nature of fMRI designs in which rest and task conditions should ideally be less than one minute due to scanner drift, wavelet analysis of HRV offers a way to compute time-varying variations in R-R interval over much shorter periods.

Wavelet analysis refers to a signal processing technique that uses wavelets to measure time-varying, non-stationary signals (112). A wavelet is a short sample waveform with oscillating amplitude functions of time that is used as a filter to decompose the time series R-R interval into a time-frequency space (135). Wavelet analysis of HRV in this thesis was assessed using the methods outlined by Toledo et al. (2003). Using a continuous wavelet transform of the R-R intervals, a time-frequency decomposition of the signal produces a time-dependent component of the low frequency and high frequency peaks of the oscillations in R-R intervals (134). This method provides information on autonomic control of cardiac activity, as reflected by HRV, over short periods of time, allowing determinations of how such frequency content varies with time.

In an effort to validate the use of the wavelet analysis algorithm used here, and determine its ability to track expected changes in HRV a pilot study was performed comparing supine rest to upright sitting (N=8). As shown in Appendix A, the wavelet analysis was able to track changes in HRV, with anticipated decreases in HRV on going from supine to seated rest due to baroreflex-mediated increases in HR that occur with postural change. Notably, decreases in the high frequency power (HFP) component of HRV occurred on moving from supine to seated rest when HR increased. In two

subjects, HFP increased during seated rest and HR decreased. Thus, the wavelet analysis is a reliable technique to measure autonomic control of the heart.

This approach provided an opportunity to quantify the impact of the study interventions (e.g., handgrip exercise, lower-body negative pressure, and forearm electrical stimulation) on parasympathetic outflow, focusing on the high frequency changes in wavelet spectra.

## 1.7 Summary

The neuroimaging literature has provided substantial evidence of the role of the cerebral cortex in autonomic cardiovascular control. Characterization of CAN regions have utilized tasks that involve perceived sense of effort such as exercise (67; 147), mental stress (28; 43), as well as breath holds and Valsalva manoeuvre (51; 53; 75). While the representation of afferent baroreceptor input has been demonstrated in the insula (19), the representation of somatosensory information is less understood. A small number of fMRI studies have observed activity within the insula and ACC during electrically-stimulated somatosensory activation, in which motor threshold and shocking stimuli were used (5; 48). Tingling electrical stimulation has been observed in the posterior insula; however, autonomic activity was not assessed (32). Sub-motor threshold stimulation has been associated with depressor responses including sympatho-inhibition and hypotension (55; 59; 60; 100), but the effects on cortical autonomic regions has not been established using fMRI. Therefore, the **overall purpose** of this research was to investigate the association between somatosensory stimulation and patterns of activity within the autonomic regions of the brain. This thesis aims to address the **working hypothesis** that somatosensory inputs are represented within the

CAN and that discrete CAN regions will be associated with changes in autonomic function. The following studies were performed to address these questions:

**Study 1** entitled 'Representation of somatosensory inputs within the cortical autonomic network', tested the hypothesis that CAN regions integrate muscle sensory afferents, with differential activation patterns observed between passive and active tasks. It was also hypothesized that regions implicated with parasympathetic activity (i.e, ventral medial prefrontal cortex) will be differentially activated during electrical stimulation and handgrip exercise, and would reflect efferent measures of parasympathetic activity.

**Study 2** entitled 'Anatomical connections between autonomic regions of the brain', aimed to determine whether function is linked to structure. Specifically, it was hypothesized that the functional responses within the CAN regions associated with somatosensory stimulation and isometric handgrip exercise are reflective of structural connections between the regions, providing the anatomical basis for the CAN to act as a functional network.

**Study 3** entitled 'Forebrain organization representing integration of baroreceptor and somatosensory afferents within the cortical autonomic network', aimed to establish the effects of muscle sensory afferents on CAN activation patterns during conditions of baroreceptor unloading. It was hypothesized that muscle sensory afferent stimulation differentially impacts CAN regions involved in sympathetic activity (i.e., insular cortex) during baroreceptor loading (supine rest) and unloading (LBNP), which will be associated with changes in muscle sympathetic nerve activity.

## 1.8     Reference List

1. **Aicher SA, Saravay RH, Cravo S, Jeske I, Morrison SF, Reis DJ and Milner TA**. Monosynaptic projections from the nucleus tractus solitarii to C1 adrenergic neurons in the rostral ventrolateral medulla: comparison with input from the caudal ventrolateral medulla. *The Journal of Comparative Neurology* 373: 62-75, 1996.

2. **Alam M and Smirk FH**. Observations in man upon a blood pressure raising reflex arising from the voluntary muscles. *Journal of Physiology* 89: 372-383, 1937.

3. **An X, Bandler R, Ongur D and Price JL**. Prefrontal cortical projections to longitudinal columns in the midbrain periacqueductal gray in macaque monkeys. *The Journal of Comparative Neurology* 401: 455-479, 1998.

4. **Arezzo JC, Schaumburg HH and Spencer PS**. Structure and function of the somatosensory system: a neurotoxological perspective. *Environemental Health Perspectives* 44: 23-30, 1982.

5. **Arienzo D, Babiloni C, Ferretti A, Caulo M, Del Gratta C, Tartaro A, Rossini PM and Romani GL**. Somatotopy of anterior cingulate cortex (ACC) and supplementary motor area (SMA) for electric stimulation of the median and tibial nerves: An fMRI study. *NeuroImage* 33: 700-705, 2006.

6. **Assaf Y and Pasternak O**. Diffusion tensor imaging (DTI)-based white matter mapping in brain research: A review. *Journal of Moecular Neuroscience* 34: 51-61, 2008.

7. **Augustine JR**. The insular lobe in primates including humans. *Neurological Research* 7: 2-10, 1985.
8. **Augustine JR**. Circuitry and functional aspects of the insular lobe in primates including humans. *Brain Research Brain Research Reviews* 22: 229-244, 1996.

9. **Basser PJ, Pajevic S, Pierpaoli C, Duda J and Aldroubi A**. In vivo fiber tractography using DT-MRI data. *Magnetic Resonance in Medicine* 44: 625-632, 2000.

10. **Basser PJ and Pierpaoli C**. Microstructural and physiological features of tissues elucidated by quantitative-diffusion-tensor MRI. *Journal of Magnetic Resonance* 111: 209-219, 1996.

11. **Benarroch EE**. Functional anatomy of the central autonomic network. In: Central Autonomic Network: Functional Organization and Clinical Correlations,  Armonk, NY: Futura Publishing Company Inc., 1997, p. 29-60.

12. **Bjornsdotter M, Loken L, Olausson H, Vallbo A and Wessberg J**. Somatotopic organization of gentle touch processing in the posterior insular cortex. *The Journal of Neuroscience* 29: 9314-9320, 2009.

13. **Brown GG, Perthen JE, Liu TT and Buxton RB**. A primer on functional magnetic resonance imaging. *Neuropsychology Review* 17: 107-125, 2007.

14. **Burns SM and Wyss JM**. The involvement of the anterior cingulate cortex in blood pressure control. *Brain Research* 340: 71-77, 1985.

15. **Burnstock G**. Mechanisms of interaction of peptide and nonpeptide vascular neurotransmitter systems. *Journal of Cardiovascular Pharmacology* 10 Suppl. 12: S74-S81, 1987.

16. **Bush G, Luu P and Posner MI**. Cognitive and emotional influences in anterior cingulate cortex. *Trends in Cognitive Sciences* 4: 214-222, 2000.

17. **Calvelo MG, Abboud FM, Ballard DR and Abdel-Sayed W**. Reflex vascular responses to stimulation of chemoreceptors with nicotine and cyanide. *Circulation Research* 27: 259-276, 1970.

18. **Cechetto DF and Saper CB**. Role of the cerebral cortex in autonomic function. In: Central Regulation of Autonomic Functions, edited by Loewy AD and Spyer KM. New York: Oxford University Press, 1990, p. 208-223.

19. **Cechetto DF and Shoemaker JK**. Functional neuroanatomy of autonomic regulation. *NeuroImage* 47: 795-803, 2009.

20. **Chanraud S, Zahr N, Sullivan EV and Pfefferbaum A**. MR diffusion tensor imaging: a window into white matter integrity of the working brain. *Neuropsychology Review* 20: 209-225, 2010.

21. **Charkoudian N and Rabbitts JA**. Sympathetic neural mechanisms in human cardiovascular health and disease. *Mayo Clinic Proceedings* 84: 822-830, 2009.

22. **Chen TL, Babiloni C, Ferretti A, Perrucci MG, Romani GL, Rossini PM, Tartaro A and Del Gratta C**. Effects of somatosensory stimulation and attention on human somatosensory cortex : An fMRI study. *NeuroImage* 53: 181-188, 2010.

23. **Cheung RTF and Hachinski V**. The insula and cerebrogenic sudden death. *Neurological Review* 57: 1685-1688, 2000.

24. **Coghill RC, Talbot JD, Evans AC, Meyer E, Gjedde E, Bushell MC and Duncan GH**. Distributed processing of pain and vibration by the human brain. *The Journal of Neuroscience* 14: 4095-4108, 1994.

25. **Coote JH, Hilton SM and Perez-Gonzalez JF**. The reflex nature of the pressor response to muscular exercise. *Journal of Physiology* 215: 789-804, 1971.

26. **Craig AD**. How do you feel - now? The anterior insula and human awareness. *Nature ReviewsNeuroscience* 10: 59-70, 2009.

27. **Critchley HD**. The human cortex responds to an interoceptive challenge. *Proceedings of the National Academy of Sciences* 101: 6333-6334, 2004.

28. **Critchley HD, Corfield DR, Chandler MP, Mathias CJ and Dolan RJ**. Cerebral correlates of autonomic cardiovascular arousal: a functional neuroimaging investigation in humans. *Journal of Physiology* 523: 259-270, 2000.

29. **Critchley HD, Mathias CJ, Josephs O, O'Doherty J, Zanini S, Dewar B, Cipolotti L, Shallice T and Dolan RJ**. Human cingulate cortex and autonomic control: converging neuroimaging and clinical evidence. *Brain* 126: 2139-2152, 2003.

30. **Critchley HD, Wiens S, Rotshein P, Ohman A and Dolan RJ**. Neural systems supporting interoceptive awareness. *Nature Neuroscience* 7: 189-195, 2004.

31. **Dampney RAL, Coleman MJ, Fontes MAP, Hirooka Y, Horiuchi J, Li YW and Polson JW**. Central mechanisms underlying short- and long-term regulation of the cardiovascular system. *Clinical and Experimental Pharmacology and Physiology* 29: 261-268, 2002.

32. **Davis KD, Kwan CL, Crawley AP and Mikulis DJ**. Electrical nerve stimulation can be used as a tool in fMRI studies of pain and tingling-evoked activations. *Pain Research & Management* 5: 81-86, 2000.

33. **Devinsky O, Morrell MJ and Vogt BA**. Contributions of anterior cingulate cortex to behaviour. *Brain* 118: 279-306, 1995.

34. **Di Salle F, Formisano E, Linden DEJ, Goebel R, Bonavita S, Pepino A, Smaltino F and Tedeschi G**. Exploring brain function with magnetic resonance imaging. *European Journal of Radiology* 30: 84-94, 1999.

35. **Donadio V, Kallio M, Karlsson T, Nordin M and Wallin BG**. Inhibition of human muscle sympathetic activity by sensory stimulation. *Journal of Physiology* 544: 285-292, 2002.

36. **Dupont S, Bouilleret V, Hasboun D, Semah F and Baulac M**. Functional anatomy of the insula: new insights from imaging. *Surgical and Radiologic Anatomy* 25: 113-119, 2003.

37. **Eckberg DL and Sleight P**. *Human baroreflexes in health and disease*. Oxford: Clarendon Press, 1992.

38. **Ferretti A, Babiloni C, Arienzo D, Del Gratta C, Rossini PM, Tartaro A and Romani GL**. Cortical brain responses during passive nonpainful median nerve stimulation at low frequencies (0.5-4 Hz): An fMRI study. *Human Brain Mapping* 28: 645-653, 2007.

39. **Fisk GD and Wyss JM**. Pressor and depressor sites are intermingled in the cingulate cortex of the rat. *Brain Research* 754: 204-212, 1997.

40. **Flynn FG, Benson DF and Ardila A**. Anatomy of the insula - functional and clinical correlates. *Aphasiology* 13: 55-78, 1999.

41. **Freyschuss U**. Cardiovascular adjustments of somatomotor activation. *Acta physiologica Scandinavica* 342: 1-63, 1970.

42. **Friedman DP, Murray EA, O'Neill JB and Mishkin M**. Cortical connnections of the somatosensory fields of the lateral sulcus macaque: evidence for a corticolimbic pathway for touch. *The Journal of Comparative Neurology* 252: 323-347, 1986.

43. **Gianaros PJ, Derbyshire SWG, May JC, Siegle GJ, Gamalo MA and Jennings JR**. Anterior cingulate activity correlates with blood pressure during stress. *Psychophysiology* 42: 627-635, 2005.

44. **Gianaros PJ, Jennings JR, Sheu LK, Derbyshire SWG and Mattews KA**. Heightened functional neural activation to psychological stress covaries with exaggerated blood pressure reactivity. *Hypertension* 49: 134-140, 2007.

45. **Gianaros PJ, Van Der Veen FM and Jennings JR**. Regional cerebral blood flow correlates with heart period and high-frequency heart period variability during working-memory tasks: Implications for the cortical and subcortical regulation of cardiac autonomic activity. *Psychophysiology* 41: 521-530, 2004.

46. **Goldstein DS**. Noradrenergic Neurotransmission. In: Primer on the Autonomic Nervous System, edited by Robertson D, Biaggioni I, Burnstock G and Low PA. San Diego: Elsevier Academic Press, 2004, p. 44-49.

47. **Goodwin GM, McCloskey DI and Mitchell JH**. Cardiovascular and respiratory responses to changes in central command during isometric exercise at constant muscle tension. *Journal of Physiology* 226: 173-190, 1972.

48. **Gray M, Rylander K, Harrison NA, Wallin BG and Critchley HD**. Following one's heart: cardiac rhythms gate central initiation of sympathetic reflexes. *The Journal of Neuroscience* 29: 1817-1825, 2009.

49. **Greenfield ADM, Brown E, Goei JS and Plassaras GC**. Circulatory responses to abrupt release of blood accumulated in the legs. *Physiologist* 6: 191, 1963.

50. **Han S, Yang C, Chen X, Naes L, Cox BF and Westfall T**. Direct evidence for the role of neuropeptide Y in sympathetic nerve stimulation-induced vasoconstriction. *American Journal of Physiology - Heart and Circulatory Physiology* 43: H290-H294, 1998.

51. **Harper RM, Gozal D, Bandler R, Spriggs D, Lee J and Alger J**. Regional brain activation in humans during respiratory and blood pressure challenges. *Clinical and Experimental Pharmacology and Physiology* 25: 483-486, 1998.

52. **Henderson LA, Richard CA, Macey PM, Runquist ML, Yu PL, Galons J and Harper RM**. Functional magnetic resonance signal changes in neural structures to baroreceptor reflex activation. *Journal of Applied Physiology* 96: 693-703, 2004.

53. **Henderson LA, Woo MA, Macey PM, Macey KE, Frysinger RC, Alger JR, Yan-Go F and Harper RM**. Neural responses during Valsalva maneuvers in obstructive sleep apnea syndrome. *Journal of Applied Physiology* 94: 1063-1074, 2003.

54. **Hoff EC, Kell JF and Carroll MN**. Effects of cortical stimulation and lesions on cardiovascular function. *Physiological Reviews* 43: 68-114, 1963.

55. **Hollman JE and Morgan BJ**. Effect of transcutaneous electrical nerve stimulation on the pressor response to static handgrip exercise. *Physical Therapy* 77: 28-36, 1997.

56. **Hurley KM, Herbert H, Moga MM and Saper CB**. Efferent projections of the infralimbic cortex of the rat. *The Journal of Comparative Neurology* 308: 249-276, 1991.

57. **Jacobs MC, Goldstein DS, Willemsen JJ, Smits P, Thien T and Lenders JW**. Differential effects of low- and high-intensity lower body negative pressure on noradrenaline and adrenaline kinetics in humans. *Clinical Science* 90: 337-343, 1996.

58. **Jacobsson F, Himmelmann A, Bergbrant A, Svensson A and Mannheimer C**. The effect of transcutaneous electric nerve stimulation in patients with therapy-resistant hypertension. *Journal of Human Hypertension* 14: 795-798, 2000.

59. **Kaada B, Flatheim E and Woie L**. Low-frequency transcutaneous nerve stimulation in mild/moderate hypertension. *Clinical Physiology* 11: 161-168, 1991.

60. **Kaada B, Vik-Mo H, Rosland G, Woie L and Opstad PK**. Transcutaneous nerve stimulation in patients with coronary arterial disease: Haemodynamic and biochemical effects. *European Heart Journal* 11: 447-453, 1990.

61. **Kara T, Narkiewicz K and Somers VK**. Chemoreflexes - physiology and clinical implications. *Acta physiologica Scandinavica* 177: 377-384, 2003.

62. **Kaufman MP and Forster HV**. Reflexes controlling circulatory, ventilatory and airway responses to exercise. In: Handbook of Physiology, Exercise: Regulation and Integration of Multiple Systems, edited by Rowell LB and Shepherd JT.  Bethesda: American Physiological Society, 1996, p. 381-447.

63. **Kaufman MP, Longhurst JC, Rybicki KJ, Wallach JH and Mitchell JH**. Effects of static muscular contraction on impulse activity of groups III and IV afferents in cats. *Journal of Applied Physiology* 55: 105-112, 1983.

64. **Khan MH, Sinoway LI and MacLean D**. Effects of graded LBNP on MSNA and interstitial norepinephrine. *American Journal of Physiology - Heart and Circulatory Physiology* 283: H2038-H2044, 2002.

65. **Kiernan JA**. *Barr's The Human Nervous System: An Anatomical Viewpoint*. Lippincott Williams & Wilkins, 2004.

66. **Kimmerly DS, O'Leary DD, Menon RS, Gati JS and Shoemaker JK**. Cortical regions associated with autonomic cardiovascular regulation during lower body negative pressure in humans. *Journal of Physiology* 569: 331-345, 2005.

67. **King AB, Menon RS, Hachinski VC and Cechetto DF**. Human forebrain activation by visceral stimuli. *The Journal of Comparative Neurology* 413: 572-582, 1999.

68. **Krogh A and Lindhard J**. The regulation of respiration and circulation during the intital stages of muscular work. *Journal of Physiology* 47: 112-136, 1913.

69. **Kurth F, Ickhoff SB, Schleicher A, Hoemke L, Zilles K and Amunts K**. Cytoarchitecture and probabilistic maps of the human posterior insular cortex. *Cerebral Cortex* 20: 1448-1461, 2009.

70. **Lane RD, McRae K, Reiman EM, Chen K, Ahern GL and Thayer JF**. Neural correlates of heart rate variability during emotion. *NeuroImage* 44: 213-222, 2009.

71. **Lanfranchi PA and Somers VK**. Arterial baroreflex function and cardiovascular variability: interactions and implications. *American Journal of Physiology - Regulatory, Integrative and Comparative Physiology* 283: R815-R826, 2002.

72. **Le Bihan D, Mangin J, Poupon C, Clark CA, Pappata S, Molko N and Chabriat H**. Diffusion tensor imaging: concepts and applications. *Journal of Magetic Resonance Imaging* 13: 534-546, 2001.

73. **Li J, Hand GA, Potts JT, Wilson LB and Mitchell JH**. C-Fos expression in the medulla induced by static muscle contraction in cats. *American Journal of Physiology* 272: H48-H56, 1997.

74. **Logothetis LK**. The neural basis of the blood-oxygen-level-dependent functional magnetic resonance imaging signal. *Philosophical Transactions of the Royal Society of London* 357: 1003-1037, 2002.

75. **Macefield VG, Gandevia SC and Henderson LA**. Neural sites involved in the sustained increase in muscle sympathetic nerve activity induced by inspiratory capacity apnea: a fMRI study. *Journal of Applied Physiology* 100: 266-273, 2006.

76. **Maciel BC, Gallo L, Marin Neto JA and Martins LEB**. Autonomic nervous control of the heart rate during isometric exercise in normal man. *European Journal of Physiology* 408: 173-177, 1987.

77. **Mark AL, Victor RG, Nerhed C and Wallin BG**. Microneurographic studies of the mechanisms of sympathetic nerve responses to static exercise in humans. *Circulation Research* 57: 461-469, 1985.

78. **Martin CE, Shaver JA, Leon DF, Thompson ME, Reddy PS and Leonard JJ**. Autonomic mechanisms in the hemodynamic responses to isometric exercise. *Journal of Clinical Investigation* 54: 104-115, 1974.

79. **McCloskey DI, Matthews PBC and Mitchell JH**. Absence of appreciable cardiovascular and respiratory responses to muscle vibration. *Journal of Applied Physiology* 33: 623-626, 1972.

80. **McCloskey DI and Mitchell JH**. Reflex cardiovascular and respiratory responses originating in exercising muscle. *Journal of Physiology* 224: 173-186, 1972.

81. **Mesulam MM and Mufson EJ**. Insula of the old world monkey. III: Efferent cortical output and comments on function. *The Journal of Comparative Neurology* 212: 38-52, 1982.

82. **Mesulam MM and Mufson EJ**. The insula of Reil in man and monkey. Architectonics, connectivity, and function. In: Cerebral cortex, edited by Peters A and Jones EG. New York: Plenum, 1985, p. 179-226.

83. **Mitchell JH, Reeves DR, Rogers HB and Secher NH**. Epidural anaesthesia and cardiovascular responses to static exercise in man. *Journal of Physiology* 417: 13-24, 1989.

84. **Mitchell JH and Schmidt RF**. Cardiovascular reflex control by afferent fibers from skeletal muscle receptors. In: Handbook of Physiology, section 2, The Cardiovascular System, vol.III Peripheral Circulation and Organ Blood Flow, edited by Shepherd JT, Abboud FM and Geiger SR.  Bethesda, MD, USA: American Physiological Society, 1983, p. 623-658.

85. **Mitchell JH and Wildenthal K**. Static (isometric) exercise and the heart: Physiological and clinical considerations. *Annual Reviews in Medicine* 25: 369-381, 1974.

86. **Mori S, Crain BJ, Chacko VP and van Zijl PC**. Three-dimensional tracking of axonal projections in the brain by magnetic resonance imaging. *Annals of Neurology* 45: 265-269, 1999.

87. **Mori S and van Zijl PCM**. Fiber tracking: principles and strategies - a technical review. *NMR in Biomedicine* 15: 468-480, 2002.

88. **Mori S and Zhang J**. Principles of diffusion tensor imaging and its applications to basic neuroscience research. *Neuron* 51: 527-539, 2006.

89. **Napadow V, Dhond R, Conti G, Makris N, Brown EN and Barbieri R**. Brain correlates of autonomic modulation: combining heart rate variability with fMRI. *NeuroImage* 42: 169-177, 2008.

90. **Neafsey EJ**. Prefrontal cortical control of the autonomic nervous system: Anatomical and physiological observations. *Progress in Brain Research* 85: 147-165, 1990.

91. **Neafsey EJ, Terreberry RR, Hurley KM, Ruit KG and Frysztak RJ**. Anterior cingulate cortex in rodents: connections, visceral control functions, and implications of emotion. In: Neurobiology of cingulate cortex and limbic thalamus: a comprehensive handbook, edited by Vogt BA and Gabriel M.  Boston: Birkhauser, 1993, p. 206-223.

92. **Norris DG**. Principles of magnetic resonance assessment of brain function. *Journal of Magetic Resonance Imaging* 23: 794-807, 2006.

93. **Ogawa S, Lee TM, Nayak AS and Glynn P**. Oxygenation-sensitive contrast in magnetic resonance image of rodent brain at high magnetic fields. *Magnetic Resonance in Medicine* 14: 68-78, 1990.

94. **Oppenheimer SM and Cechetto DF**. Cardiac chronotropic organization of the rat insular cortex. *Brain Research* 533: 66-72, 1990.

95. **Oppenheimer SM, Gelb A, Girvin JP and Hachinski VC**. Cardiovascular effects of human insular cortex stimulation. *Neurology* 42: 1727-1732, 1992.

96. **Oppenheimer SM, Kedem G and Martin WM**. Left-insular cortex lesions perturb cardiac autonomic tone in humans. *Clinical Autonomic Research* 6: 131-140, 1996.

97. **Owens NC, Sartor DM and Verberne AJM**. Medial prefrontal cortex depressor response: role of the solitary tract nucleus in the rat. *Neuroscience* 89: 1331-1346, 1999.

98. **Owens NC and Verberne AJ**. An electrophysiological study of the medial prefrontal cortical projection to the nucleus of the solitary tract in rat. *Experimental Brain Research* 110: 55-61, 1996.

99.  **Owens NC and Verberne AJM**. Regional haemodynamic responses to activation of the medial prefrontal cortex depressor region. *Brain Research* 919: 221-231, 2001.

100. **Owens S, Atkinson ER and Lees DE**. Thermographic evidence of reduced sympathetic tone with transcutaneous nerve stimulation. *Anesthesiology* 50: 62-65, 1979.

101. **Paton JF, Deuchars J, Li YW and Kasparov S**. Properties of solitary tract neurones responding to peripheral arterial chemoreceptors. *Neuroscience* 105: 231-248, 2001.

102. **Pfefferbaum A and Sullivan EV**. Increased brain white matter diffusivity in normal adult aging: relationship to anisotropy and partial voluming. *Magnetic Resonance in Medicine* 49: 953-961, 2003.

103. **Pierpaoli C and Basser PJ**. Towards a quantitative assessment of diffusion anisotropy. *Magnetic Resonance in Medicine* 36: 893-906, 1996.

104. **Pierpaoli C, Jezzard P, Basser PJ, Barnett A and Di Chiro G**. Diffusion tensor MR imaging of the human brain. *Radiology* 201: 637-648, 1996.

105. **Price RR, Allison J, Massoth RJ, Clarke GD and Drost DJ**. Practical aspects of functional MRI. *Medical Physics* 29: 1892-1912, 2002.

106. **Raichle ME, MacLeod AM, Snyder AZ, Powers WJ, Gusnard DA and Shulman GL**. A default mode of brain function. *Proceedings of the National Academy of Sciences* 98: 676-682, 2001.

107. **Rea RF and Wallin BG**. Sympathetic nerve activity in arm and leg muscles during lower body negative pressure in humans. *Journal of Applied Physiology* 66: 2778-2781, 1989.

108. **Rolls ET, Inoue K and Browning A**. Activity of primate subgenual cingulate cortex neurons is related to sleep. *Journal of Neurophysiology* 90: 134-142, 2003.

109. **Rowell LB**. *Human Cardiovascular Control*. New York: Oxford University Press, Inc., 1993.

110. **Rowell LB and O'Leary DS**. Reflex control of the circulation during exercise: chemoreflexes and mechanoreflexes. *Journal of Applied Physiology* 69: 407-418, 1990.

111. **Rubin MF, Brunelli SM and Townsend RR**. Variability - the drama of the circulation. *The Journal of Clinical Hypertension* 12: 284-287, 2010.

112. **Samar VJ, Bopardikar A, Rao R and Swartz K**. Wavelet analysis of neuroelectric waveforms: a conceptual tutorial. *Brain and Language* 66: 7-60, 1999.

113. **Sanderson JE, Tomlinson B, Lau MSW, So KWH, Cheung AHK, Critchley JAJH and Woo KS**. The effect of transcutaneous electrical nerve stimulation (TENS) on autonomic cardiovascular reflexes. *Clinical Autonomic Research* 5: 81-84, 1995.

114. **Sato A and Schmidt RF**. Somatosympathetic reflexes: afferent fibers, central pathways, discharge characteristics. *Physiological Reviews* 53: 916-947, 1973.

115. **Schreihofer AM and Guyenet PG**. The baroreflex and beyond: control of sympathetic vasomotor tone by gabaergic neurons in the ventrolateral medulla. *Clinical and Experimental Pharmacology and Physiology* 29: 514-521, 2002.

116. **Seals DR**. Sympathetic neural discharge and vascular resistance during exercise in humans. *Journal of Applied Physiology* 67: 1801-1806, 1989.

117. **Seals DR, Chase PB and Taylor JL**. Autonomic mediation of the pressor responses to isometric exercise in humans. *Journal of Applied Physiology* 64: 2190-2196, 1988.

118. **Sherry JE, Oehrlein KM, Hegge KS and Morgan BJ**. Effect of burst-mode transcutaneous electrical nerve stimulation on peripheral vascular resistance. *Physical Therapy* 81: 1183-1191, 2001.

119. **Shields RW**. Functional anatomy of the autonomic nervous system. *Journal of Clinical Neurophysiology* 10: 2-13, 1993.

120. **Sinoway LI and Li J**. A perspective on the muscle reflex: implications for congestive heart failure. *Journal of Applied Physiology* 99: 5-22, 2005.

121. **Smith SA, Mitchell JH and Garry MG**. The mammalian exercise pressor reflex in health and disease. *Experimental Physiology* 91: 89-102, 2006.

122. **Somers VK, Zavala DC, Mark AL and Abboud FM**. Influence of ventilation and hypocapnia on sympathetic nerve responses to hypoxia in normal humans. *Journal of Applied Physiology* 67: 2095-2100, 1989.

123. **Stauss HM**. Baroreceptor reflex function. *American Journal of Physiology - Regulatory, Integrative and Comparative Physiology* 283: R284-R286, 2002.

124. **Stein PK, Bosner MS, Kleiger RE and Conger BM**. Heart rate variability: a measure of cardiac autonomic tone. *American Heart Journal* 127: 1376-1381, 1994.

125. **Sullivan EV and Pfefferbaum A**. Diffusion tensor imaging and aging. *Neuroscience and Behavioral Reviews* 30: 749-761, 2006.

126. **Sun M-K and Reis DJ**. Medullary vasomotor activity and hypoxic sympathoexcitation in pentobarbital-anesthetized rats. *American Journal of Physiology - Regulatory, Integrative and Comparative Physiology* 270: R348-R355, 1996.

127. **Sundlof G and Wallin BG**. The variability of muscle nerve sympathetic activity in resting recumbent man. *Journal of Physiology* 272: 383-397, 1977.

128. **Sundlof G and Wallin BG**. Effect of lower body negative pressure on human muscle sympathetic nerve activity. *Journal of Physiology* 278: 525-532, 1978.

129. **Swett JE and Bourassa CM**. Electrical stimulation of peripheral nerve. In: Electrical Stimulation Research Techniques, edited by Patterson MM and Kesner RP. New York: Academic Press, 1981, p. 244-284.

130. **Task Force of the European Society of Cardiology**. Heart rate variability: Standards of measurement, physiological interpretation, and clinical use. *Circulation* 93: 1043-1065, 1996.

131. **Taylor JA, Hand GA, Johnson DG and Seals DR**. Sympathoadrenal-circulatory regulation of arterial pressure during orthostatic stress in young and and older men. *American Journal of Physiology - Regulatory, Integrative and Comparative Physiology* 263: R1147-R1155, 2002.

132. **Terreberry RR and Neafsey EJ**. Rat medial frontal cortex: a visceral motor region with a direct projection to the solitary nucleus. *Brain Research* 278: 245-249, 1983.

133. **Thomas GD and Segal SS**. Neural control of muscle blood flow during exercise. *Journal of Applied Physiology* 97: 731-738, 2004.

134. **Toledo E, Gurevitz O, Hod H, Eldar M and Akselrod S**. Wavelet analysis of instantaneous heart rate: a study of autonomic control during thrombolysis. *American Journal of Physiology - Regulatory, Integrative and Comparative Physiology* 284: R1079-R1091, 2003.

135. **Torrence C and Compo GP**. A practical guide to wavelet analysis. *Bulletin of the American Meterological Society* 79: 61-78, 1998.

136. **Vallbo AB, Hagbarth KE, Torebjork HE and Wallin.B.G.** Somatosensory, priorioceptive, and symapthetic activity in human peripheral nerves. *Physiological Reviews* 59: 919-957, 1979.

137. **Vallbo AB, Hagbarth KE and Wallin BG**. Microneurography: how the technique developed and its role in the investigation of the sympathetic nervous system. *Journal of Applied Physiology* 96: 1262-1269, 2004.

138. **van Ravenswaaij-Arts CMA, Kollee LAA, Hopman JCW, Stoelinga GBA and van Geijn HP**. Heart rate variability. *Annals of Internal Medicine* 118: 436-447, 1993.

139. **Vanderlei LCM, Pastre CM, Hoshi RA, de Carvalho TD and de Godoy MC**. Basic notions of heart rate variability and its clinical applicability. *Revista Brasileira De Cirurgia Cardiovascular* 24: 205-217, 2009.

140. **Verberne AJM and Owens NC**. Cortical modulation of the cardiovascular system. *Progress in Neurobiology* 54: 149-168, 1998.

141. **Victor RG and Leimbach WN**. Effects of lower body negative pressure on sympathetic discharge to leg muscles in humans. *Journal of Applied Physiology* 63: 2558-2562, 1987.

142. **Victor RG, Pryor SL, Secher NH and Mitchell JH**. Effects of partial neuromuscular blockade on sympathetic nerve responses to static exercise in humans. *Circulation Research* 65: 468-476, 1989.

143. **Vogt BA, Finch DM and Olson CR**. Functional heterogeneity in cingulate cortex: the anterior executive and posterior evaluative regions. *Cerebral Cortex* 2: 435-443, 1992.

144. **Vogt BA and Pandya DN**. Cingulate cortex of the rhesus monkey: II. Cortical afferents. *The Journal of Comparative Neurology* 262: 271-289, 1987.

145. **Waldrop TG, Rybicki KJ and Kaufman MP**. Chemical activation of group I and II muscle afferents has no cardiorespiratory effects. *Journal of Applied Physiology* 56: 1223-1228, 1984.

146. **Wallin BG and Fagius J**. Peripheral sympathetic neural activity in conscious humans. *Annual Reviews in Physiology* 50: 565-576, 1988.

147. **Williamson JW, McColl R and Mathews D**. Evidence for central command activation of the human insular cortex during exercise. *Journal of Applied Physiology* 94: 1726-1734, 2003.

148. **Williamson JW, McColl R, Mathews D, Ginsburg M and Mitchell JH**. Activation of the insular cortex is affected by the intensity of exercise. *Journal of Applied Physiology* 87: 1213-1219, 1999.

149. **Williamson JW, McColl R, Mathews D, Mitchell JH, Raven PB and Morgan WP**. Brain activation by central command during actual and imagined handgrip under hypnosis. *Journal of Applied Physiology* 92: 1317-1324, 2002.

150. **Willis WD**. The somatosensory system, with emphasis on structures important for pain. *Brain Research Reviews* 55: 297-313, 2007.

151. **Wong SW, Masse N, Kimmerly DS, Menon RS and Shoemaker JK**. Ventral medial prefrontal cortex and cardiovagal control in conscious humans. *NeuroImage* 35: 698-708, 2007.

152. **Yamada K, Sakai K, Akazawa K, Yuen S and Nishimura T**. MR tractography: a review of its clinical applications. *Magnetic Resonance in Medical Sciences* 8: 165-174, 2009.

153. **Yao T, Andersson S and Thoren P**. Long lasting cardiovascular depression induced by acupuncture-like stimulation of the sciatic nerve in unanaesthetized spontaneously hypertensive rats. *Brain Research* 240: 240-277, 1982.

154. **Yuan W, Ming Z, Hai L, Chen-wang J and Shao-hui M**. A functional magnetic resonance imaging study of human brain in pain-related areas induced by electrical stimulation with different intensities. *Neurology India* 58: 922-927, 2010.

155. **Zhang ZH and Oppenheimer SM**. Characterization, distribution and lateralization of baroreceptor-related neurons in the rat insular cortex. *Brain Research* 760: 243-250, 1997.

# Chapter 2 - Representation of somatosensory inputs within the cortical autonomic network[1]

## 2.1    INTRODUCTION

Muscle contractions produce autonomic arousal and cardiovascular adjustments to support blood flow distribution and blood pressure (BP). This autonomic arousal is thought to include ascending sensory signals from muscle as well as descending "drive" signals from primary and supplementary cortical motor areas. In this context, a cortical autonomic network (CAN) has been described in humans based on sympathetic and cardiac responses to physical and cognitive tasks. The insula, ventral medial prefrontal cortex (vMPFC), and anterior cingulate cortex (ACC) form part of the CAN that modulates efferent responses (22; 33; 37; 57; 60). However, the sensory component of the CAN is not known with respect to the peripheral stimuli it processes. For instance, in humans (58; 60), and rodents (45), the insula and vMPFC are implicated in heart rate (HR) control during effortful tasks. However, whether such cortical activation patterns reflect somatosensory signals from activated muscle, cardiac or baroreceptor inputs, cortical-cortical pathways, or efferent visceromotor signals that target changes in cardiovascular function, has not been determined.

It is known that afferent signals arising from muscle affect autonomic cardiovascular control. Of the four muscle sensory nerve types, namely types I, II, III and IV, the type III and IV afferents are functionally involved in cardiovascular arousal during fatiguing contractions (32; 40). The type I and II afferent projections and outcomes have received less attention. While vibration-induced activation of type Ia muscle spindles fail to produce cardiovascular responses (39), sensory level electrical stimulation of type I and II afferent nerves reduced reflex-mediated sympathetic and BP responses (27; 47). This association between the somatosensory and autonomic nervous system prompts the hypothesis that large diameter type I and II afferents are reflected

within the CAN and that such integration is associated with suppression of cardiovascular state.

As stated above, the CAN sites involved in integrating peripheral signals from muscle are not clearly defined.  Activation in the insula has been shown in response to muscle afferent input during postexercise circulatory occlusion (58); however, it is difficult to dissociate this response from concurrent baroreceptor input.  In an anaesthetized animal model, altered cell activity in insular neurons has been reported during ventral root stimulation, independent of BP changes (28).  In humans, activation within the insula and ACC was observed during motor threshold electrical stimulation of peripheral nerves (2; 19).  However, these models will activate multiple sensory and motor neurons that produce nonspecific CAN activation patterns and cardiovascular responses.

Therefore, the purpose of this study was to establish the functional representation of muscle sensory afferents in the CAN and separate these from top-down signals arising during volitional muscle activation.  The left insula has been associated with a bradycardic response, increased parasympathetic activity (46; 61) and integration of afferent information regarding BP changes (10).  The vMPFC is implicated in parasympathetic function, evidenced by deactivation  during handgrip exercise (60) when parasympathetic activity is withdrawn (38), and has extensive anatomical connections with the insula (3; 44).  Therefore, we expect the left insula and vMPFC to represent primary sites associated with somatosensory nerve stimulation.

## 2.2    MATERIALS AND METHODS

### 2.2.1    Participants

Twelve healthy participants (8 females, 4 males; aged $25 \pm 3$ yr; height $167 \pm 7$ cm; weight $65 \pm 12$ kg) volunteered in this study.  All subjects were non-smokers, not taking any medication, and had no prior history of cardiovascular, neurological, or musculoskeletal disorders.  In addition, each participant was deemed to be right-handed according to the Edinburgh Handedness Inventory (43).

Prior to the experimental day, each participant was familiarized with transcutaneous electrical nerve stimulation and the parameters for the stimulus intensities were determined.  All participants provided informed written consent to the experimental procedures that were approved by the Health Sciences Research Ethics Board at *The University of Western Ontario.*

### 2.2.2    Experimental Approach

Overall, our approach was to assess CAN regions of interest while muscle sensory afferents were stimulated electrically at sub-motor and motor levels that do not affect HR.  Cortical responses to these passive trials were compared to volitional trials of mild wrist flexion and strong handgrip exercise.  The two volitional conditions achieve muscle afferent activation as well as top-down signals from the motor cortical regions but only the VOL35% produces a HR response (60).  Sub-motor threshold electrical stimulation (sensory intensity) activates type I and II afferent nerve fibres (27; 48).  Motor threshold stimulation recruits type I, II and III and possibly group IV (30; 48).

### 2.2.2.1  Electrical Stimulation Procedures

The electrical stimulus was delivered as symmetrical biphasic square waves using a portable stimulator (JACE Systems, Cherry Hill, NJ) that was modified for MRI compatibility.  Two self-adhesive electrodes (4cm x 4cm) (StimCare, Empi, St. Paul, MN) were positioned on the right forearm flexors over the muscle belly; this position was identified by palpation during resisted wrist flexion.  Similar stimulation settings were used across all trials with a pulse frequency of 100 Hz and duration of 50 μsec. Two levels of intensity were used with current levels set individually: sub-motor (SUB; mean value $24 \pm 4$ mA) and motor (MOT; mean value $34 \pm 7$ mA).  The sub-motor threshold was determined by increasing the stimulation intensity until a muscle contraction was elicited, and then decreased to a level just below motor threshold.  The MOT stimulation was used to elicit a sustained wrist flexion at approximately 5% of maximal voluntary contraction (MVC).  MOT stimulation was not considered painful for the participants according to subjective perceptions.

### 2.2.2.2 Volitional Procedures

A series of active wrist flexions that mimicked the 5% MVC force induced by MOT stimulation were also performed.  This volitional task (VOL5%) was performed to induce movement that was similar to MOT as well as to include motor cortex activation and descending neural drive.  Importantly, this contraction was sufficiently low in intensity that average HR did not change.  In addition, a moderate intensity isometric handgrip exercise at 35% MVC (VOL35%) was performed to study a stronger volitional task that did increase HR.  Short bouts of moderate intensity handgrip exercise have been shown to elicit a robust increase in HR via parasympathetic nervous

system (PNS) withdrawal as opposed to an increase in sympathetic nerve activity (38) and the HR response is negatively correlated with deactivation in the vMFPC (60).

### 2.2.3   Experimental Paradigm

Participants arrived at the laboratory after having been instructed to fast 3 hr prior to testing and to refrain from caffeine, nicotine, alcohol and physical activity for at least 12 hr.  Cutaneous afferent blockade of the forearm was achieved with EMLA cream (Astra Pharmaceuticals, Wayne, PA) through its application 2 hr prior to the start of the experiment.  The cream was applied to the sites of the forearm beneath the stimulation electrodes and covered with Tegaderm dressings (3M, St. Paul, MN). Sensory blockade was verified over the course of the protocol by stroking the skin upon the start and end of the experiments.  Prior to testing, calibration of the handgrip device was made by asking participants to complete two MVC's.  The higher of two MVC's was calibrated as 100%.

Three trials for each of SUB, MOT, and VOL5% conditions were combined in each of four runs, which were completed in a randomized order.  For VOL5%, participants were able to replicate the force of flexion elicited by MOT stimulation using visual feedback.  Within the run, each trial lasted 30 s and was repeated three times within a single run with 15 s of rest provided between trials.  Each run lasted 7.75 min, producing 36 trials in four runs.  The last 25 s of each trial were analyzed to capture steady state levels, as well as to a) avoid transient activation patterns associated with wrist movement during MOT and VOL5%  and b) account for a short lag time associated with switching the screen display from visual cues to handgrip force.  Visual cues were given prior to the delivery of each stimuli to avoid surprise and to compare

MOT with VOL5%, since volitional tasks involve a preparatory phase within motor areas of the cortex (14). Specifically, the visual cues 'SUBMOTOR', 'MOTOR', and 'VOLITIONAL' were observed on screen at the onset of sub-motor stimulation, motor stimulation and volitional wrist flexion, respectively. For the VOL5% condition, upon seeing the visual cue, the screen was switched to the PowerLab data acquisition screen with a cursor pointed at the line indicating the level of force to which the participants were required to reach by flexing their wrists. As the visual cues were similarly presented during each trial this was not expected to elicit confounding attentional or motor processes between trials. Participants were asked not to actively move their forearm or count during the stimulations to avoid confounding influences of cortical attentional processes.

The VOL35% protocol was tested as a separate block design consisting of an initial baseline recording period of 1 min followed by three 30 s blocks of handgrip exercise each separated by 1 min of rest. Two identical runs of VOL35% were performed with 2 min of rest between each run to ensure stable baseline levels. Participants were instructed to avoid holding their breath or performing a Valsalva manoeuvre during handgrip, which was verified by a stable rate and depth of breathing on the pneumotrace recording (Siemens, Pi-Products, Amberg, Germany). After each run, participants rated their level of perceived exertion on a scale from 6-20 (7).

### 2.2.4   Physiological Recording

Heart rate was acquired from an MRI-compatible pulse oximeter (Nonin Medical Inc., 8600FO MRI, Plymouth, MN) secured over the left middle finger.

Analog signals of the pulse oximeter and handgrip dynamometer were sampled at 1

KHz and stored for analysis (Powerlab, ADInstruments, Colorado Springs, CO).

### 2.2.4.1 Physiological Data Analysis

For the SUB, MOT, VOL5% protocol, beat-by-beat measures of HR were

averaged for 15 s of each rest period and the final 25 s of stimulation and VOL5% trials.

For each individual, an average HR was calculated for each condition in every run,

resulting in an average rest, SUB, MOT, and VOL5% HR value for each of the 4 runs.

These average values from each run were then taken together for an overall average HR

for each condition.  In the VOL35% protocol, beat-by-beat measures of HR were

averaged over 1 min of each rest period and during the 30 s handgrip periods for each

individual in both runs.  An overall average HR for rest and handgrip were calculated

from the combined values of all participants obtained in each run.

The frequency-specific levels of variability in beat-by-beat R-R intervals during

the intervention segments was assessed with a wavelet-based spectral analysis approach

(55).  This heart rate variability (HRV) analysis focused on the respiratory frequency

modulations in R-R interval which varied across individuals but typically were in the

range of 0.15 – 0.3 Hz.

### 2.2.4.2 Physiological Statistical Analysis

The effect of condition on HR and HRV for the SUB, MOT, VOL5% protocol

was assessed using a one-way ANOVA and for VOL35% was assessed using a two-

tailed Student's T-Test.  The HRV data from the VOL35% protocol was normalized to

the natural logarithm (ln) prior to statistical analysis.  The probability level was set at

$p<0.05$.  Data are reported as mean ± standard deviation (S.D.).

### 2.2.5   Neuroimaging Recording

MRI was performed at 3-Tesla (Magnetom TRIO TIM, Siemens Medical Solutions, Erlangen, Germany) with a 32-channel head coil.  A high resolution $T_1$-weighted structural volume was acquired with a 3D MPRAGE sequence at the beginning of the scanning session (sagittal, field of view $256 \times 240$ mm, voxel size $1 \times 1 \times 1$ mm, 1 mm slice thickness, no gap, flip angle 9º, TR = 2300 ms, TE = 2.98 ms). Whole brain blood-oxygenation level-dependent (BOLD) contrast fMRI data were acquired by $T_2^*$-weighted gradient echo planar imaging (EPI) pulse sequence with the following parameters: TE = 30 ms; flip angle = 90º; field of view (FOV) = $240 \times 240$ mm; in-plane voxel resolution = $3 \times 3$ mm.  Forty-five interleaved axial slices (3 mm slice thickness, no gap) were acquired in each volume with a time-to-repetition (TR) of 2500 ms.  For each of the runs in the paradigm involving SUB, MOT and VOL5%, 186 volumes were acquired; 147 volumes were acquired during each of the VOL35% runs. The first two images of each run were automatically discarded to allow for analysis of an equilibrated MRI signal.

### 2.2.5.1 Neuroimaging Data Analysis

Raw fMRI data were analyzed by SPM2 (Wellcome Department of Imaging Neuroscience, London, UK).  The EPI images were spatially realigned and unwarped to correct for head motion using the mean functional image in the time series and normalized to stereotaxic space (Montreal Neurological Institute; MNI).  The functional scans were co-registered with the T1-weighted scan and were smoothed with a 6 mm FWHM Gaussian kernel.  To reduce low frequency noise, a high-pass filter with 128 s cutoff was applied to the dataset.

Two levels of analysis were performed. First, individual design matrices were constructed with the epochs of each trial (consisting of SUB, MOT, VOL5%) modeled by a box-car and convolved with a canonical hemodynamic response function (HRF). Similarly, the handgrip period of the VOL35% trials was modeled with a box-car function convolved with a canonical HRF. The cortical activities of the handgrip tasks were also correlated with the HR response in a third design matrix using a HR regressor. For each participant, an average HR regressor was calculated using 2.5 s bins of HR data from an entire run, and averaged across the two runs. Individual subject regressors were then averaged into one HR regressor that was entered into the analysis. The HR responses to handgrip were consistent between both runs. The General Linear Model was used to create a statistical parametric map on a voxel-by-voxel basis (21). Second, the average contrast images from each individual representing the SUB, MOT, VOL5% trials from protocol 1 and VOL35% from protocol 2 were entered into separate repeated measures ANOVA and T-test models, respectively, as a random effects group analysis. Significant changes in signal intensity were determined for the SUB, MOT, VOL5% protocol, as well as the VOL35% paradigm. The VOL35% analysis using the box-car function was not different from that using the average HR regressor (data not shown). Thus, the reported results are those obtained from the analysis using the HR regressor, similar to our previous report (60).

Subtraction analyses were performed to establish relative differences in regional activation with expected differences in the afferent signals across the protocols. Note, this subtraction analysis was performed only on sites where increased activation was observed in each of the SUB, MOT and VOL5% conditions. These contrasts included

the following: SUB > MOT and MOT > SUB (masked inclusively with SUB and MOT), MOT > VOL5% and VOL5% > MOT (masked inclusively with MOT and VOL5%), and SUB > VOL5% and VOL5% > SUB (masked inclusively with SUB and VOL5%).

BOLD responses compared to rest were corrected for multiple comparisons [false discovery rate (FDR), $p<0.05$] and in some cases a more lenient threshold of $p<0.001$, uncorrected, was used. As subtraction analyses include a stricter statistical threshold, a probability level of $p<0.005$ (uncorrected for multiple comparisons) was used in these contrasts. A minimum cluster size of 10 voxels was used.

### 2.2.6 Region of Interest Analysis

A region-of-interest identification was performed that was based on previous data relating cortical and sub-cortical structures with sensory stimuli and isometric handgrip exercise. Specifically, in human fMRI studies, the insula was found to process somatosensory information during non-painful and painful electrical stimulation (2) and gentle tactile brushing (6). Somatotopic sensory organization has also been found in the ACC during nerve stimulations (2). Furthermore, the amygdala, insula and pons were involved in the autonomic responses to surprising electrical stimuli depending upon cardiac cycle timing (24). Moderate intensity isometric handgrip exercise increases activation in the bilateral insula (58; 60), and decreases activity of the vMFPC and posterior cingulate cortex (PCC) (60). Therefore, the insula, medial prefrontal cortex and ACC formed the *a priori* foci of analysis.

## 2.3    RESULTS

### 2.3.1    Physiological Responses

Compared to rest (61 ± 8 bpm), HR did not change with SUB (60 ± 9 bpm), MOT (61 ± 8 bpm), or VOL5% (60 ± 8 bpm).  Compared with baseline (61 ± 7 bpm), VOL35% increased HR to 67 ± 9 bpm ($p<0.001$) with a Borg scale rating of 12 ± 3, corresponding to moderate intensity effort (7).

The beat-to-beat variations in HR in one participant are illustrated in Figure 2.1 during VOL35% (Figure 2.1A) and SUB (Figure 2.1B); these data reflect reduced HR variations during VOL35% and increased fluctuations during SUB.  Using a wavelet analysis, the total power representing the high frequency component of HRV (normalized units), was decreased from 4.21 ± 1.09 ms$^2$ during rest to 3.93 ± 1.05 ms$^2$ during VOL35% ($p<0.005$) (Figure 2.1C).  High frequency power during rest was 29.42 ± 18.87 ms$^2$ and was 39.85 ± 27.60 ms$^2$ (non-normalized units) during SUB in a wavelet analysis of beat-by-beat R-R intervals (Effect size = 0.43; Power = 0.57; $p=0.06$) (Figure 2.1D).
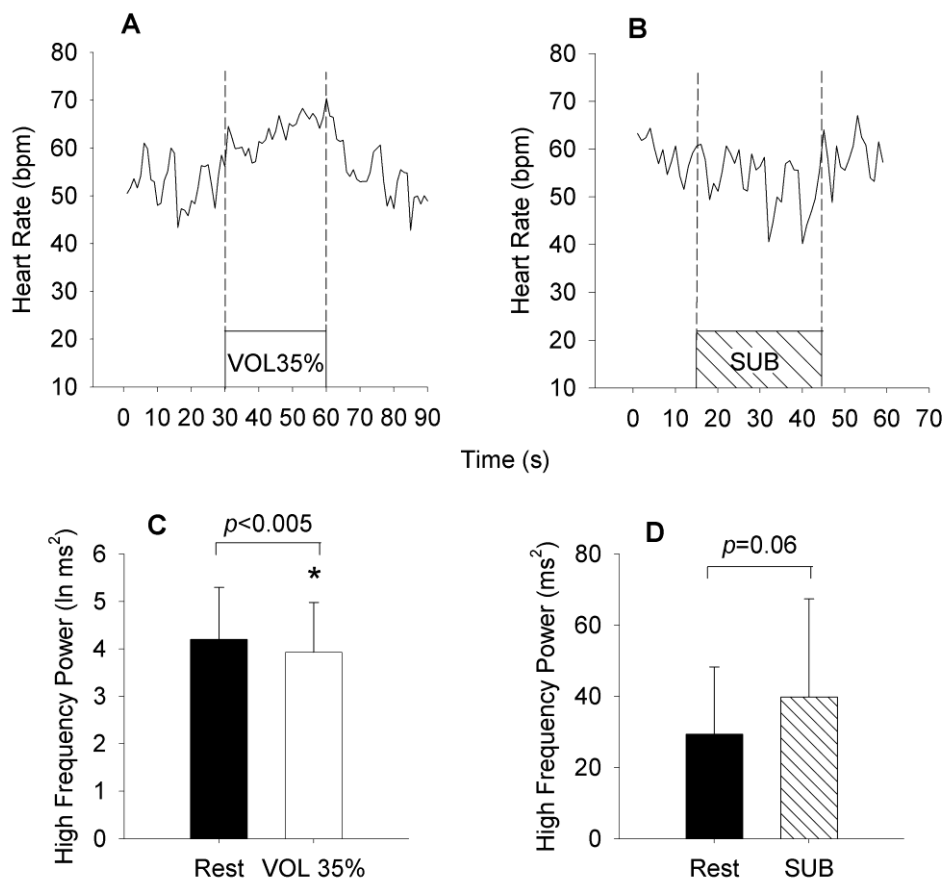
**Figure 2.1-- Panels A and B illustrate the time courses of beat-by-beat heart rate fluctuations during handgrip exercise (VOL35%) modified with 30 s of rest, and sub-motor stimulation (SUB) from a representative individual. Panels C and D represent the group changes in high frequency power observed during VOL35% and SUB.**

**2.3.2    Functional MRI responses**

**2.3.2.1 Global Responses**

In the overall global response, SUB was associated with activation in the vMPFC, bilateral posterior insula, subgenual ACC, mid-cingulate cortex (MCC), and PCC (Table 2.1, Figures 2.2, 2.3).  Additionally, sensori-motor areas were involved including the right supplementary motor area (SMA; T-value 4.35), the bilateral primary motor cortices (M1; T-value 2.37 on left, 2.75 on right), and the bilateral primary somatosensory cortices (S1; T-value 2.38 on left, 3.76 on right) ($p<0.05$, corrected).  The MNI $x,y,z$ co-ordinates for S1 activation were -42, -24, 64 and 46, -20, 52 on the left and right side, respectively, corresponding with the arm area of the somatosensory cortex homunculus.

In response to MOT, increased neural activity was observed in the left posterior insula and MCC (Table 2.2, Figures 2.2, 2.3) ($p<0.05$, corrected).  Other regions displaying increased activity during MOT were the left putamen (T-value 3.82), left SMA (T-value 3.51), and left S1 (T-value 3.42), as well as the left M1 (T-value 3.26) and left thalamus (T-value 4.18) ($p<0.05$, corrected).

During VOL5%, brain regions displaying increased activity included the right anterior and posterior insula (Table 2.3, Figure 2.2), the bilateral putamen (T-value 4.15 on left, 4.53 on right), the left SMA (T-value 3.77), right S1 (T-value 4.15) the bilateral M1 (T-value 3.37 on left, 3.71 on right), the bilateral thalamus (T-value 3.74 on left, 2.83 on right), the bilateral cerebellum (T-value 5.29 on left, 3.77 on right), and the bilateral precuneus (T-value 4.80 on left, 4.42 on right) ($p<0.05$, corrected).

In response to handgrip exercise (VOL35%), the bilateral insula increased activity (Table 2.5, Figure 2.2), as well as the bilateral thalamus (T-value 4.33 on left, 4.36 on right), SMA (T-value 4.33 on left, 4.36 on right), S1 (T-value 5.12 on left, 6.19 on right), M1 (T-value 4.71 on left, 3.62 on right), and cerebellum (T-value 6.18 on left, 7.08 on right).  Regions demonstrating decreased neural activity during VOL35% were the vMPFC, bilateral PCC, right dorsal ACC, and bilateral subgenual ACC (Table 2.5, Figure 2.3).  Additional regions included the bilateral superior temporal pole (T-score 6.01 on left, 5.96 on right) and angular gyrus (T-score 7.05 on left, 5.56 on right) ($p<0.05$, corrected).

### 2.3.2.2  CAN Regional Responses

In the group analysis, the SUB protocol elicited increased activity in the posterior regions of the bilateral insula (Table 2.1, Figure 2.2).  SUB also increased activity in the vMPFC, the left subgenual ACC, the right MCC as well as the left PCC ($p<0.05$, corrected) (Table 2.1, Figure 2.3).  The time course of vMPFC activation is shown in Figure 2.4.  Decreased activity during SUB was observed in the bilateral anterior insula ($p<0.05$, corrected) (Table 2.1, Figure 2.2).

Brain regions that increased neural activity during the electrically-induced wrist flexion (MOT) included the left posterior insula and left MCC ($p<0.05$, corrected) (Table 2.2, Figures 2.2, 2.3).  Decreased neural activity during MOT occurred in the right dorsal ACC ($p<0.001$, uncorrected) (Table 2.2, Figure 2.3).

In response to VOL5%, increased signal intensity was observed in the anterior-posterior portions of the right insula ($p<0.05$, corrected) (Table 2.3, Figure 2.2).  Also,

decreased activity was observed in the right subgenual ACC and bilateral dorsal ACC ($p<0.001$, uncorrected) (Table 2.3, Figure 2.3).

The VOL35% protocol was associated with activity within the bilateral insula (Table 2.4, Figure 2.2; $p<0.05$, corrected).  Similar to our previous report (60), deactivation was observed in the vMPFC with a time course that correlated negatively with HR changes ($p<0.05$, corrected) (Table 2.4, Figure 2.4).  Decreased activity was also observed in the left PCC, right dorsal ACC and bilateral subgenual ACC (Table 2.4, Figure 2.3; $p<0.05$, corrected).

**2.3.2.3 Contrasting BOLD responses between SUB, MOT, and VOL5%**

Comparisons of activated regions between the SUB, MOT and VOL5% conditions are shown in Table 2.5.  In subtraction analyses for SUB > MOT, greater activation was observed in the left subgenual ACC and right MCC.  The contrast MOT > SUB showed activation in left posterior insula and left MCC.  Compared with VOL5%, MOT displayed greater activation in the left posterior insula.  In contrast, VOL5% displayed greater activation in the right anterior insula compared with MOT. With VOL5% > SUB, greater activity was seen in the right posterior and anterior insula. Lastly, the SUB > VOL5% contrast was associated with bilateral posterior insula and subgenual ACC ($p<0.005$, uncorrected).

**Table 2.1 -- Brain region responses during sub-motor stimulation versus rest**

| Region | Side | x | y | z | T-score |
|--------|------|-----|-----|-----|---------|
| *A.* Increased activation during SUB stimulation | | | | | |
| vMPFC | | 0 | 48 | -8 | 3.27 |
| Insula (posterior) | L | -38 | -18 | 14 | 3.53 |
| | R | 40 | -16 | 10 | 3.38 |
| Subgenual ACC | L | -6 | 34 | -8 | 4.93 |
| MCC | R | 10 | -8 | 40 | 3.87 |
| PCC | L | -2 | -52 | 28 | 3.92 |
| | | | | | |
| *B.* Decreased activation during SUB stimulation | | | | | |
| Insula (anterior) | L | -34 | 18 | 6 | 3.66 |
| | R | 34 | 24 | 4 | 4.06 |

*p*<0.05, FDR corrected

SUB, sub-motor stimulation; vMPFC, ventral medial prefrontal cortex; ACC, anterior cingulate cortex; MCC, middle cingulate cortex; PCC, posterior cingulate cortex; L, left; R, right; MNI co-ordinates (*x, y, z*).
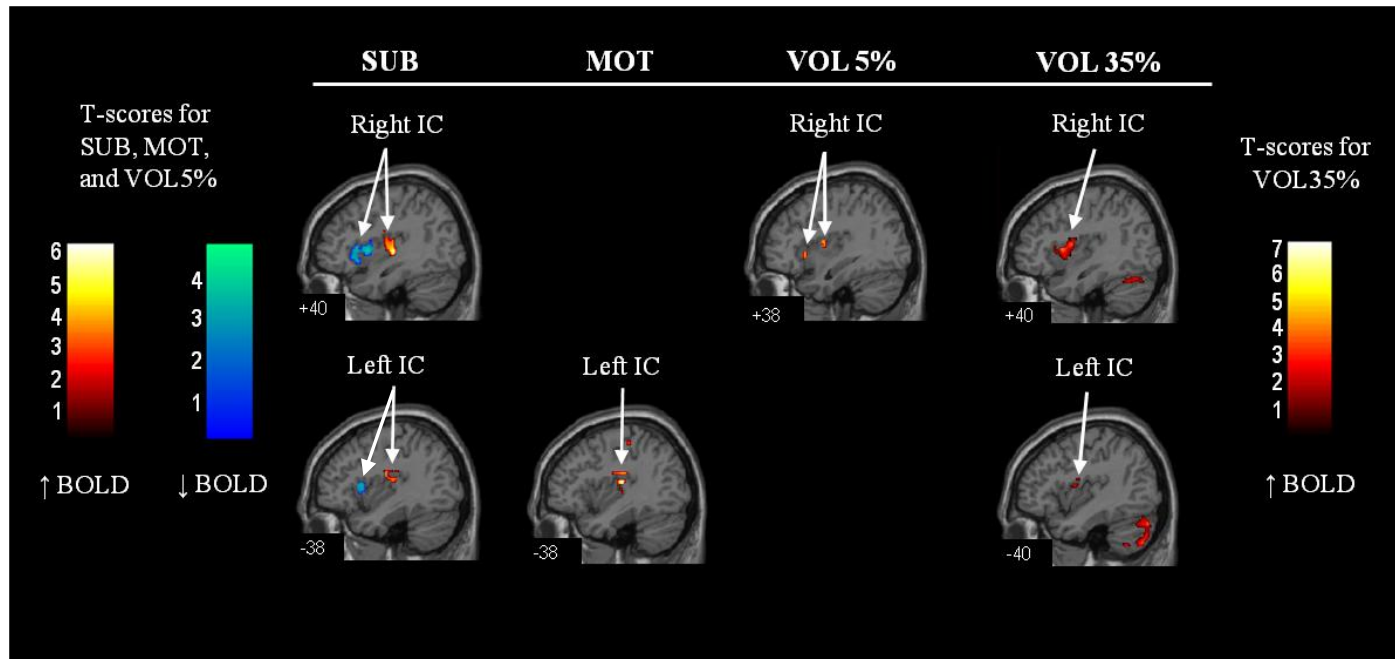
**Figure 2.2 -- BOLD responses in the insula during sub-motor threshold stimulation (SUB), motor threshold stimulation (MOT), 5% MVC volitional wrist flexion (VOL5%), and 35% MVC volitional handgrip exercise (VOL35%) versus rest. IC, insular cortex.**
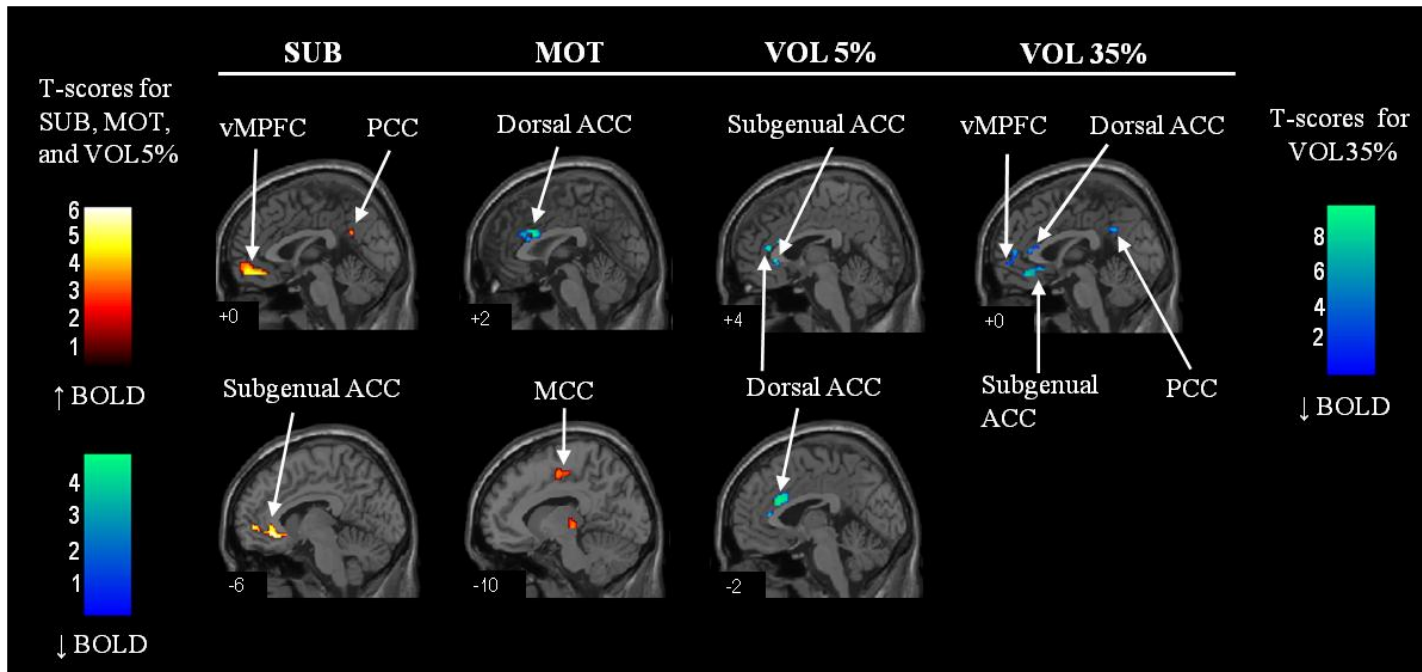
**Figure 2.3 -- BOLD responses in the cingulate cortex and ventral medial prefrontal cortex (vMPFC) during sub-motor threshold stimulation (SUB), motor threshold stimulation (MOT), 5% MVC volitional wrist flexion (VOL5%), and 35% MVC volitional handgrip exercise (VOL35%) versus rest.**
**vMPFC, ventral medial prefrontal cortex; ACC, anterior cingulate cortex; PCC, posterior cingulate cortex; MCC, middle cingulate cortex.**
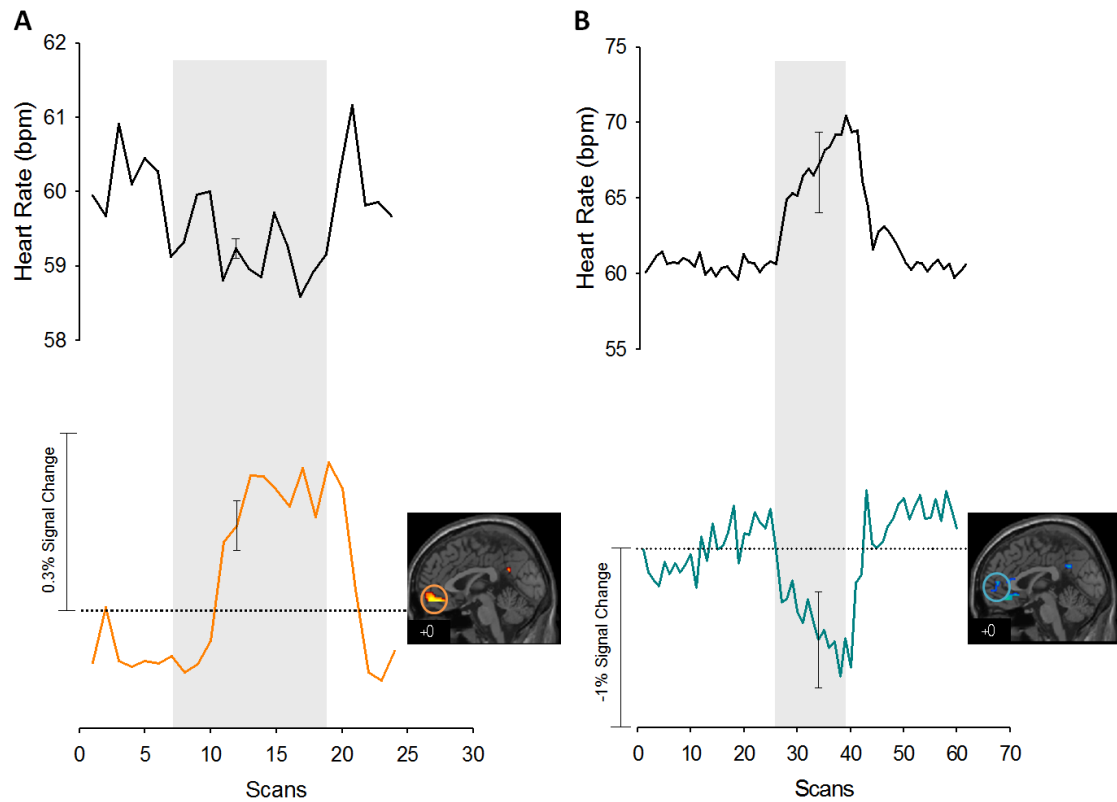
**Figure 2.4 -- Panel A (top) shows the averaged time course of the HR response during SUB. Below is the BOLD response of activity in the vMPFC during SUB. Shaded area indicates 30 s of sub-motor stimulation. Panel B (top) shows the averaged time course of the HR response during VOL35%. Below is the BOLD response of deactivation in the vMPFC during VOL35%. Shaded area indicates 30 s of handgrip exercise period. The standard error bars are shown in the middle of the VOL35% and SUB.**

**Table 2.2 -- Brain region responses during motor stimulation versus rest**

| Region | Side | x | y | z | T-score |
|--------|------|-----|-----|-----|---------|
| *A.* Increased activation during MOT stimulation | | | | | |
| Insula (posterior) | L | -38 | -18 | 14 | 6.59 |
| MCC | L | -10 | -8 | 50 | 3.84 |
| | | | | | |
| *B.* Decreased activation during MOT stimulation | | | | | |
| Dorsal ACC | R | 2 | 18 | 24 | 5.41 |

Increased activation: $p<0.05$, FDR corrected. Decreased activation: $p<0.001$, uncorrected.

MOT, motor stimulation; MCC, middle cingulate cortex; ACC, anterior cingulate cortex; L, left; R, right; MNI co-ordinates (*x, y, z*).

**Table 2.3 -- Brain region responses during 5% MVC volitional wrist flexion versus rest**

| | Region | Side | Co-ordinates | | | T-score |
|---|---|---|---|---|---|---|
| | | | *x* | *y* | *z* | |
| *A.* | Increased activation during VOL5% | | | | | |
| | Insula (posterior) | R | 38 | -2 | 10 | 3.34 |
| | (anterior) | R | 32 | -10 | 4 | 3.58 |
| *B.* | Decreased activation during VOL5% | | | | | |
| | Subgenual ACC | R | 2 | 28 | -2 | 4.27 |
| | Dorsal ACC | L | -2 | 34 | 10 | 3.63 |
| | | R | 4 | 38 | 12 | 3.83 |

Increased activation: $p<0.05$, FDR corrected. Decreased activation: $p<0.001$, uncorrected.

VOL5%, volitional wrist flexion; ACC, anterior cingulate cortex; L, left; R, right; MNI co-ordinates (*x, y, z*).

**Table 2.4 -- Brain region responses during 35% MVC volitional handgrip exercise**

| | Region | Side | Co-ordinates | | | T-score |
|---|---|---|---|---|---|---|
| | | | $x$ | $y$ | $z$ | |
| *A.* | Increased activation during VOL35% | | | | | |
| | Insula | L | -40 | 0 | 12 | 4.46 |
| | | R | 40 | 2 | 12 | 6.31 |
| *B.* | Decreased activation during VOL35% | | | | | |
| | vMPFC | | 0 | 50 | -2 | 5.25 |
| | PCC | L | -6 | -42 | 32 | 6.29 |
| | | R | 6 | -46 | 32 | 7.14 |
| | Dorsal ACC | R | 2 | 32 | 8 | 9.49 |
| | Subgenual ACC | L | -4 | 34 | -10 | 9.26 |
| | | R | 2 | 22 | -6 | 7.77 |

$p<0.05$, FDR corrected.
VOL35%, volitional handgrip exercise; vMPFC, ventral medial prefrontal cortex; PCC, posterior cingulate cortex; ACC, anterior cingulate cortex, L, left; R, right; MNI co-ordinates (*x, y, z*).

**Table 2.5 -- Brain regions active during subtraction contrasts of sub-motor stimulation, motor stimulation, and 5% MVC volitional wrist flexion**

| Region | Side | Co-ordinates | | | T-score |
|---|---|---|---|---|---|
| | | $x$ | $y$ | $z$ | |
| *A.* Increased activity during SUB > MOT | | | | | |
| Subgenual ACC | L | -6 | 34 | -6 | 3.81 |
| MCC | R | 10 | -8 | 40 | 4.28 |
| *B.* Increased activity during MOT > SUB | | | | | |
| Insula (posterior) | L | -36 | 0 | 16 | 3.54 |
| MCC | L | -8 | -8 | 50 | 3.57 |
| *C.* Increased activity during MOT > VOL5% | | | | | |
| Insula (posterior) | L | -38 | -18 | 14 | 5.91 |
| *D.* Increased activity during VOL5% > MOT | | | | | |
| Insula (anterior) | R | 32 | 18 | 4 | 3.80 |
| *E.* Increased activity during SUB > VOL5% | | | | | |
| Insula (posterior) | L | -38 | -20 | 14 | 3.90 |
| | R | 42 | -10 | 6 | 3.69 |
| Subgenual ACC | L | -6 | 34 | 0 | 3.44 |
| *F.* Increased activity during VOL5% > SUB | | | | | |
| Insula (posterior) | R | -38 | 0 | 6 | 3.04 |
| Insula (anterior) | R | 32 | 18 | 4 | 4.16 |

$p<0.005$, uncorrected

SUB, sub-motor stimulation; MOT, motor stimulation; VOL5%, volitional wrist flexion; ACC, anterior cingulate cortex; MCC, middle cingulate cortex; L, left; R, right; MNI co-ordinates (*x, y, z*).

**2.3.2.4 Signal Change in Left Posterior Insula and vMPFC**

The group average effect size (%Δ) of the BOLD signal in the left posterior insula was 0.41 ± 0.12% (effect size ± S.E.) during SUB, 1.43 ± 0.19% during MOT was and 0.90 ± 0.20% during VOL35% (Figure 2.5). For the vMPFC group analysis, activation was observed during SUB (effect size: 1.03 ± 0.31%), and deactivation was observed during VOL35% (effect size: -0.86 ± -0.25%) (Figure 2.5).
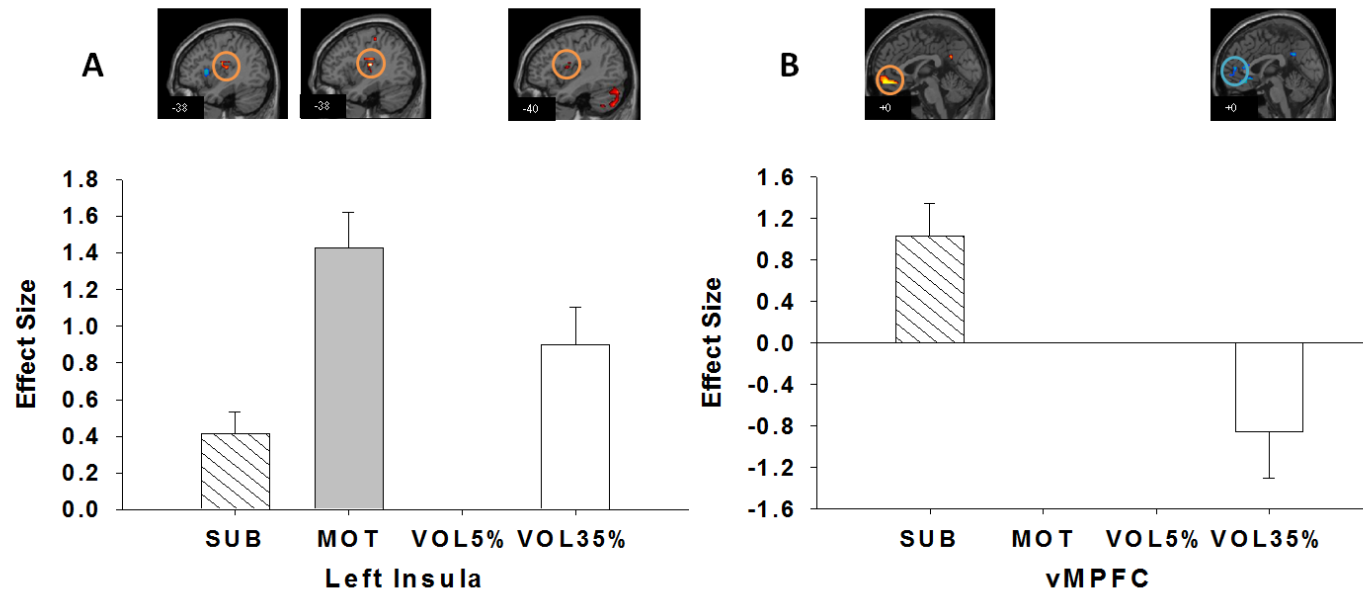
**Figure 2.5 -- Panel A shows the effect sizes (percent signal change ± S.E.) in the left insula during SUB, MOT, VOL5% and VOL35%. Panel B shows effect sizes in the vMPFC during SUB, MOT, VOL5% and VOL35% .**

## 2.4     DISCUSSION

The major new finding of the current study was the representation of muscle sensory pathways within the CAN, particularly the insula, vMPFC and cingulate cortex. In line with the hypothesis, left posterior insula activity was increased in graded fashion from SUB to MOT suggesting a somatosensory role of this region for Type I and II afferent stimulation.  Activity in the vMPFC and subgenual ACC was increased during SUB and this occurred with a tendency towards elevated HRV.  In contrast, vMPFC activity and HRV were reduced, and HR increased during VOL35%.  Further, differences between electrically-stimulated and centrally-driven tasks were noted in insular and cingulate sub-regions and these were distributed along anterior-posterior and ventral-dorsal axes.  The results suggest that Type I and II afferents from muscle are functionally represented in the CAN but that their functional impact is modulated by other signals during effortful contractions.

In the current study, the cortical patterns observed were not related to superficial cutaneous afferents as these were anesthetized.  However, a major assumption of the current study is that CAN patterns during SUB and MOT were isolated to muscle afferents and avoided concurrent sensory patterns from cardiac or baroreflex afferents. Changes in sensory information from cardiac afferents are minimized in this study because average HR was unchanged in the protocols.  Further, data obtained in a previous pilot study indicated that BP (Finometer) is unchanged during SUB, MOT and VOL5% protocols.  These stable hemodynamics replicate observations during stimulation of the peroneal and tibial nerves (29; 51) and suggest that the current model emphasized representation of muscle sensory afferent projections within the CAN.

### 2.4.1   Insular Cortex

The insula is involved in a wide range of stimuli but determination of its motor

versus sensory roles has been difficult in conscious humans within the context of

muscle afferents and CAN studies.  Previously, fatiguing handgrip exercise was used to

characterize the cortical regions associated with Type III and IV muscle afferents where

insular activation was observed (58).  However, this pattern was confounded by the

concomitant increase in arterial pressure and possible involvement of baroreceptor input

to CAN regions (58).  In the current study, SUB was associated with activity in the

bilateral posterior insulae, whereas MOT was associated with activation in the left

posterior insula only.  As outlined above, activation of the insula during SUB and MOT

does not appear to represent afferent signals reflecting changes in HR or BP as these

were not changed during SUB or MOT.  Thus, these findings are in line with previous

reports demonstrating that the insula plays a significant role in somatosensory

processing (2; 19) with involvement of this region in somatosensory mapping of the

body (1; 42).  The specificity of posterior insula activation for somatosensory function

is consistent with recent efforts to understand the cytoarchitectonic subdivisions of this

region which has been labelled as anterior, mid and posterior insula (11; 16; 35).  In

addition, the posterior insula may play a multimodal sensory role (11).  The current

findings support this architectural description, and the higher effect size of the left

posterior insula in MOT compared to SUB, supports increased somatosensory input

during MOT.  Furthermore, the current findings indicate that Type I and II pathways

project to the posterior insula and, from here, may extend to integrate motor and

cardiovascular control.  The absence of left posterior insula activation during both

volitional tasks suggests conjecture that reciprocal projections from the primary and supplementary motor regions inhibit excitatory muscle sensory signals in the insula. This speculation is supported by anatomical evidence that the posterior insula receives afferent projections from the SMA and sends efferent pathways to the basal ganglia (20; 35) and that the anterior insula is an interface between the posterior insular cortex and motor cortex (52).

In contrast to activation within the posterior insula, SUB resulted in concurrent deactivation in the bilateral anterior insula. The purpose of this pattern is not known, but may be related to the potential role of this region in a sense of urgency and awareness (11; 18) or subjective emotional experience (13). This interpretation is consistent with the concurrent observation of increased vMPFC activation during SUB (see below) and the role of this frontal region in a vegetative and unfocused state of awareness; that is, inhibition of an area of awareness (insula) with concurrent activation of a region involved enhanced vegetative state (vMPFC). This interpretation is also consistent with increased activation of the anterior insula during VOL5% which required focused attention and effort.

### 2.4.2   Cingulate Cortex and vMPFC

The ACC carries out executive functions that extend to visceromotor, skeletomotor and endocrine systems (8) and has been shown to be involved with somatosensory processing of electrical stimulation (2; 19). The ACC can be further differentiated into functionally specific sub-regions. In the present study, SUB was associated with activity in the left subgenual ACC and right MCC, whereas MOT showed activity in the left MCC compared to rest and to SUB. Mid-cingulate cortex

activity was previously observed during painful and non-painful stimulations of the median and tibial nerves at motor threshold (2). The current findings support the involvement of the MCC in sensori-motor control (12; 36).

Importantly for the current study, the subgenual region of the rostral ACC has been implicated with PNS activity (12) with projections to the parasympathetic nucleus of the solitary tract (54). Close by, the vMPFC exhibits reciprocal projections to limbic structures including the amygdala, hypothalamus, and autonomic nuclei in the brainstem (4; 44). Functionally, activity in the vMFPC and subgenual ACC is reduced during attention-demanding, goal-oriented tasks (25; 49) and particularly tasks associated with cardioacceleration (10; 22; 60). Thus, the vMPFC has been linked with PNS rather than sympathetic outflow (12; 60), at least for mild to moderate intensity stress.

However, the new finding of this study was *increased* activation of the vMPFC and subgenual ACC during sensory (non-volitional) levels of electrical stimulation. Such elevations in vMPFC activation are important because, as outlined above, this structure is associated with PNS elevation and implicated as the 'default brain network' (25) that is active in resting humans (49).

Given that reductions in vMPFC activation are associated with reduced PNS and elevated HR, it is conceivable that increased vMPFC activation would be associated with elevated PNS outflow to the heart. Direct measures of PNS activity are difficult in humans, but indirect measures of HRV provide some insight. Analysis of the respiratory frequency-specific oscillations described a statistical trend towards enhanced HRV with SUB. This observation is consistent with an enhanced parasympathetic or

cardiovagal state. Previously, acupuncture enhanced the high frequency component of HR variations (26). Also, sub-motor threshold electrical stimulation attenuated the sympathetic and systolic BP response to fatiguing handgrip exercise, an effect that was attributed to the gating of signals from Type III and IV afferent fibres by Type I and II afferents (27). Electrical nerve stimulation has also been shown to decrease BP and sympathetic tone in healthy and hypertensive individuals (31; 47). Of note, SUB displayed greater activation of the subgenual ACC compared to MOT and VOL. Thus, the interesting hypothesis from these observations is that stimulation of Type I and II sensory afferents may exert a depressor effect on autonomic outflow that is modulated cortically in the vMPFC and/or subgenual ACC.

The current study employed sub-motor electrical stimulation of a small region of forearm muscle and observed important activation patterns with the insula and vMPFC. Whether this pattern is scaled to the number of muscle sensory afferents engaged is not known. Neither is it known if this pattern is applicable or consistent across other sensory inputs to the CAN. It is known that the trigeminocardiac reflex and stimulation of the nasal passage produces bradycardia (5; 41). These earlier observations, and the current results, support a hypothesis that the sensory inputs to the brain that produce reflex bradycardia, involve the modulatory effects of the vMPFC.

### 2.4.3    Methodological Considerations of the Study

Concurrent cortical activation patterns during handgrip or sensory afferent stimulation raise the possibility that they are part of an interconnected network involved in autonomic processing; however, such connections have yet to be established in humans. Nonetheless, a growing body of experimental evidence supports this

hypothesis. In particular, reciprocal connections between the prefrontal cortex and insula have been demonstrated in primates (3; 9). New developments in diffusion tensor imaging and high-field imaging may aid in identifying the pathways involved with somatosensory afferents and how, or why, they affect the vMPFC.

Second, inter-individual variability, including sex differences, exists in terms of efferent autonomic responses and neural patterns of activity during various tasks (34, 53, 59). In the current study, individuals had varying magnitudes of change in HR and HRV during electrical stimulation and handgrip exercise, and not all participants displayed similar neural activity across conditions. This was observed in previous literature in which not all the participants displayed activity in the insula and ACC during various thresholds of electrical stimulation, perhaps due to differences in stimuli processing (2; 15).

While the results agree with previous research relating MPFC associations with vagal function and HRV (23), the role of the vMPFC is likely to be more complex. For example, the vMPFC has many reciprocal connections with sub-cortical and brainstem regions involved in sympathetic activation (57). This region has also been experimentally linked to functional reductions and increases in sympathetic activation in a manner that depends upon anesthetization status and disease (50).

Lastly, as a region that integrates viscerosensory information with autonomic cardiovascular control suggests important implications for the MPFC. For instance, autonomic consequences of chemical stimulation of the MPFC are altered with hypertension (50). Also, the study of age and disease-related changes in the vMPFC is

warranted given evidence that aging and stroke are associated with decreased HRV (17; 56).

### 2.4.4 Conclusions

Cortical patterns that mediate autonomic responses to muscle activation may be associated with ascending input from muscle receptors and/or descending signals from supplementary and primary motor regions. While spino-medullary pathways of muscle afferents have been demonstrated, our results show muscle somatosensory organization within CAN regions such as the insula, vMPFC and ACC. Insular activation appeared to be associated with somatosensory processing. Specifically, posterior insular activation was explained by a sensory input while the anterior insula was involved in the volitional tasks, consistent with its known role in somatosensory and emotive processing during muscular contractions. Sensory level stimulation without movement was associated with robust activation in the vMPFC and subgenual ACC, as well as enhanced HRV, suggesting a role of these regions in heightened PNS activity.

## 2.5 Reference List

1. **Allen GV, Saper CB, Hurley KM and Cechetto DF**. Organization of visceral and limbic connections in the insular cortex of the rat. *The Journal of Comparative Neurology* 311: 1-16, 1991.

2. **Arienzo D, Babiloni C, Ferretti A, Caulo M, Del Gratta C, Tartaro A, Rossini PM and Romani GL**. Somatotopy of anterior cingulate cortex (ACC) and supplementary motor area (SMA) for electric stimulation of the median and tibial nerves: An fMRI study. *NeuroImage* 33: 700-705, 2006.

3. **Augustine JR**. Circuitry and functional aspects of the insular lobe in primates including humans. *Brain Research Brain Research Reviews* 22: 229-244, 1996.

4. **Barbas H**. Anatomic basis of cognitive-emotional interactions in the primate prefrontal cortex. *Neuroscience & Biobehavioral Reviews* 19: 499-510, 1995.

5. **Barnard NA and Bainton R**. Bradycardia and the trigeminal nerve. *Journal of Cranio-Maxillofacial Surgery* 18: 359-360, 1990.

6. **Bjornsdotter M, Loken L, Olausson H, Vallbo A and Wessberg J**. Somatotopic organization of gentle touch processing in the posterior insular cortex. *The Journal of Neuroscience* 29: 9314-9320, 2009.

7. **Borg GA**. Psychophysical bases of perceived exertion. *Medicine and Science in Sports and Medicine* 14: 377-381, 1982.

8. **Bush G, Luu P and Posner MI**. Cognitive and emotional influences in anterior cingulate cortex. *Trends in Cognitive Sciences* 4: 214-222, 2000.

9. **Cavada C, Company TTJ, Cruz-Rizzolo RJ and Reinoso-Suarez F**. The anatomical connections of the macaque monkey orbitofrontal cortex. *Cerebral Cortex* 10: 220-242, 2000.

10. **Cechetto DF and Shoemaker JK**. Functional neuroanatomy of autonomic regulation. *NeuroImage* 47: 795-803, 2009.

11. **Craig AD**. How do you feel - now? The anterior insula and human awareness. *Nature ReviewsNeuroscience* 10: 59-70, 2009.

12. **Critchley HD**. The human cortex responds to an interoceptive challenge. *Proceedings of the National Academy of Sciences* 101: 6333-6334, 2004.

13. **Critchley HD, Wiens S, Rotshein P, Ohman A and Dolan RJ**. Neural systems supporting interoceptive awareness. *Nature Neuroscience* 7: 189-195, 2004.

14. **Cunnington R, Windischberger C, Deecke L and Moser E**. The preparation and readiness for voluntary movement: a high-field event-related fMRI study of the Bereitschafts-BOLD response. *NeuroImage* 20: 404-412, 2003.

15. **Davis KD, Kwan CL, Crawley AP and Mikulis DJ**. Electrical nerve stimulation can be used as a tool in fMRI studies of pain and tingling-evoked activations. *Pain Research & Management* 5: 81-86, 2000.

16. **Dupont S, Bouilleret V, Hasboun D, Semah F and Baulac M**. Functional anatomy of the insula: new insights from imaging. *Surgical and Radiologic Anatomy* 25: 113-119, 2003.

17. **Dutsch M, Burger M, Dorfler C, Schwab S and Hilz MJ**. Cardiovascular autonomic function in poststroke patients. *Neurology* 69: 2249-2255, 2007.

18. **Farrer C and Frith CD**. Experiencing oneself vs another person as being the cause of an action: The neural correlates of the experience of agency. *NeuroImage* 15: 596-603, 2002.

19. **Ferretti A, Babiloni C, Arienzo D, Del Gratta C, Rossini PM, Tartaro A and Romani GL**. Cortical brain responses during passive nonpainful median nerve stimulation at low frequencies (0.5-4 Hz): An fMRI study. *Human Brain Mapping* 28: 645-653, 2007.

20. **Flynn FG, Benson DF and Ardila A**. Anatomy of the insula - functional and clinical correlates. *Aphasiology* 13: 55-78, 1999.

21. **Friston KJ, Holmes AP, Worsley KJ, Poline JP, Frith CD and Frackowiak RSJ**. Statistical parametric maps in functional imaging: a general linear approach. *Human Brain Mapping* 2: 189-210, 2005.

22. **Gianaros PJ, Derbyshire SWG, May JC, Siegle GJ, Gamalo MA and Jennings JR**. Anterior cingulate activity correlates with blood pressure during stress. *Psychophysiology* 42: 627-635, 2005.

23. **Gianaros PJ, Van Der Veen FM and Jennings JR**. Regional cerebral blood flow correlates with heart period and high-frequency heart period variability during working-memory tasks: Implications for the cortical and subcortical regulation of cardiac autonomic activity. *Psychophysiology* 41: 521-530, 2004.

24. **Gray M, Rylander K, Harrison NA, Wallin BG and Critchley HD**. Following one's heart: cardiac rhythms gate central initiation of sympathetic reflexes. *The Journal of Neuroscience* 29: 1817-1825, 2009.

25. **Gusnard DA and Raichle ME**. Searching for a baseline: functional imaging and the resting human brain. *Nature Reviews Neuroscience* 2: 685-694, 2001.

26. **Haker E, Egekvist H and Bjerring P**. Effect of sensory stimulation (acupuncture) on sympathetic and parasympathetic activities in healthy subjects. *Journal of the Autonomic Nervous System* 79: 52-59, 2000.

27. **Hollman JE and Morgan BJ**. Effect of transcutaneous electrical nerve stimulation on the pressor response to static handgrip exercise. *Physical Therapy* 77: 28-36, 1997.

28. **Ichiyama RM, Waldrop TG and Iwamoto GA**. Neurons in and near insular cortex are responsive to muscular contraction and have sympathetic and/or cardiac-related discharge. *Brain Research* 1008: 273-277, 2004.

29. **Indergand HJ and Morgan BJ**. Effects of high-frequency transcutaneous electrical nerve stimulation on limb blood flow in healthy humans. *Physical Therapy* 74: 361-367, 1994.

30. **Johnson MJ, Lortie G, Simoneau JA and Boulay MR**. Glycogen depletion of human skeletal muscle fibers in response to high-frequency electrical stimulation. *Canadian Journal of Applied Physiology* 28: 424-433, 2003.

31. **Kaada B, Flatheim E and Woie L**. Low-frequency transcutaneous nerve stimulation in mild/moderate hypertension. *Clinical Physiology* 11: 161-168, 1991.

32. **Kaufman MP, Longhurst JC, Rybicki KJ, Wallach JH and Mitchell JH**. Effects of static muscular contraction on impulse activity of groups III and IV afferents in cats. *Journal of Applied Physiology* 55: 105-112, 1983.

33. **Kimmerly DS, O'Leary DD, Menon RS, Gati JS and Shoemaker JK**. Cortical regions associated with autonomic cardiovascular regulation during lower body negative pressure in humans. *Journal of Physiology* 569: 331-345, 2005.

34. **Kimmerly DS, Wong SW, Menon RS and Shoemaker JK**. Forebrain neural patterns associated with sex differences in autonomic and cardiovascular function during baroreceptor unloading. *American Journal of Physiology - Regulatory, Integrative and Comparative Physiology* 292: R715-R722, 2006.

35. **Kurth F, Eickhoff SB, Schleicher A, Hoemke L, Zilles K and Amunts K**. Cytoarchitecture and probabilistic maps of the human posterior insular cortex. *Cerebral Cortex* 20: 1448-1461, 2010.

36. **Lowell SY, Knorr CJ, Chung BR, Reynolds RC, Simonyan K and Ludlow CL**. Sensory stimulation activates both motor and sensory components of the swallowing system. *NeuroImage* 42: 285-295, 2008.

37. **Macefield VG, Gandevia SC and Henderson LA**. Neural sites involved in the sustained increase in muscle sympathetic nerve activity induced by inspiratory capacity apnea: a fMRI study. *Journal of Applied Physiology* 100: 266-273, 2006.

38. **Mark AL, Victor RG, Nerhed C and Wallin BG**. Microneurographic studies of the mechanisms of sympathetic nerve responses to static exercise in humans. *Circulation Research* 57: 461-469, 1985.

39. **McCloskey DI, Matthews PBC and Mitchell JH**. Absence of appreciable cardiovascular and respiratory responses to muscle vibration. *Journal of Applied Physiology* 33: 623-626, 1972.

40. **McCloskey DI and Mitchell JH**. Reflex cardiovascular and respiratory responses originating in exercising muscle. *Journal of Physiology* 224: 173-186, 1972.

41. **McCulloch PF and Panneton WM**. Fos immunohistochemical determination of brainstem neuronal activation in the muskrat after nasal stimulation. *Neuroscience* 78: 913-925, 1997.

42. **Mesulam M and Mufson EJ**. Insula of the old world monkey. I: Architectonics in the insulo-orbito-temporal component of the paralimbic brain. *The Journal of Comparative Neurology* 212: 1-22, 1982.

43. **Oldfield RC**. The assessment and analysis of handedness: the Edinburgh inventory. *Neuropsychologia* 9: 97-113, 1971.

44. **Ongur D and Price JL**. The organization of networks within the orbital and medial prefrontal cortex of rats, monkeys and humans. *Cerebral Cortex* 10: 206-219, 2000.

45. **Oppenheimer SM and Cechetto DF**. Cardiac chronotropic organization of the rat insular cortex. *Brain Research* 533: 66-72, 1990.

46. **Oppenheimer SM, Gelb A, Girvin JP and Hachinski VC**. Cardiovascular effects of human insular cortex stimulation. *Neurology* 42: 1727-1732, 1992.

47. **Owens S, Atkinson ER and Lees DE**. Thermographic evidence of reduced sympathetic tone with transcutaneous nerve stimulation. *Anesthesiology* 50: 62-65, 1979.

48. **Radhakrishnan R and Sluka KA**. Deep tissue afferents, but not cutaneous afferents, mediate transcutaneous electrical nerve stimulation-induced antihyperalgesia. *The Journal of Pain* 6: 673-680, 2005.

49. **Raichle ME, MacLeod AM, Snyder AZ, Powers WJ, Gusnard DA and Shulman GL**. A default mode of brain function. *Proceedings of the National Academy of Sciences* 98: 676-682, 2001.

50. **Resstel LBM and Correa FMA**. Involvement of the medial prefrontal cortex in central cardiovascular modulation of the rat. *Autonomic Neuroscience: Basic and Clinical* 126-127: 130-138, 2006.

51. **Sherry JE, Oehrlein KM, Hegge KS and Morgan BJ**. Effect of burst-mode transcutaneous electrical nerve stimulation on peripheral vascular resistance. *Physical Therapy* 81: 1183-1191, 2001.

52. **Shi CJ and Cassell MD**. Cortical, thalamic, and amygdaloid connections of the anterior and posterior insular cortices. *The Journal of Physiology* 399: 440-468, 1998.

53. **Shoemaker JK, Hogeman C, Khan M, Kimmerly DS and Sinoway LI**. Gender affects sympathetic and hemodynamic response to postural stress. *American Journal of Physiology - Heart and Circulatory Physiology* 281: H2028-H2035, 2001.

54. **Terreberry RR and Neafsey EJ**. Rat medial frontal cortex: a visceral motor region with a direct projection to the solitary nucleus. *Brain Research* 278: 245-249, 1983.

55. **Toledo E, Gurevitz O, Hod H, Eldar M and Akselrod S**. Wavelet analysis of instantaneous heart rate: a study of autonomic control during thrombolysis. *American Journal of Physiology - Regulatory, Integrative and Comparative Physiology* 284: R1079-R1091, 2003.

56. **Umetani K, Singer DH, McCraty R and Atkinson M**. Twenty-four hour time domain heart rate variability and heart rate: relations to age and gender over nine decades. *Journal of the American College of Cardiology* 31: 593-601, 1998.

57. **Verberne AJM and Owens NC**. Cortical modulation of the cardiovascular system. *Progress in Neurobiology* 54: 149-168, 1998.

58. **Williamson JW, McColl R and Mathews D**. Evidence for central command activation of the human insular cortex during exercise. *Journal of Applied Physiology* 94: 1726-1734, 2003.

59. **Wong SW, Kimmerly DS, Masse N, Menon RS, Cechetto DF and Shoemaker JK**. Sex differences in forebrain and cardiovagal responses at the onset of isometric handgrip exercise: a retrospective fMRI study. *Journal of Applied Physiology* 103: 1402-1411, 2007.

60. **Wong SW, Masse N, Kimmerly DS, Menon RS and Shoemaker JK**. Ventral medial prefrontal cortex and cardiovagal control in conscious humans. *NeuroImage* 35: 698-708, 2007.

61. **Zhang ZH, Dougherty PM and Oppenheimer SM**. Characterization of baroreceptor-related neurons in the monkey insular cortex. *Brain Research* 796: 303-306, 1998.

**Chapter 3 Anatomical connections between regions of the human cortical autonomic network**

## 3.1    INTRODUCTION

A cortical autonomic network (CAN) comprising the insular cortex, ventral medial prefrontal cortex (vMPFC), and anterior cingulate cortex (ACC) has been established in previous rodent studies (11; 40; 53). Functional magnetic resonance imaging (fMRI) studies in humans have also found these CAN regions to be commonly activated during physiological and behavioural tasks that affect autonomic function (15; 16; 23; 29; 57). The common recruitment of these regions during autonomic challenges raises the possibility that these regions form a network, or perhaps an integrated group of subnetworks. In turn, the definition of 'network' implies physical connections for information exchange. In non-human primates, the insula, ACC, and MFPC are reciprocally linked to one another with distinct connectional features (35; 43). Further the anterior insula contains reciprocal projections with the ventral ACC, including Brodmann areas 24a and 24b (4; 19; 35). In contrast, the mid and posterior insula has connections with area 24c of the dorsal cingulate and area 23 of the posterior cingulate cortex (PCC) (35). Reciprocal connections also exist between the prefrontal cortex and insula (3; 20). However, the structural connectivity in the context of the autonomic network in humans has not been elucidated. Cortical stimulation during human surgery is a powerful model for directly determining regions involved in specific functions. For instance, intra-operative insular stimulation has demonstrated a role for the insula in heart rate (HR) control (44). However, this procedure provides information on single site responses and does not give insight into the anatomy of the region. In addition, cortical damage models involving the ACC (16; 18) and insula (45) show evidence of diminished autonomic cardiovascular responses, demonstrating the importance of

distinct regions without providing information of how the regions function as a network. Functional connectivity studies correlating low-frequency fluctuations of BOLD signals have suggested connectivity between the insula and ACC as a resting-state network (50), as well as in a salience network, in which the anterior insula and ACC segregate internal and extrapersonal stimuli to guide behaviour (48). However, functional connectivity describes spatiotemporal correlations between discrete brain regions (22), but does not demonstrate axonal linkages between the regions.

Diffusion tensor imaging (DTI) is a recent technique used to exploit the white matter fibre tract connections between brain sites. This approach is based on the diffusion direction of water molecules, providing connectivity maps of the neural networks (5; 13; 38). In a recent DTI study, functional patterns of activity during sensory stimulation were associated with tract connections between the insula and ACC (37). However, DTI has not been used to study the anatomical connections between the regions associated with autonomic function.

Our previous fMRI studies involving isometric handgrip exercise, a simple manoeuvre that elicits rapid reduction in parasympathetic activity, and muscle sensory afferent stimulation, to acutely increase parasympathetic activity, were associated with differential activity in subdivisions of the insula, as well as in the vMPFC, subgenual ACC and PCC (25; 57). In addition, studies examining the forebrain architecture associated with baroreflex modulations suggest a reproducible pattern of cortical activation with the CAN regions (29). The involvement of similar CAN regions during a volitional task, during passive electrically-stimulated activation of muscle afferents, and during alterations in baroreceptor sensory information, each with correlated

cardiovascular responses, prompts the need to assess the anatomical relationships between functionally complementary pathways within the CAN.

Based on our studies involving handgrip exercise and stimulation of muscle sensory afferents and their associations with the anterior and posterior insula, as well as the vMPFC, subgenual ACC and PCC, we aimed to establish whether these regions form a network facilitating inter-regional communication to support autonomic function. To this end, DTI was used to test the hypothesis that the anterior and posterior insular projections with the subgenual ACC, vMPFC and PCC constitute a structural network for autonomic regulation and sensory processing.

## 3.2 METHODS

### 3.2.1 Participants

Twelve healthy participants (8 females, 4 males; mean age ± SD: 25 ± 3 yr) with no history of cardiovascular, neurological, or musculoskeletal disorders volunteered for this study. All participants were right-handed determined using the Edinburgh handedness inventory (42). All participants provided informed written consent to experimental procedures that were approved by the Health Sciences Research Ethics Board at *The University of Western Ontario*.

### 3.2.2 Data Acquisition

A Siemens 3T TIM Trio MRI scanner with a 32-channel head coil was used to acquire both T1-weighted anatomical and diffusion weighed images. A high resolution $T_1$-weighted structural volume was acquired with a 3-dimensional magnetization-prepared rapidly acquired gradient echo (MPRAGE) pulse sequence (sagittal orientation, field of view $256 \times 240$ mm, voxel size $1 \times 1 \times 1$ mm, no gap, flip angle 9º,

TR = 2300 ms, TE= 2.98 ms).  The diffusion data were obtained using a twice

refocused diffusion weighted echo planar imaging (EPI) acquisition (TR = 6000 ms, TE

= 75 ms, field of view = 200 x 200 mm).  The b-values used were 0 s/mm$^2$ and 700

s/mm$^2$, and diffusion gradients were applied across 64 spatial directions (27).  Fifty-six

axial slices were acquired with a slice thickness of 2 mm and no gap.

### 3.2.3   DTI Image Processing and Analysis

Analyses of the MRI-DTI data were performed using Brain Voyager QX v 2.1

(Brain Innovation, Maastricht, Netherlands).  After the diffusion tensor reconstruction,

fractional anisotropy (FA) and mean diffusivity (MD) values in each voxel were

calculated.  The data were aligned into AC-PC orientation and the whole brain FA, MD

maps and MPRAGE were normalised to standard Talairach space using sinc

interpolation (R=3).  Regions of interest (anterior insula, posterior insula, vMPFC,

subgenual ACC, PCC, thalamus; Figure 3.1) were placed manually based on anatomical

atlas labelling on a single subjects' MPRAGE image which was in Talairach space.

Three-dimensional tract reconstruction was done based on the Fiber Assignment

by Continuous Tracking (FACT) algorithm and a brute-force reconstruction approach.

The continuous tracking method used the following termination criteria: FA value of 0.2

and angle threshold of 50 degrees.  All analysis was performed by the same individual

(RG) and biased analysis of the tractography was avoided by the use of standardized

seed regions that were placed on normalized brain spaces (Talairach), by presenting

individual results, and by stringent determination of connectivity based on visualization

of a bundle rather than few, individual fibres.

## 3.3    RESULTS

Due to low signal-to-noise ratio in one of the participants' diffusion data,

analysis is based on 11 individuals.  Figure 3.2 illustrates representative data for the

inter-connections observed between the regions of interest.  Common connections were

observed between the anterior insula and subgenual ACC (7/11 subjects on left side;

9/11 on right side), as well as between the posterior insula and PCC (10/11 on left side;

8/11 on right side).  As well, other insular tract projections considered were with the

thalamus, which were present in 9 individuals (8/11 on the left side; 9/11 on right side),

as well as to the S1/S2 region with mostly left-sided dominance (10/11 on left; 3/11 on

right).  In 5 participants, fibre tracts in the cingulate gyrus were seen between the

subgenual ACC and PCC, whereas 4 subjects displayed such connections between the

vMPFC and PCC.  Less commonly, connections were observed between the vMPFC

and anterior insula (2/11 on left side; 1/11 on right side).  FA was highest in the right

posterior insula and lowest in the vMPFC (Table 3.1).
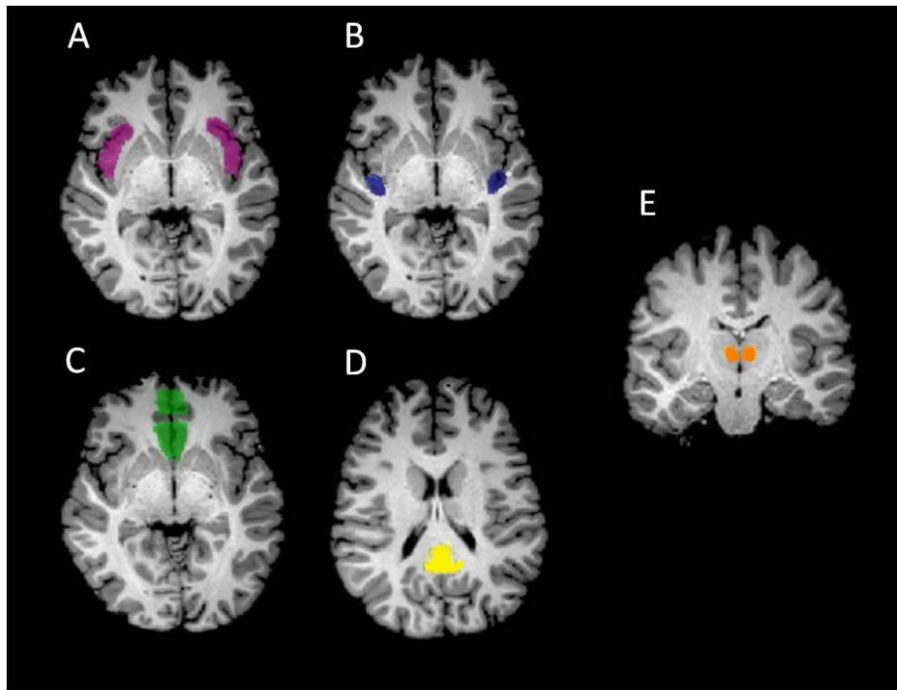
**Figure 3.1 -- Regions of interest upon which tracking of white matter fibres was performed. A: anterior insula; B: posterior insula; C: ventral medial prefrontal cortex and subgenual anterior cingulate cortex; D: posterior cingulate cortex; E: thalamus.**
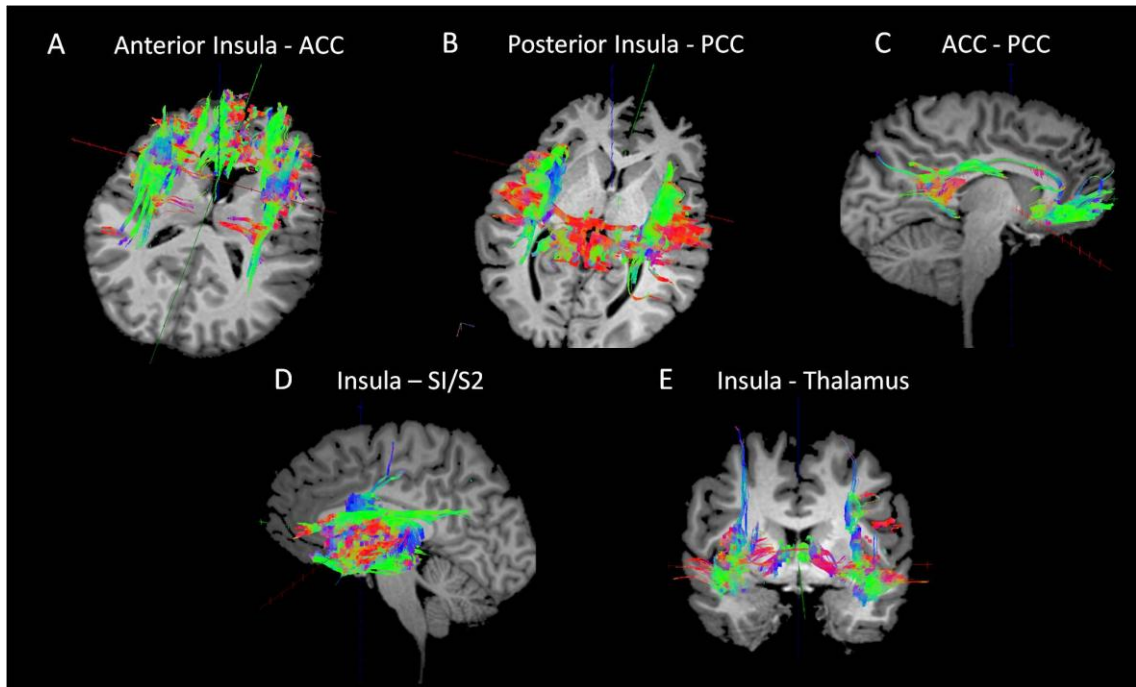
**Figure 3.2 -- Representative data of connections observed between** A: **anterior insula and the anterior cingulate cortex (ACC);** B: **posterior insula and the posterior cingulate cortex (PCC);** C: **anterior cingulate cortex (ACC) and the posterior cingulate cortex (PCC);** D: **insula and the somatosensory cortex (S1/S2);** E: **insula and the thalamus. Red fibres indicate left-right, blue fibres indicate inferior-superior, green fibres indicate anterior-posterior.**

**Table 3.1 -- Fractional anisotropy values for each region.**

| Region | Fractional Anisotropy |
|---|---|
| Left anterior insula | 0.2930 |
| Right anterior insula | 0.2701 |
| Left posterior insula | 0.2956 |
| Right posterior insula | 0.3318 |
| Posterior cingulate cortex | 0.2445 |
| Subgenual anterior cingulate cortex | 0.3021 |
| Ventral medial prefrontal cortex | 0.1841 |
| Thalamus | 0.2492 |

*Fractional anisotropy's for above regions represent average values for gray matter areas (0.2-0.3).*

**3.4     DISCUSSION**

These data provide structural evidence supporting previously observed

functional relationships between the CAN regions associated with the modulation of

autonomic function and somatosensory afferent processing.  This study focused on the

insular connections given the multifaceted functions and location of this region within

the cortex to receive and direct input to various cortical and subcortical sites.  In this

analysis, cortical projections fell into clusters defined by those that were associated with

a) the anterior insula, b) the posterior insula, and c) the midline anterior-posterior axis

along the cingulate cortex.  Specifically, connections were observed between a) the

anterior insula and subgenual ACC, b) the posterior insula and PCC, and c) the

subgenual ACC and PCC were observed.  In addition to these three patterns, we also

found structural linkages between the insula and S1/S2 as well as the insula with

thalamus.  These findings support the hypothesis that these regions are linked in a

manner that lends credence to their function as a network during various stimuli that

elicit an autonomic response.  Further, these anatomical linkages provide the anatomical

basis for specificity of roles associated with the subdivisions of the insula.

**3.4.1   Anterior Insula Projections**

We observed connections between the anterior insula and the subgenual ACC.

These observations support known insular connections with the medial network in the

rodent forebrain (43).  It is postulated that the von Economo neurons, which are

contained within both the anterior insula and ACC, form the basis for the connections

between these two regions (14).  The current observations also provide the structural

substrate for resting-state connectivity based on correlated low-frequency oscillations in

the blood-oxygenation level dependent (BOLD) signal (50).  Furthermore, using DTI

methods, structural connections in humans have been observed between functionally

linked regions of the resting-state network including the insula and ACC (52).  The

current observations also provide the structural basis for earlier observations implicating

a sensory pathway between the anterior insula and the subgenual ACC (25).  These

results are consistent with observations in visceral sensory processing (37).

The structural connectivity between the insula and ACC is supplemented by

retrograde and anterograde tracing experiments in the rat (49), rabbit (7) and cat (47),

showing projections from area 25 of the infralimbic cortex to the anterior insula.  Our

analysis focused on the subgenual ACC (area 25) and vMPFC (area 10), and inter-

connections of the subgenual ACC with the medial prefrontal and orbital areas has been

shown (9).  The current observations of insular and MPFC connections lend support to

their functional roles.

The connections between the anterior insula and the subgenual ACC observed in

the current study are consistent with involvement of the ACC and anterior insula in

control of the autonomic nervous system (11; 53).  Behavioural cognitive tasks, such as

working memory, decrease heart rate variability in a manner that is correlated with

activity in the MPFC, ACC and insula (24).  The anterior insula has been related to

viscero-autonomic roles (28; 31; 44), and afferent and efferent linkages of the insula

exist with prominent subcortical autonomic centres including the amygdala,

hypothalamus, parabrachial nuclei and nucleus of the solitary tract (NTS) (10; 20).

Anatomically, the subgenual ACC contains direct projections to the parasympathetic

nucleus of the solitary tract (51) and dorsal motor nucleus of the vagus (26).  Efferent

projections also have been observed from the vMPFC and subgenual ACC to the

hypothalamus (1), NTS (46) and periaqueductal gray (PAG) (53). Such connections,

observed in rodents, are consistent with measured behavioural outcomes observed in

humans. For example, the tachycardic response to isometric handgrip exercise is due to

parasympathetic withdrawal (33) and is also associated with activation of the anterior-

mid insula as well as decreased activity in the vMPFC/subgenual ACC (25; 57). In

turn, sub-motor simulation of muscle sensory afferents leads to enhanced

parasympathetic modulation of HR and concurrent decreased activity in the anterior

insula and increased activity within the vMPFC (25). The role of the vMPFC and

subgenual ACC with parasympathetic activity is highly supported by other researchers

correlating cardiac behaviour with activity patterns in these regions (17; 40; 57).

Together, there is homology between discrete pathways observed in rodent work and

with DTI in humans of the current study. Together, these observations provide further

anatomical support for the conclusion that these forebrain linkages among the anterior

insula and ACC impact parasympathetic vasomotor function.

Thus, the combined evidence leads to the conjecture that the anterior insula

provides projections to the subgenual ACC/vMPFC region to subserve sensory input to

neurogenic cardiovascular control. This hypothesis is consistent with conclusions that

the insula is also involved in the affective and conscious perception of sensory

processing (58). More specifically, it is suggested that proprioceptive information from

somatosensory stimulation is integrated within the interoceptive domain of the anterior

insula and translated by the prefrontal and ACC regions to impact heart rate variability

(25), supporting the notion of a joint system of awareness of self involving the anterior

insula and ACC (34). It is important to note that the vMPFC and subgenual ACC are also associated with affective and emotional components of sensory processing; thus, the structural linkages between the anterior insula and ACC may subserve both cognitive and autonomic responses.

### 3.4.2 Posterior Insula Projections

In the current study we observed connections between the posterior insula and PCC. These data support previous experimental tracing studies observations in monkeys (35) and correlative functional connectivity analysis in humans (8), based on resting state fluctuations of the BOLD signal. Together, these different methods highlight differences in anatomical connectivity along the anterio-posterior axis of the insula. We previously observed concurrent activation in the posterior insula and PCC during sub-motor somatosensory stimulation of the forearm muscle (25), and deactivation in the PCC during volitional handgrip exercise (25; 57). These observations suggest that the regions may act conjointly to affect some action. The posterior insula acts as an anatomical substrate for processing sensory information (12; 30; 58). In contrast, while the PCC has been attributed with an evaluative function, it has not been credited with any role in emotion or autonomic control (54). Rather, the functional underpinnings of the posterior insula and PCC connections may relate to a role in visuospatial orientation (54).

In addition to the posterior insula and ACC linkages, our current findings provide an anatomical basis for previously-observed functional activity in the posterior insula and S1/S2 during somatosensory stimulation (25). Unlike the anterior insula, the posterior insula contains direct connections with the somatosensory areas, including

secondary and primary cortices (21; 35; 36). This is in line with the established role of the 'sensory' posterior insula, which includes integration of vibrotactile stimuli (12), baroreceptors (59), and touch (6).

Lastly, connections between the insula and thalamus were observed in the current analysis, consistent with previous observations in monkeys (4; 39) and humans (37). Muscle nerve afferent stimulation in the cat has shown group I afferent projections to the nuclei of the thalamus (2; 32). Also, marked differences in the connections of the anterior and posterior insula with various thalamic nuclei are also related to the functions of the anterior insula in autonomic regulation and the posterior insula with somesthetic-skeletomotor function (35).

### 3.4.3   Midline Cingulate Cortex Projections

Additionally, projections between the vMPFC/subgenual ACC and PCC were observed in approximately 45% of the participants in the current study. These low numbers likely reflect the conservative analysis performed on a small portion of the rostral ACC. While we did not differentiate between the dorsal and ventral portions of the PCC, histological staining in post-mortem human brains confirms connectivity between the ventral PCC and subgenual ACC (56). Monosynaptic connections are also present between these regions in the monkey (55). It is proposed that the ventral PCC provides ongoing self-monitoring and evaluates emotion and non-emotion events through its interactions with the ACC (56). The information exchange between the ACC and PCC regions may enable the storage of memory and autonomic responses to emotion as driven by the ACC (41).

### 3.4.4 Methodological Considerations

Within our seed-based approach and placement of regions of interest, it is possible that connections were missed from areas not seeded. It is also not possible to infer direct connections between the regions using tractography; however, the results are consistent with tracts reported in previous tracer, histological, functional connectivity and DTI studies, as reported above. More detailed DTI analysis of subject-specific seed regions based on individual BOLD coordinates may improve the determination of the true variability and/or homogeneity in anatomical linkages between regions of the CAN. Nonetheless, the current approach was intended to capture the global context of CAN connectivity. Indeed, this more generalized approach revealed homogeneity in several linkage combinations, particularly the anterior insula-subgenual ACC, the posterior insula-PCC, and ACC-PCC axes.

### 3.5 Conclusions

In conclusion, we have demonstrated structural connectivity between subdivisions of the insula and cingulate cortex that are associated with tasks that affect autonomic cardiovascular function. Specifically, the anterior insula was linked to the subgenual ACC whereas the posterior insula was connected with the PCC and with the somatosensory cortex. The anterior insula and subgenual ACC appear to conjointly modulate autonomic function, while the posterior insula and PCC are suggested to support somatosensory integration and monitoring of the internal milieu, which may in turn affect autonomic arousal by the ACC. Thus, the current study supports the involvement of the anterior and posterior insula within two distinct functional networks

(8; 50) and further establishes the anatomical substrates for the expected functional

relationships between the CAN regions of interest.

## 3.6    Reference List

1.  **An X, Bandler R, Ongur D and Price JL**. Prefrontal cortical projections to longitudinal columns in the midbrain periacqueductal gray in macaque monkeys. *The Journal of Comparative Neurology* 401: 455-479, 1998.

2.  **Andersson SA, Landgren S and Wolsk D**. The thalamic relay and cortical projection of group I muscle afferents from the forelimb of the cat. *Journal of Physiology* 183: 576-591, 1966.

3.  **Augustine JR**. The insular lobe in primates including humans. *Neurological Research* 7: 2-10, 1985.

4.  **Augustine JR**. Circuitry and functional aspects of the insular lobe in primates including humans. *Brain Research Brain Research Reviews* 22: 229-244, 1996.

5.  **Basser PJ, Pajevic S, Pierpaoli C, Duda J and Aldroubi A**. In vivo fiber tractography using DT-MRI data. *Magnetic Resonance in Medicine* 44: 625-632, 2000.

6.  **Bjornsdotter M, Loken L, Olausson H, Vallbo A and Wessberg J**. Somatotopic organization of gentle touch processing in the posterior insular cortex. *The Journal of Neuroscience* 29: 9314-9320, 2009.

7.  **Buchanan S, Thompson RH, Maxwell BL and Powell DA**. Efferent connections of the medial prefrontal cortex in the rabbit. *Experimental Brain Research* 100: 469-483, 1994.

8.  **Cauda F, D'Agata F, Sacco K, Duca S, Geminiani G and Vercelli A**. Functional connectivity of the insula in the resting brain. *NeuroImage* 55: 8-23, 2011.

9.  **Cavada C, Company TTJ, Cruz-Rizzolo RJ and Reinoso-Suarez F**. The anatomical connections of the macaque monkey orbitofrontal cortex. *Cerebral Cortex* 10: 220-242, 2000.

10. **Cechetto DF and Chen SJ**. Subcortical sites mediating sympathetic responses from insular cortex in rats. *American Journal of Physiology - Regulatory, Integrative and Comparative Physiology* 258: R245-R255, 1990.

11. **Cechetto DF and Saper CB**. Role of the cerebral cortex in autonomic function. In: Central Regulation of Autonomic Functions, edited by Loewy AD and Spyer KM.  New York: Oxford University Press, 1990, p. 208-223.

12. **Coghill RC, Talbot JD, Evans AC, Meyer E, Gjedde E, Bushell MC and Duncan GH**. Distributed processing of pain and vibration by the human brain. *The Journal of Neuroscience* 14: 4095-4108, 1994.

13. **Conturo TE, Lori NF, Cull TS, Akbudak E, Snyder AZ, Shimony JS, McKinstry RC, Burton H and Raichle ME**. Tracking neuronal fiber pathways in the living human brain. *Proceedings of the National Academy of Sciences* 96: 10422-10427, 1999.

14. **Craig AD**. How do you feel - now? The anterior insula and human awareness. *Nature ReviewsNeuroscience* 10: 59-70, 2009.

15. **Critchley HD, Corfield DR, Chandler MP, Mathias CJ and Dolan RJ**. Cerebral correlates of autonomic cardiovascular arousal: a functional neuroimaging investigation in humans. *Journal of Physiology* 523: 259-270, 2000.

16. **Critchley HD, Mathias CJ, Josephs O, O'Doherty J, Zanini S, Dewar B, Cipolotti L, Shallice T and Dolan RJ**. Human cingulate cortex and autonomic control: converging neuroimaging and clinical evidence. *Brain* 126: 2139-2152, 2003.

17. **Critchley HD, Wiens S, Rotshein P, Ohman A and Dolan RJ**. Neural systems supporting interoceptive awareness. *Nature Neuroscience* 7: 189-195, 2004.

18. **Devinsky O, Morrell MJ and Vogt BA**. Contributions of anterior cingulate cortex to behaviour. *Brain* 118: 279-306, 1995.

19. **Dupont S, Bouilleret V, Hasboun D, Semah F and Baulac M**. Functional anatomy of the insula: new insights from imaging. *Surgical and Radiologic Anatomy* 25: 113-119, 2003.

20. **Flynn FG, Benson DF and Ardila A**. Anatomy of the insula - functional and clinical correlates. *Aphasiology* 13: 55-78, 1999.

21. **Friedman DP, Murray EA, O'Neill JB and Mishkin M**. Cortical connnections of the somatosensory fields of the lateral sulcus macaque: evidence for a corticolimbic pathway for touch. *The Journal of Comparative Neurology* 252: 323-347, 1986.

22. **Friston KJ, Frith CD, Liddle PF and Frackowiak RSJ**. Functional connectivity: the principal-component analysis of large (PET) data sets. *Journal of Cerebral Blood Flow & Metabolism* 13: 5-14, 1993.

23. **Gianaros PJ, Derbyshire SWG, May JC, Siegle GJ, Gamalo MA and Jennings JR**. Anterior cingulate activity correlates with blood pressure during stress. *Psychophysiology* 42: 627-635, 2005.

24. **Gianaros PJ, Van Der Veen FM and Jennings JR**. Regional cerebral blood flow correlates with heart period and high-frequency heart period variability during working-memory tasks: Implications for the cortical and subcortical regulation of cardiac autonomic activity. *Psychophysiology* 41: 521-530, 2004.

25. **Goswami R, Frances MF and Shoemaker JK**. Representation of somatosensory inputs within the cortical autonomic network. *NeuroImage* 54: 1211-1220, 2011.

26. **Hurley KM, Herbert H, Moga MM and Saper CB**. Efferent projections of the infralimbic cortex of the rat. *The Journal of Comparative Neurology* 308: 249-276, 1991.

27. **Jones DK, Horsfield MA and Simmons A**. Optimal strategies for measuring diffusion in anisotropic systems by magnetic resonance imaging. *Magnetic Resonance in Medicine* 42: 515-525, 1999.

28. **Kaada BR**. Cingulate, posterior orbital, anterior insular and temporal pole cortex. In: Handbook of Physiology, edited by J.Field et al. Washington: Americal Physiological Society, 1960, p. 1345-1372.

29. **Kimmerly DS, O'Leary DD, Menon RS, Gati JS and Shoemaker JK**. Cortical regions associated with autonomic cardiovascular regulation during lower body negative pressure in humans. *Journal of Physiology* 569: 331-345, 2005.

30. **Kurth F, Ickhoff SB, chleicher A, oemke L, illes K and munts K**. Cytoarchitecture and probabilistic maps of the human posterior insular cortex. *Cerebral Cortex* 20: 1448-1461, 2009.

31. **Macefield VG, Gandevia SC and Henderson LA**. Neural sites involved in the sustained increase in muscle sympathetic nerve activity induced by inspiratory capacity apnea: a fMRI study. *Journal of Applied Physiology* 100: 266-273, 2006.

32. **Mallart A**. Thalamic projection of muscle nerve afferents in the cat. *Journal of Physiology* 194: 337-353, 1968.

33. **Mark AL, Victor RG, Nerhed C and Wallin BG**. Microneurographic studies of the mechanisms of sympathetic nerve responses to static exercise in humans. *Circulation Research* 57: 461-469, 1985.

34. **Medford N and Critchley HD**. Conjoint activity of anterior insular and anterior cingulate cortex: awareness and response. *Brain Structure and Function* 214: 535-549, 2010.

35. **Mesulam MM and Mufson EJ**. Insula of the old world monkey. III: Efferent cortical output and comments on function. *The Journal of Comparative Neurology* 212: 38-52, 1982.

36. **Mesulam MM and Mufson EJ**. The insula of Reil in man and monkey. Architectonics, connectivity, and function. In: Cerebral cortex, edited by Peters A and Jones EG. New York: Plenum, 1985, p. 179-226.

37. **Moisset X, Bouhassira D, Ducreux D, Glutron D and Coffin B**. Anatomical connections between brain areas activated during rectal distension in healthy volunteers: A visceral pain network. *European Journal of Pain* 14: 142-148, 2010.

38. **Mori S and van Zijl PCM**. Fiber tracking: principles and strategies - a technical review. *NMR in Biomedicine* 15: 468-480, 2002.

39. **Mufson EJ and Mesulam M**. Thalamic connections of the insula in the rhesus monkey and comments on the paralimbic connectivity of the medial pulvinar nucleus. *The Journal of Comparative Neurology* 227: 109-120, 1984.

40. **Neafsey EJ**. Prefrontal cortical control of the autonomic nervous system: Anatomical and physiological observations. *Progress in Brain Research* 85: 147-165, 1990.

41. **Neafsey EJ, Terreberry RR, Hurley KM, Ruit KG and Frysztak RJ**. Anterior cingulate cortex in rodents: connections, visceral control functions, and implications of emotion. In: Neurobiology of cingulate cortex and limbic thalamus: a comprehensive handbook, edited by Vogt BA and Gabriel M. Boston: Birkhauser, 1993, p. 206-223.

42. **Oldfield RC**. The assessment and analysis of handedness: the Edinburgh inventory. *Neuropsychologia* 9: 97-113, 1971.

43. **Ongur D and Price JL**. The organization of networks within the orbital and medial prefrontal cortex of rats, monkeys and humans. *Cerebral Cortex* 10: 206-219, 2000.

44. **Oppenheimer SM, Gelb A, Girvin JP and Hachinski VC**. Cardiovascular effects of human insular cortex stimulation. *Neurology* 42: 1727-1732, 1992.

45. **Oppenheimer SM, Kedem G and Martin WM**. Left-insular cortex lesions perturb cardiac autonomic tone in humans. *Clinical Autonomic Research* 6: 131-140, 1996.

46. **Owens NC and Verberne AJ**. An electrophysiological study of the medial prefrontal cortical projection to the nucleus of the solitary tract in rat. *Experimental Brain Research* 110: 55-61, 1996.

47. **Room P, Russchen FT, Groenewegen HJ and Lohman AHM**. Efferent connections of the prelimbic (area 32) and the infralimbic (area 25) cortices: an anterograde tracing study in the cat. *The Journal of Comparative Neurology* 242: 40-55, 1985.

48. **Seeley WW, Menon V, Schatzberg AF, Keller J, Glover GH, Kenna H, Reiss AL and Greicius MD**. Dissociable intrinsic connectivity networks for salience processing and executive control. *The Journal of Neuroscience* 27: 2349-2356, 2007.

49. **Takagishi M and Chiba T**. Efferent projections of the infralimbic (area 25) region of the medial prefrontal cortex in the rat: an anteriograde tracer PHA-L study. *Brain Research* 566: 26-39, 1991.

50. **Taylor KS, Seminowicz DA and Davis KD**. Two systems of resting state connectivity between the insula and cingulate cortex. *Human Brain Mapping* 30: 2731-2745, 2009.

51. **Terreberry RR and Neafsey EJ**. Rat medial frontal cortex: a visceral motor region with a direct projection to the solitary nucleus. *Brain Research* 278: 245-249, 1983.

52. **van den Heuvel MP, Mandl RCW, Kahn RS and Hulshoff Pol HE**. Functionally linked resting-state networks reflect the underlying structural connectivity architecture of the human brain. *Human Brain Mapping* 30: 3127-3141, 2009.

53. **Verberne AJM and Owens NC**. Cortical modulation of the cardiovascular system. *Progress in Neurobiology* 54: 149-168, 1998.

54. **Vogt BA, Finch DM and Olson CR**. Functional heterogeneity in cingulate cortex: the anterior executive and posterior evaluative regions. *Cerebral Cortex* 2: 435-443, 1992.

55. **Vogt BA and Pandya DN**. Cingulate cortex of the rhesus monkey: II. Cortical afferents. *The Journal of Comparative Neurology* 262: 271-289, 1987.

56. **Vogt BA, Vogt L and Laureys S**. Cytology and functionally correlated circuits of human posterior cingulate areas. *NeuroImage* 29: 452-466, 2006.

57. **Wong SW, Masse N, Kimmerly DS, Menon RS and Shoemaker JK**. Ventral medial prefrontal cortex and cardiovagal control in conscious humans. *NeuroImage* 35: 698-708, 2007.

58. **Zhang ZH, Dougherty PM and Oppenheimer SM**. Monkey insular cortex neurons respond to baroreceptive and somatosensory convergent inputs. *Neuroscience* 94: 351-360, 1999.

59. **Zhang ZH and Oppenheimer SM**. Characterization, distribution and lateralization of baroreceptor-related neurons in the rat insular cortex. *Brain Research* 760: 243-250, 1997.

**Chapter 4 Forebrain organization representing integration of baroreceptor and somatosensory afferents within the cortical autonomic network**

## 4.1 INTRODUCTION

Central processing of afferent feedback from baroreceptors modulates autonomic cardiovascular function, with increased baroreceptor firing inhibiting muscle sympathetic nerve activity (MSNA) (9). Baroreflex activity affects the regulation of various components of autonomic function, including a role for carotid sinus baroreceptors in pulmonary modulation of the autonomic nervous system (11). Baroreceptor activity also has an influence on the processing of somatosensory stimuli and subsequent effects on autonomic function. Specifically, afferent input from arterial baroreceptors is a powerful modulator of the excitatory cardiovascular response evoked by skeletal muscle afferents during muscle contractions (41). Furthermore, unpredicted somatosensory stimuli delivered 200-400 ms after the R wave of the cardiac cycle inhibits MSNA, whereas no change in MSNA is observed with delivery synchronous with the ECG-R wave (10). Thus, ongoing feedback from baroreflex activity plays an important role in the integration of somatosensory stimuli and the resultant effects on autonomic control of cardiovascular function.

The large diameter type I and II afferents may be particularly important as somatosensory afferents that produce depressor cardiovascular responses mediated by changes in autonomic outflow (22; 23; 38). For instance, the increase in MSNA during static handgrip exercise is depressed by concurrent ipsilateral sub-motor threshold electrical stimulation of the type I and II afferents (21). These authors postulated that the depressor effect on MSNA depends on an interaction of the III and IV afferents that are active during handgrip exercise with the type I and II afferents at the spinal level (21). However, sites of somatosensory integration within the forebrain have also been

recently observed. Specifically, in non-human primates, somatosensory and baroreceptive inputs converge on the same neurons within the insula (57). Also, we have demonstrated changes in activity within major centers of the CAN in conscious humans during sub-motor forearm stimulation, a manoeuvre that activates type I and II afferents (14).

There is evidence that somatosensory afferent neural integration occurs at the brainstem and even supramedullary sites. In particular, afferent projections from both muscle and baroreceptor sensory afferents synapse in discrete regions of the brainstem, such as the nucleus tractus solitarii (NTS) (24; 40). Further, Gray and colleagues (2009) have demonstrated an involvement of cortical and sub-cortical structures including the insula, amygdala and brainstem nuclei in the integration of somatosensory stimuli during different phases of baroreflex activity (15).

The first human evidence of cortical involvement of baroreflex-mediated changes in autonomic function during an orthostatic stressor (lower-body negative pressure; LBNP) was demonstrated using functional magnetic resonance imaging (fMRI) (25). These regions included the insular cortex, anterior cingulate cortex (ACC), medial prefrontal cortex (MFPC), cerebellum and amygdala (25; 26), supporting an established cortical and sub-cortical network responsible for regulating visceromotor activity (2; 6; 8; 51). In addition, we recently identified forebrain centers involved with sensory level type I/II afferent stimulation, including the insula and ventral MFPC (vMPFC), during supine conditions at basal levels of baroreceptor loading (14). Whether the central organization of somatosensory inputs is altered during episodes of reduced baroreceptor afferent input is unknown.

Therefore, the purpose of the present study was to examine the hypothesis of a sympathoinhibitory effect of type I and II sensory stimulation that is attenuated by baroreceptor loading and that this depressor effect of somatosensory stimulation (exhibited during reductions in baroreceptor afferent activity with lower body suction) would be associated with alterations in activation patterns within the cortical autonomic network (CAN), particularly the insula, dorsal ACC and/or MPFC. In particular, evidence from primates suggests that significant convergence of somatosensory and baroreceptive input exists on the same neurons within the insula (57). Thus, it was expected that insula activation during somatosensory stimulation would be altered during LBNP in a manner that is associated with a depressed sympathetic response to baroreceptor unloading.

## 4.2    MATERIALS AND METHODS

### 4.2.1    Ethical Approval

Experimental procedures were conducted with approval by the Health Sciences Research Ethics Board at *The University of Western Ontario*. All participants provided informed written consent to the study which was in accordance with the standards set by the *Declaration of Helsinki*.

### 4.2.2    Participants

Fifteen healthy participants [6 females, 9 males; age range 18-31 yr, mean(SD) = 25(3) yrs; height 175(8) cm; weight 74(12) kg] volunteered for this study. All subjects were non-smokers, not taking any medication, and had no prior history of cardiovascular, neurological, or musculoskeletal disorders. In addition, each participant was classified as right-handed according to the Edinburgh Handedness Inventory (35).

Prior to the experimental day, each participant was familiarized with transcutaneous electrical nerve stimulation at sub-motor threshold levels and the parameters for the stimulus intensities were determined (see below).  As well, each participant was assessed for their tolerance to perform 20 s end-expiratory apneas.

### 4.2.3   Experimental Approach

Our approach was to assess cortical activation patterns and autonomic responses to somatosensory stimulation while baroreceptor loading was varied.  Secondly, we studied the autonomic and brain responses to end-expiratory apneas, a significant stimulus known to activate the sympathetic nervous system (12) in the absence of orthostasis.  Baroreceptor unloading was achieved using 30 mmHg LBNP (49). Transcutaneous electrical nerve stimulation at sub-motor threshold stimulation was used to activate the type I and II afferent nerve fibers (21; 43).

The participants were tested on two separate experimental days to obtain: 1) the cardiovascular and neural recordings (PHYS session), and 2) the neuroimaging data (fMRI session).  The PHYS session was always performed first in order to assess tolerance of LBNP and establish forearm electrical stimulation levels.

### 4.2.4   Experimental Stimuli and Procedures

The somatosensory stimuli were generated electrically by a neurostimulator (Digitimer DS7A, Hertfordshire, England) with a symmetrical and biphasic stimulation waveform delivered at a frequency of 100 Hz and pulse width duration of 50 μs.  Two self-adhesive electrodes with modified wiring for MRI compatibility (4cm x 4cm; StimCare, Empi, St. Paul, MN) were placed over the right forearm flexors, identified by palpation during resisted flexion.  The location for the electrodes and stimulation

intensity were each individually adjusted to attain sub-motor threshold at an intensity just below motor threshold. On fMRI testing days, levels of stimulations for each participant were determined outside the scanner and verified once inside the scanner just prior to the imaging session. The average intensity at sub-motor threshold was achieved at $15 \pm 3$ mA.

Minimizing head movement during LBNP was achieved in the fMRI session through the use of MAST antishock trousers (David Clark Company Inc., Worcester, MA, USA), as well as an adjustable bicycle seat and footplate within the LBNP chamber. The suction within the lower body chamber was applied continuously while the MAST trousers controlled the venous pooling. Specifically, during LBNP, inflation of the antishock trousers countered venous pooling and reflected baseline, supine conditions, whereas deflation of the trousers induced venous pooling and orthostatic stress. The viability and reproducibility of the use of antishock trousers with LBNP has previously been demonstrated by Kimmerly et al (2006), who showed that measures of central venous pressure were not different between LBNP sessions with and without antishock trousers (26). During the fMRI sessions, the participants' head was immobilized within a head cradle with foam padding and were instructed to refrain from performing any active tasks and to avoid head movements.

### 4.2.5   Experimental Protocol

Participants were asked to fast for a minimum of 3 hr and to refrain from caffeine, nicotine, alcohol and physical activity for at least 12 hr prior to testing. Participants were also asked to arrive to the laboratory two hours prior to the experimental testing to determine the stimulation parameters and perform cutaneous

anesethization.  In order to achieve cutaneous afferent blockade, the forearm was treated with EMLA cream (Astra Pharmaceuticals, Wayne, PA) at the location of optimal electrode placement.  The experimental session began by having subjects lay in the supine position, sealed in the LBNP chamber at the level of the iliac crest.

The somatosensory stimulation (SS) session was a block design consisting of four repetitions of stimulation lasting 30 s with 15 s rest provided between.  Two runs were performed, with a total of 8 SS trials.

The LBNP session was a block design which exposed participants to three 60-s bouts of LBNP with 30 s rest in between.  Two runs were performed, producing a total of 6 LBNP trials.  The LBNP + somatosensory stimulation (LBNP+SS) session was a similar block design consisting of three 60 s trials of LBNP.  Somatosensory stimulation was applied during the last 30 s of LBNP to allow for steady state conditions.  Like the LBNP session, the LBNP+SS session was repeated twice for a total of 6 LBNP+SS trials.

Apnea sessions consisted of two conditions, including Apnea and Apnea + somatosensory stimulation (Apnea+SS).  The apneas were performed as maximal end-expiratory breath holds, each lasting 20 s with 45 s rest provided between trials to ensure that MSNA, HR and blood pressure (BP) returned to baseline values after the transient sympathetic withdrawal that occurs after breath holds (48; 53).  Apnea and Apnea+SS were each repeated three times within a single run in randomized order.  Two runs were performed, producing a total of 6 Apnea and 6 Apnea+SS trials over two runs.

The PHYS and fMRI sessions were identical except for a 2 min baseline allotted at the beginning of each run during the PHYS sessions to allow for calculation of baseline MSNA.

### 4.2.6 Physiological Recording Session (PHYS)

### 4.2.6.1 Data Acquisition

HR was acquired from a standard lead II electrocardiogram (ECG; Pilot 9200, Colin Medical Instruments, San Antonio, TX, USA). Arterial BP was measured continuously on a beat-by-beat basis from the left middle finger with a photoplethysmograph finger cuff (Finometer; Finapres Medical Systems BV, Amsterdam, Netherlands), from which mean (MAP) was obtained. Cardiac output (Q) was acquired using the Finometer Modelflow algorithm (54). Pneumotrace recordings were used to measure rate and depth of breathing (Siemens, Pi-Products, Amberg, Germany). Multi-fibre MSNA was recorded from the right fibular (peroneal) nerve using microneurography (16). A tungsten microelectrode (length=35mm, diameter=200 μm) tapered to a 1-5 μm uninsulated tip was inserted percutaneously into the fibular nerve posterior to the fibular head. A reference electrode was placed subcutaneously 1-3 cm from the recording site. Confirmation of a suitable MSNA site was determined by bursts exhibiting pulse synchrony, as well as a burst pattern that did not produce skin paresthesias and increased in response to voluntary apnea but not during arousal to a loud noise (16).

### 4.2.6.2 Data Analysis

ECG, BP, Q and rectified and integrated neurogram signals were collected at a sampling rate of 1 KHz , the amplified and filtered neurogram signals were sampled at

10 KHz, and stored offline for further analysis (Powerlab software, ADInstruments Inc.,

Colorado Springs, CO, USA).

MSNA bursts exhibiting pulse synchrony with characteristic rising and falling

slopes and having a signal-to-noise-ratio of at least 2:1 (i.e., the ratio of the amplitude of

the burst and baseline), were included in the analysis. MSNA was quantified as the

number of bursts per min (burst frequency), burst incidence (bursts per 100 heartbeats),

and total MSNA activity (sum of all burst amplitudes in sampling period). Burst size

was normalized to the mean amplitude to account for any electrode repositioning.

### 4.2.6.3 Statistical Analysis

The effect of each condition on each hemodynamic and MSNA variable versus

baseline was assessed using a two-tailed Student's T-test. Statistical analyses were

performed using SAS (SAS, Cary, NC, USA). Statistical significance was set at

$P<0.05$. Data are reported as mean[standard deviation (SD)].

### 4.2.7   MRI Session

### 4.2.7.1 Data Acquisition

Heart rate was calculated from pulse intervals obtained from an MRI-compatible

pulse oximeter (Nonin Medical Inc., 8600FO MRI, Plymouth, MN, USA) secured over

the left middle finger. Absolute levels of LBNP were acquired using a pressure

transducer (Edwards Lifesciences, PX272, Irvine, CA, USA) that was connected to a

bridge amplifier outside the MRI suite. Analog signals of the pulse oximeter and LBNP

levels were sampled at 1 KHz and stored for analysis (Powerlab, ADInstruments,

Colorado Springs, CO, USA).

Imaging data were collected on a 3-Tesla scanner (Magnetom TRIO TIM, Siemens Medical Solutions, Erlangen, Germany) with a 32-channel head coil. A high resolution $T_1$-weighted structural volume was acquired with a 3D MPRAGE sequence at the beginning of the scanning session (sagittal, field of view $256 \times 240$ mm, voxel size $1 \times 1 \times 1$ mm, 1 mm slice thickness, no gap, flip angle 9º, TR = 2300 ms, TE = 2.98 ms). Whole brain blood-oxygenation level-dependent (BOLD) contrast fMRI data were acquired by $T_2^*$-weighted gradient echo planar imaging (EPI) pulse sequence (TE, 30 ms; flip angle, 90º; field of view, $240 \times 240$ mm; in-plane voxel resolution, $3 \times 3$ mm). Functional volumes consisted of 45 interleaved axial slices (TR 2500ms, 3 mm slice thickness, no gap). For each of the runs in the SS session, 78 volumes were acquired, 174 volumes were acquired in the Apnea paradigm, and 120 volumes were acquired during each of the LBNP and LBNP+SS runs. The first two images of each run were automatically discarded to allow for analysis of an equilibrated MRI signal.

### 4.2.7.2 Data Analysis

Raw fMRI data were analyzed by SPM8 (Wellcome Department of Imaging Neuroscience, London, UK). The EPI images were motion corrected using a fourth degree B-spline interpolation to create a mean EPI image, which was co-registered to the same space as each individual's structural image. Images were then segmented into grey matter, white matter, and cerebrospinal fluid (1), and normalized to the Montreal Neurological Institute (MNI) coordinate system. The scans were spatially smoothed using a full-width half-maximum (FWHM) Gaussian kernel of 6 mm, and normalized for global activations. To reduce low frequency noise due to scanner drift, a high-pass filter with 128 s cutoff was applied to the dataset (autoregressive model).

**4.2.7.3 Statistical Analysis**

Two levels of analysis were performed. First, within-subject analyses were constructed to form a General Linear Model (GLM) modeled with a conventional block design using a canonical hemodynamic response function. Second, each individual's contrast images reflecting differences in signal intensity between the conditions of interest and baseline, were entered into a random effects group analysis. Subtraction analyses were also performed to compare between conditions. BOLD responses containing information of increased and decreased activation patterns were thresholded at $P<0.005$ (uncorrected), and a minimum cluster size of 10 voxels was used. The effect size (mean $\pm$ SE percent change) of the BOLD signal was obtained from each significant cluster.

A region of interest (ROI) analysis was performed based on previous literature pertaining to baroreflex-mediated changes in autonomic activity (19; 25), as well as somatosensory processing (14; 15). These ROI's include the insula, MFPC and ACC. Identification of anatomical locations was obtained using the Talairach Daemon software (27). All figures are represented in neurological convention (i.e., left is on the left).

**4.3    RESULTS**

**4.3.1    Physiological Responses**

Due to a loss of somatosensory stimuli from one participant during the fMRI recording session, neuroimaging data are based on 14 participants. Similarly, good quality MSNA recordings for all the conditions were successfully obtained in 11 participants upon which the analysis was performed.

Baseline measures were similar amongst all runs.  Baseline HR's were not

different between SS, LBNP, LBNP+SS and Apnea runs in both the PHYS and MRI

sessions (Tables 4.1, 4.2 and 4.3).  Baseline MAP and Q were not different between SS,

LBNP, LBNP+SS and Apnea runs in PHYS sessions (Tables 4.1, 4.2 and 4.3).  Baseline

MSNA burst frequency, MSNA incidence, MSNA amplitude and total MSNA were

similar between SS, LBNP, LBNP+SS and Apnea sessions (Tables 4.1, 4.2, and 4.3).

**4.3.1.1 SS**

SS alone did not affect HR, MAP or Q (Table 4.1).  Nor did SS have a

significant impact on MSNA burst frequency, burst incidence, burst amplitude or total

MSNA (Table 4.1).  Representative physiological responses to SS are shown in Figure

4.1A.

**Table 4.1-- Hemodynamic and sympathetic nerve activity measures during baseline and somatosensory stimulation.**

| Measure | Baseline | SS |
|---|---|---|
| HR (fMRI) (beats/min) | 59 (9) | 59 (9) |
| HR (LAB) (beats/min) | 57 (9) | 56 (9) |
| MAP (LAB) (mmHg) | 93 (6) | 93 (7) |
| Q (LAB) (L/min) | 5.3 (1.4) | 5.3 (1.4) |
| MSNA (LAB) (bursts/min) | 22 (10) | 22 (10) |
| MSNA (LAB) (amplitude, mV) | 49 (6) | 49 (5) |
| MSNA (LAB) (total activity, a.u.) | 1086 (536) | 1036 (531) |
| MSNA (LAB) (bursts/100 heart beats) | 40 (16) | 39 (17) |

All values are expressed as means (SD).  fMRI indicates measures collected during the neuroimaging session.  LAB indicates measures collected during the laboratory session. SS, somatosensory stimulation; HR, heart rate; MAP, mean arterial pressure; Q, cardiac output; MSNA, muscle sympathetic nerve activity.
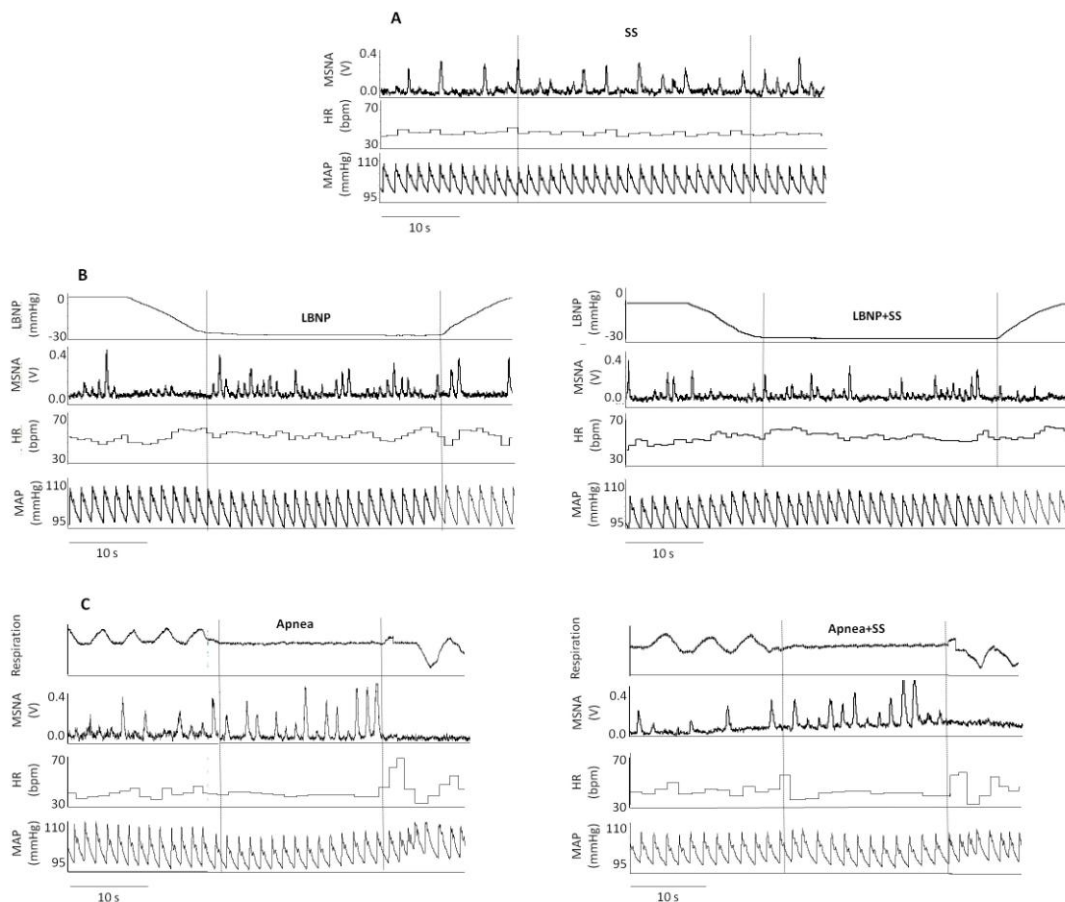
**Figure 4.1 -- Panel A illustrates representative data during somatosensory stimulation (SS) with no changes observed in muscle sympathetic nerve activity (MSNA), heart rate (HR), and blood pressure (BP). Panel B is representative data showing differences in the rise in MSNA burst frequency during lower-body negative pressure (LBNP) and lower-body negative pressure + somatosensory stimulation (LBNP+SS), with similar changes in HR. Panel C illustrates representative data during Apnea demonstrating similar increases in MSNA and no change in HR and BP.**

**4.3.1.2 LBNP and LBNP+SS**

Representative physiological responses to LBNP and LBNP+SS are shown in Figure 4.1B. In response to LBNP, HR increased in the fMRI ($\Delta$6 bpm, P<0.05) and PHYS ($\Delta$3 bpm, P<0.05) sessions, Q tended to decrease ($\Delta$-0.3 L/min, P=0.06), and MAP was unchanged compared to baseline (Table 4.2). Similarly in the LBNP+SS session, increases in HR in the fMRI ($\Delta$5 bpm, P<0.05) and PHYS ($\Delta$2 bpm P<0.05) sessions, and decreased Q ($\Delta$-0.3 L/min, P<0.05) were observed, with no difference in MAP (Table 4.2). No differences were observed when comparing the changes in HR from baseline between LBNP and LBNP+SS sessions (fMRI, $\Delta$6 vs. $\Delta$5 bpm, respectively; PHYS, $\Delta$3 vs. $\Delta$2 bpm, respectively).

In response to LBNP, all indices of MSNA were increased above baseline levels, including burst frequency ($\Delta$12 bursts/min, P<0.05), burst amplitude ($\Delta$6 mV, P<0.05), total MSNA ($\Delta$686 a.u., P<0.05) and burst incidence ($\Delta$20 bursts/100 heart beats, P<0.05) (Table 4.2). Whereas, compared with baseline, LBNP+SS elicited elevations in burst frequency ($\Delta$8 bursts/min, P<0.05), burst amplitude ($\Delta$7 mV, P<0.05), total MSNA ($\Delta$531 a.u., P<0.05), and burst incidence ($\Delta$15 bursts/100 heart beats, P<0.05) (Table 4.2), the absolute increase in MSNA burst frequency ($\Delta$frequency) was smaller during LBNP+SS compared to that of LBNP (8 vs. 12 bursts/min, respectively, P<0.05) (Figure 4.2A). No differences between LBNP and LBNP+SS were observed with respect to changes in burst amplitude, total MSNA and burst incidence compared to baseline (Figure 4.2B-D).

**Table 4.2 -- Hemodynamic and sympathetic nerve activity measures during lower-body negative pressure and lower-body negative pressure +somatosensory stimulation versus respective baselines.**

| Measure | Baseline 1 | LBNP | Baseline 2 | LBNP+SS |
|---|---|---|---|---|
| HR (fMRI) (beats/min) | 58 (8) | 65 (10)* | 59 (8) | 64 (10)† |
| HR (LAB) (beats/min) | 58 (10) | 61 (10)* | 58 (9) | 60 (10)† |
| MAP (LAB) (mmHg) | 98 (11) | 98 (11) | 97 (10) | 96 (11) |
| Q (LAB) (mmHg) | 5.3 (1.3) | 5.0 (1.2) | 5.3 (1.3) | 5.0 (1.0) † |
| MSNA (LAB) (bursts/min) | 19 (7) | 31 (8)* | 20 (8) | 28 (7)† |
| MSNA (LAB) (amplitude, mV) | 43 (7) | 50 (7)* | 43 (9) | 50 (7)† |
| MSNA (LAB) (total activity, a.u.) | 822 (314) | 1507 (404)* | 856 (405) | 1387 (449)† |
| MSNA (LAB) (bursts/100 heart beats) | 33 (13) | 54 (14)* | 35 (14) | 49 (14)† |

All values are expressed as means (SD). fMRI indicates measures collected during the neuroimaging session. LAB indicates measures collected during the laboratory session. LBNP, lower-body negative pressure; SS, somatosensory stimulation; HR, heart rate; MAP, mean arterial pressure; Q, cardiac output; MSNA, muscle sympathetic nerve activity. *Significant difference from Baseline 1 (P<0.05); †Significant difference from Baseline 2 (P<0.05).

**Figure 4.2 -- Changes in MSNA Burst Frequency (Panel A), Burst Amplitude (Panel B), Total MSNA (Panel C) and Burst Incidence (Panel D) during lower-body negative pressure (LBNP) and lower-body negative pressure + somatosensory stimulation (LBNP+SS). *Significant difference from LBNP (P<0.05).**

**4.3.1.3 Apnea and Apnea+SS**

Representative physiological responses to Apnea and Apnea+SS are shown in Figure 4.1C. HR was not different from baseline during Apnea and Apnea+SS, in either the PHYS or fMRI sessions (P>0.05; Table 4.3). As well, MAP and Q during Apnea and Apnea+SS were not altered compared to baseline in the PHYS session (P>0.05; Table 4.3).

Apnea elicited increases in MSNA burst frequency (Δ13 bursts/min, P<0.05), burst amplitude (Δ9 mV, P<0.05), total MSNA (Δ783 a.u., P<0.05) as well as burst incidence (Δ23 bursts/100 heart beats, P<0.05) above baseline (Table 4.3). Increases in MSNA burst frequency (Δ12 bursts/min, P<0.05), burst amplitude (Δ7 mV, P<0.05), total MSNA (Δ671 a.u., P<0.05) and burst incidence (Δ22 bursts/100 heart beats, P<0.05) were also observed during Apnea+SS (Table 4.3). There were no differences in the absolute increase of any of the MSNA measures during Apnea compared to Apnea+SS (Figure 4.3A-D).

**Table 4.3 -- Hemodynamic and sympathetic nerve activity measures during baseline, apnea and apnea+somatosensory stimulation.**

| Measure | Baseline | Apnea | Apnea+SS |
|---|---|---|---|
| HR (fMRI) (beats/min) | 61 (10) | 60 (11) | 61 (12) |
| HR (LAB) (beats/min) | 58 (9) | 59 (10) | 58 (10) |
| MAP (LAB) (mmHg) | 95 (9) | 97 (8) | 97 (9) |
| Q (LAB) (L/min) | 5.5 (1.3) | 5.6 (1.4) | 5.6 (1.4) |
| MSNA (LAB) (bursts/min) | 20 (9) | 33 (6)* | 32 (9)* |
| MSNA (LAB) (amplitude, mV) | 38 (8) | 48 (6)* | 45 (7)* |
| MSNA (LAB) (total activity, a.u.) | 760 (416) | 1543 (354)* | 1431 (499)* |
| MSNA (LAB) (bursts/100 heart beats) | 35 (17) | 58 (13)* | 57 (16)* |

All values are expressed as means (SD). fMRI indicates measures collected during the neuroimaging session. LAB indicates measures collected during the laboratory session. SS, somatosensory stimulation; HR, heart rate; MAP, mean arterial pressure; Q, cardiac output; MSNA, muscle sympathetic nerve activity. *Significant difference from Baseline ($P<0.05$).
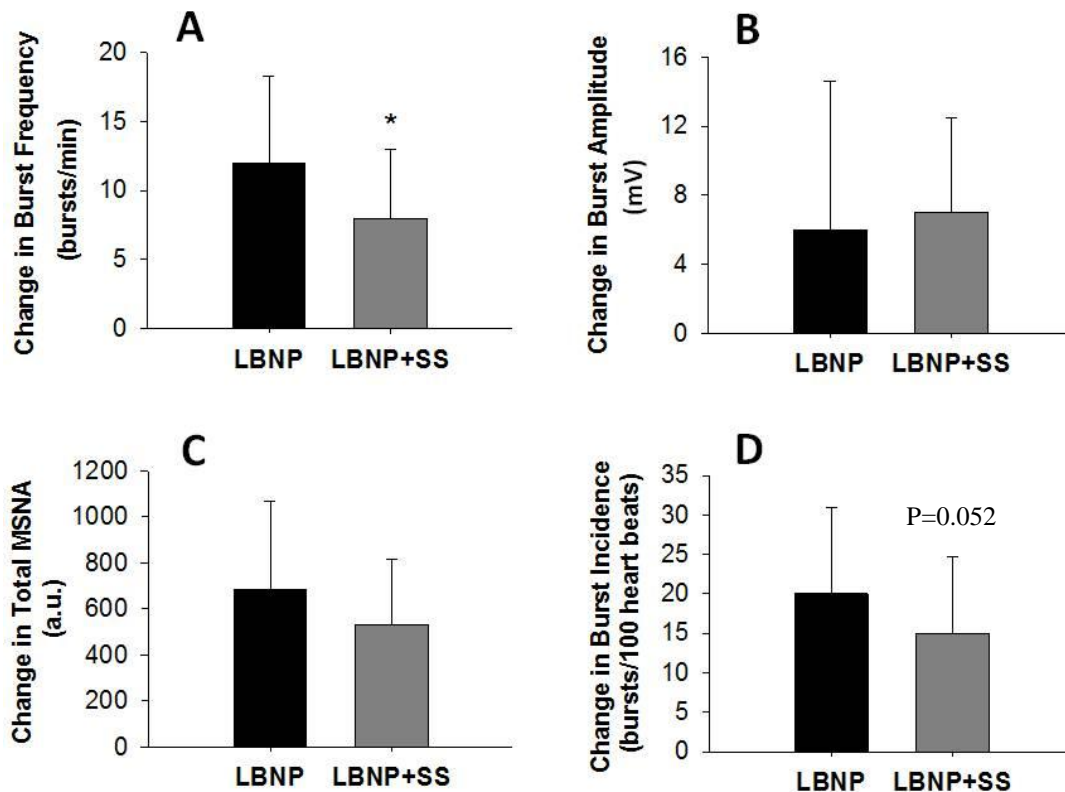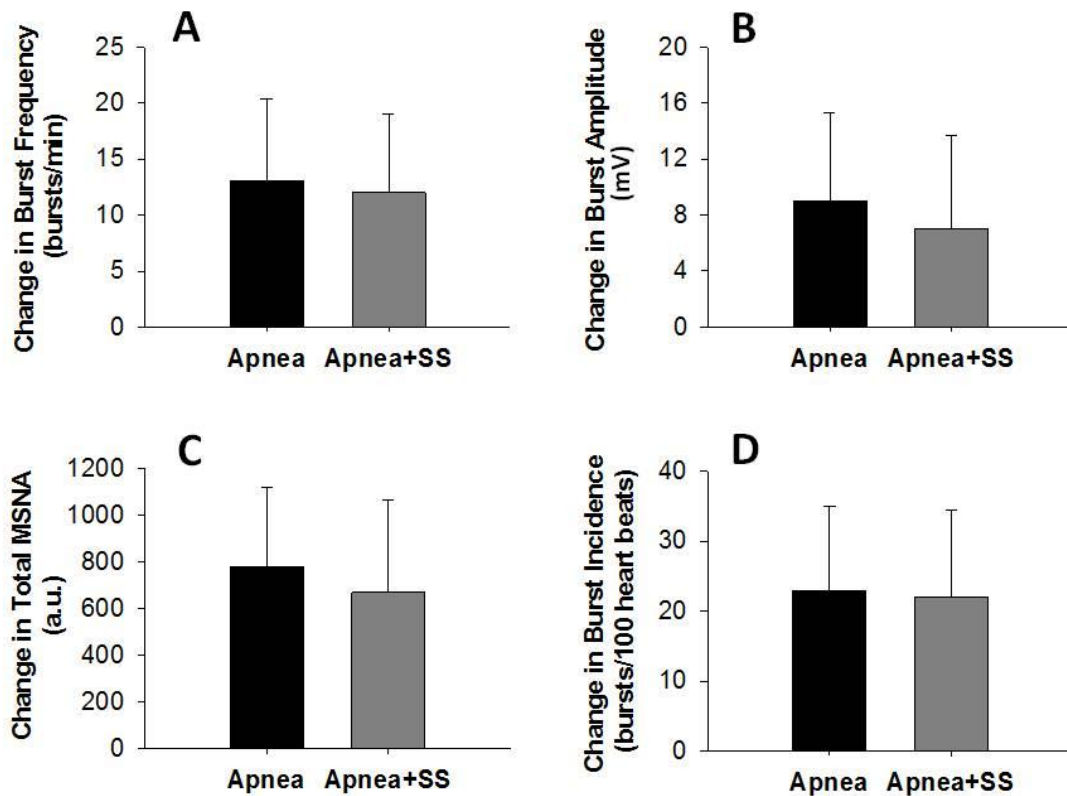
**Figure 4.3 -- Changes in MSNA Burst Frequency (Panel A), Burst Amplitude (Panel B), Total MSNA (Panel C) and Burst Incidence (Panel D) during expiratory apnea (Apnea) and apnea+somatosensory stimulation (Apnea+SS).**

**4.3.2   Neuroimaging Responses**

**4.3.2.1 SS**

Regions of interest associated with increased activity during SS included the left mid-superior insula and left prefrontal cortex (Table 4.4, Figure 4.4).

**4.3.2.2 LBNP and LBNP+SS**

LBNP was associated with increased activity in the right mid-superior insula and right dorsal ACC, and subtraction analysis showed absence of activity in these regions during LBNP+SS (Table 4.4, Figures 4.5, 4.6).  In response to LBNP and LBNP+SS, increased signal intensity was observed in the amygdala and cerebellum (Table 4.4, Figure 4.5).  Decreased activity during LBNP as well as LBNP+SS occurred in the subgenual ACC, prefrontal cortex, and mediodorsal thalamus (Table 4.4, Figure 4.5).  Decreased BOLD activity observed during LBNP+SS and not during LBNP occurred in the right posterior insula (Table 4.4, Figures 4.5, 4.6).

**4.3.2.3 Apnea and Apnea+SS**

Brain regions showing increased BOLD activation during both Apnea and Apnea+SS included the anterior insula, dorsal ACC, mediodorsal thalamus and cerebellar nuclei (Table 4.5, Figure 4.7).  The effect size (BOLD percent signal change) in the right anterior insula was greater during Apnea+SS compared to Apnea alone, whereas activity in the right dorsal ACC was greater during Apnea compared to Apnea+SS (Figure 4.6).  Decreased activity in both conditions was observed in the cerebellum (Table 4.5, Figure 4.7).  Apnea but not Apnea+SS was associated with decreased activity in the right posterior insula (Table 4.5, Figures 4.6, 4.7).

**Table 4.4 -- Brain regions associated with somatosensory stimulation (SS), lower-body negative pressure (LBNP), and lower-body negative pressure+ somatosensory stimulation (LBNP+SS)**

| Location | Side | MNI (x, y, z) | T-score | Z-score |
|---|---|---|---|---|
| **A.  SS  - Increased Activity** | | | | |
| Insula (middle superior) | L | -40, 4, 18 | 3.04 | 3.69 |
| Prefrontal cortex | L | -4, 48, -12 | 3.26 | 2.77 |
| **B.  LBNP - Increased Activity** | | | | |
| Insula (middle superior) | R | 32, 12, 14 | 3.74 | 3.45 |
| Dorsal anterior cingulate | R | 16, 40, 20 | 4.25 | 3.83 |
| Amygdala | R | 28, -2, -26 | 3.06 | 2.88 |
| Cerebellum | L | -32, -50, -36 | 4.71 | 4.16 |
| Cerebellum | R | 44, -58, -36 | 3.60 | 3.32 |
| **C.  LBNP - Decreased Activity** | | | | |
| Subgenual anterior cingulate | R | 8, 34, -8 | 4.07 | 3.69 |
| Prefrontal cortex | L | -4, 32, -18 | 3.70 | 3.40 |
| Prefrontal cortex | R | 4, 42, -22 | 3.53 | 3.27 |
| Thalamus (medial dorsal nucleus) | L | -10, -18, 0 | 3.01 | 2.84 |
| **D.  LBNP+SS - Increased Activity** | | | | |
| Amygdala | R | 30, -4, -22 | 3.03 | 2.86 |
| Cerebellum | L | -36, -54, -40 | 4.70 | 4.16 |
| Cerebellum | R | 42, -56, -38 | 3.45 | 3.21 |
| **E.  LBNP+SS - Decreased Activity** | | | | |
| Insula (posterior) | R | 34, -26, 16 | 4.42 | 3.96 |
| Subgenual anterior cingulate | R | 8, 34, -8 | 4.68 | 4.14 |
| Prefrontal cortex | L | -2, 34, -16 | 3.67 | 3.38 |
| Prefrontal cortex | R | 4, 42, -22 | 3.85 | 3.52 |
| Thalamus (medial dorsal nucleus) | L | -10, -20, 6 | 3.27 | 3.05 |
| Thalamus (medial dorsal nucleus) | R | 12, -20, 6 | 3.23 | 3.02 |

MNI, Montreal Neurologic Institute co-ordinates; L, left; R, right.
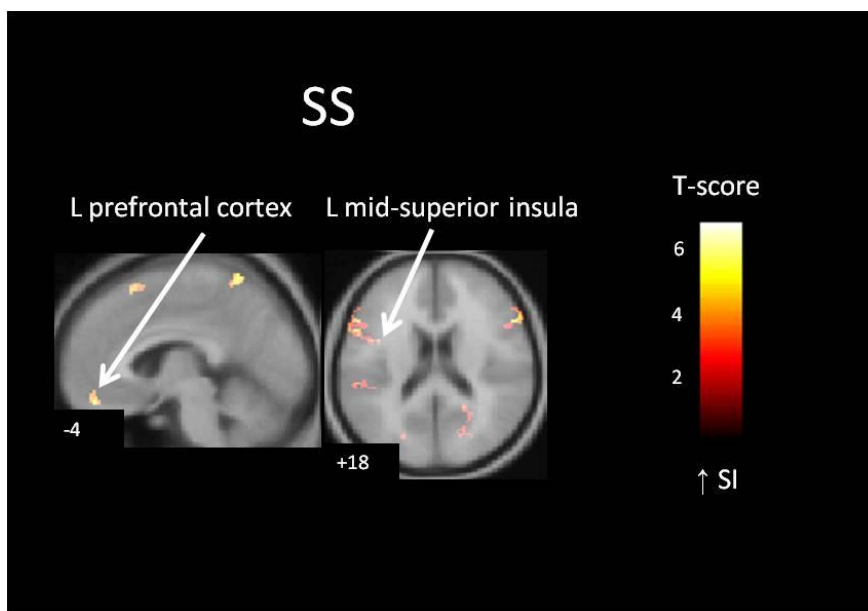
**Figure 4.4 – Blood-oxygenation level-dependent signal intensity (SI) changes in brain regions associated with somatosensory stimulation (SS).**

**Figure 4.5 – Blood-oxygenation level-dependent signal intensity (SI) changes in brain regions associated with lower-body negative pressure (LBNP), and lower-body negative pressure + somatosensory stimulation (LBNP+SS).**

**Table 4.5 -- Brain regions associated with apnea, and apnea+somatosensory stimulation (Apnea+SS)**

| Location | Side | MNI (x, y, z) | T-score | Z-score |
|---|---|---|---|---|
| **A.   Apnea - Increased Activity** | | | | |
| Insula (anterior) | L | -38, 16, -4 | 3.40 | 3.16 |
| Insula  (anterior) | R | 40, 20, -6 | 5.26 | 4.55 |
| Dorsal anterior cingulate | L | -4, 30, 34 | 4.11 | 3.73 |
| Dorsal anterior cingulate | R | 4, 32, 32 | 4.78 | 4.21 |
| Cerebellum | L | -20, -52, -28 | 3.10 | 2.91 |
| Cerebellum | L | -22, -78, -50 | 3.49 | 3.23 |
| Thalamus (medial dorsal nucleus) | L | -10, -16, 6 | 5.72 | 4.84 |
| Thalamus (medial dorsal nucleus) | R | 12, -16, 6 | 4.89 | 4.30 |
| **B.   Apnea - Decreased Activity** | | | | |
| Insula (posterior) | R | 42, -8, 14 | 3.47 | 3.22 |
| Cerebellum | R | 34, -38, -28 | 4.80 | 4.23 |
| Cerebellum | R | 44, -60, -26 | 4.32 | 3.88 |
| **C.   Apnea+SS - Increased Activity** | | | | |
| Insula (anterior) | R | 48, 16, -2 | 3.85 | 3.53 |
| Dorsal anterior cingulate | R | 6, 30, 30 | 3.24 | 3.03 |
| Cerebellum | L | -16, -52, -32 | 3.13 | 2.94 |
| Thalamus (medial dorsal nucleus) | L | -10, -16, 6 | 5.99 | 5.02 |
| Thalamus (medial dorsal nucleus) | R | 10, -16, 8 | 5.12 | 4.45 |
| **D.   Apnea+SS - Decreased Activity** | | | | |
| Cerebellum | R | 40, -68, -24 | 3.54 | 3.28 |

MNI, Montreal Neurologic Institute co-ordinates; L, left; R, right.
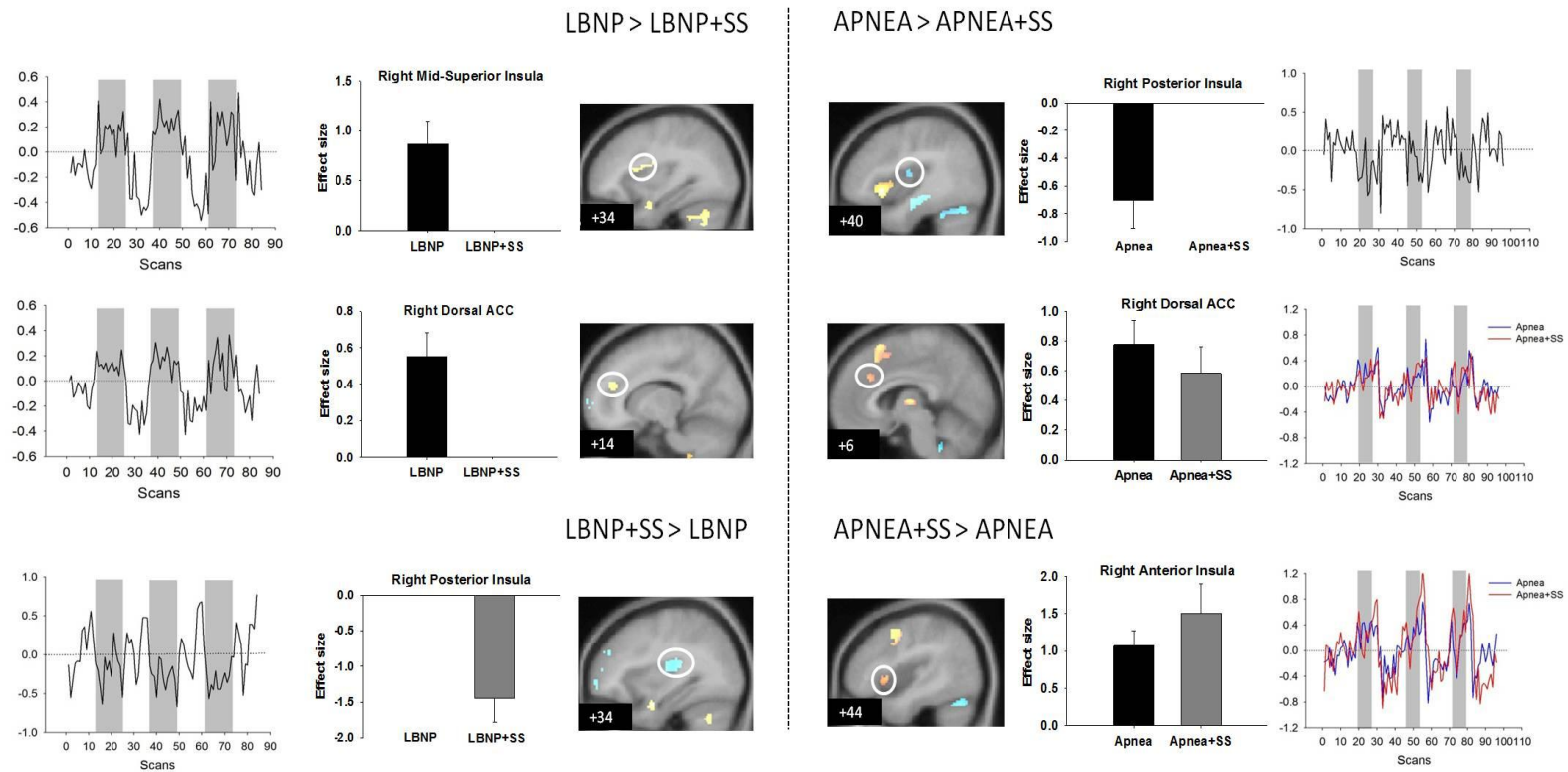
**Figure 4.6 -- Effect sizes (percent signal change ± SE) and time courses of the BOLD responses. Left side shows areas with increased and decreased activity during lower-body negative pressure (LBNP) and lower-body negative pressure + somatosensory stimulation (LBNP+SS). Right side shows areas with increased and decreased activity during apnea and apnea + somatosensory stimulation (Apnea+SS). ACC, anterior cingulate cortex.**
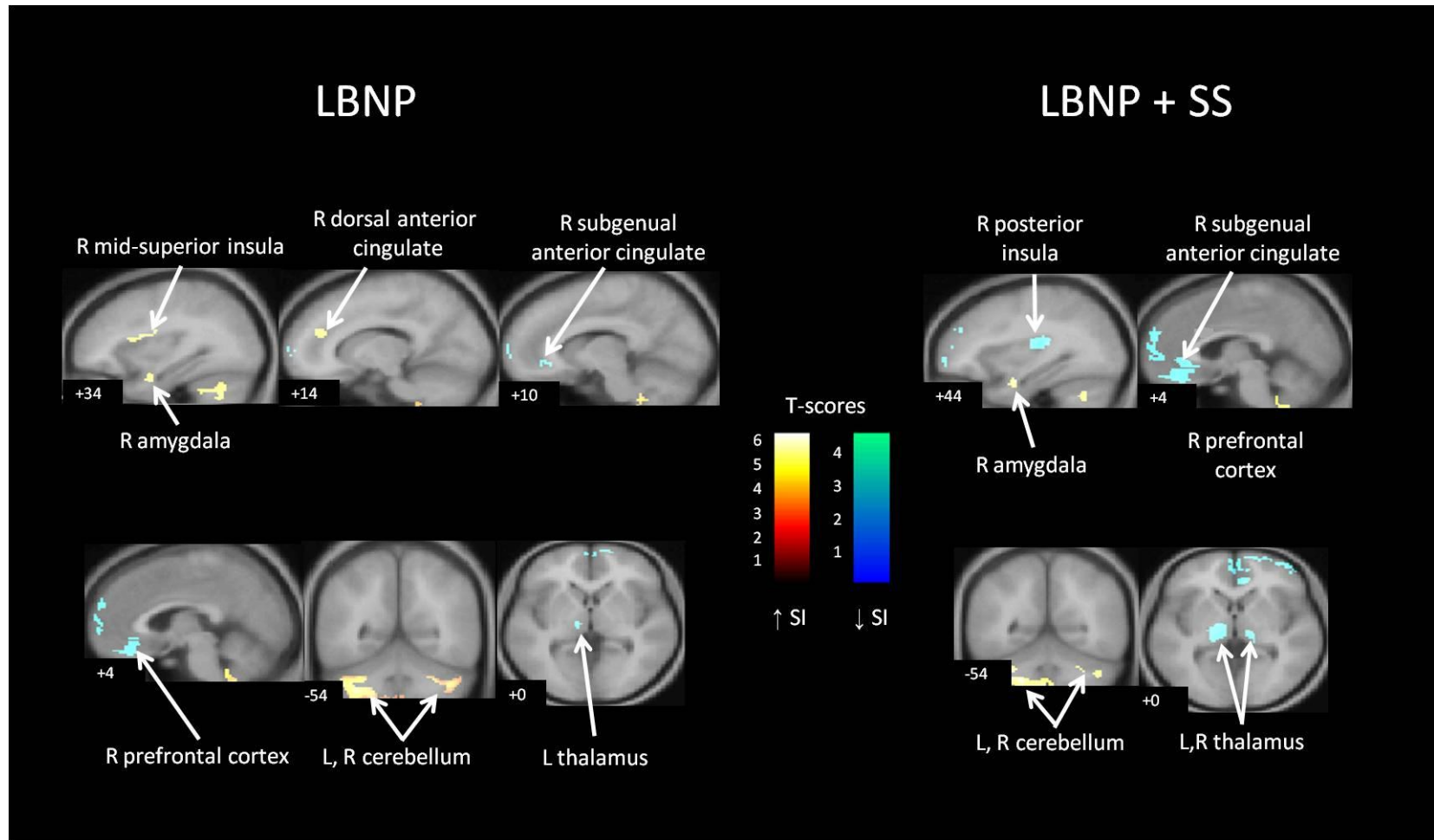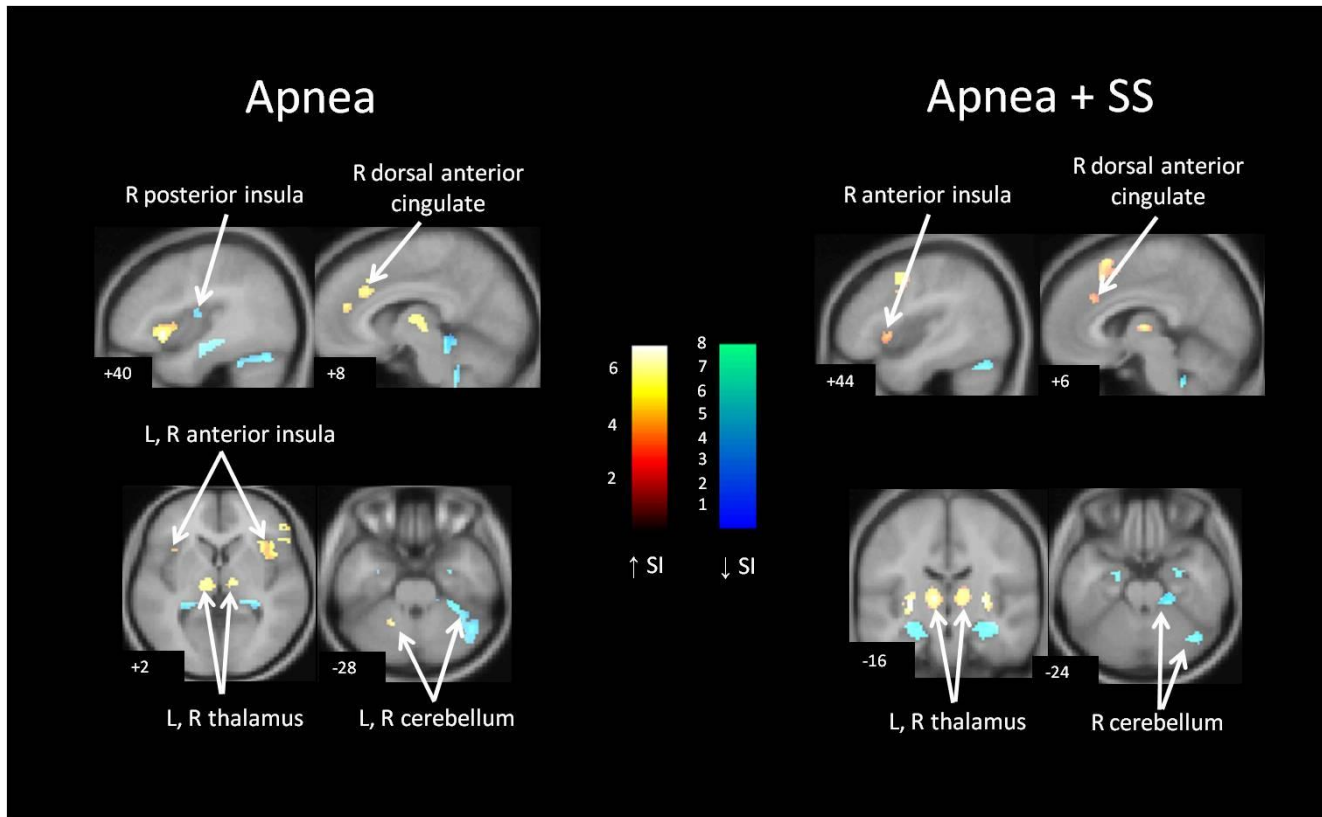
**Figure 4.7 – Blood-oxygenation level-dependent signal intensity (SI) changes in brain regions associated with expiratory apnea (Apnea), and expiratory apnea + somatosensory stimulation (Apnea+SS).**

**4.4    DISCUSSION**

This study presents the first observations of the forebrain organization associated with sensory gating interactions between baroreceptor and skeletal muscle sensory afferents with concurrent outcome measures of sympathetic nerve activity. By itself, SS did not affect baseline MSNA and was associated with activity in the left insula and prefrontal cortex. Baroreceptor unloading during LBNP was associated with increased activity in the right insula and dorsal ACC, as well as decreased activity in the subgenual ACC and prefrontal cortex, consistent with increased MSNA and HR during LBNP. However, SS during baroreceptor unloading attenuated the LBNP-induced increase in MSNA burst frequency and reversed the concurrent activation of the right insula and dorsal ACC. In addition, SS did not affect the LBNP-induced deactivation in the subgenual ACC and prefrontal cortex. In contrast, SS during expiratory apnea did not affect the rise in MSNA nor abolish the activity in the right insula and dorsal ACC. These findings suggest that the effect of muscle afferent input on neural patterns of activity and on sympathetic outflow is dependent upon, and are specific to, the levels of baroreceptor afferent input and not just a state of elevated sympathetic outflow. The sympatho-inhibitory effect of somatosensory stimulation, observed only during LBNP, was associated with a lack of activation within the right insula and dorsal ACC but without change to the deactivation patterns observed during baroreceptor unloading alone. Thus, baroreceptor activity may operate as a gating mechanism for the distribution of somatosensory afferents.

### 4.4.1   Physiological Responses

We utilized sensory level stimulation to recruit the large diameter type I and II afferents during low baroreceptor input and observed an inhibitory effect on MSNA. Previously, a reduction in systolic BP as well as a smaller increase in MSNA burst frequency and total activity was reported during concurrent handgrip exercise and TENS (21).  This inhibition was attributed to an interaction between type III and IV afferent fibers activated during exercise with type I and II fibers at the spinal cord. While that interpretation may apply for fatiguing muscular contractions, the current observations suggest that the type I and II afferents interact with baroreceptor afferents in higher cortical centers.  In addition, it has been found that the increase in diastolic BP is lower during a 2 min moderate intensity handgrip test during TENS at a non-painful intensity (45).  However, no changes in HR or BP were observed when TENS was applied during Valsalva's manoeuvre (45).  In-as-much as LBNP and Valsalva's manoeuvre engage baroreflex mechanisms, the current data support the idea that somatosensory inputs do not affect HR or BP per se, but rather focus on a modest attenuation of sympathetic outflow.  We found no change in arterial pressure or MSNA during apnea combined with SS compared to apnea alone.  These observations suggest that the impact on sympathetic tone depends on baroreceptor activity and not just a state of heightened sympathetic outflow.

Although Hollman and Morgan (1997) suggested the depressor effect of SS was due to integration of sensory afferents within the spinal cord, the current evidence suggests that the reduction in MSNA with sensory stimulation during baroreceptor unloading may be attributed to processing within cortical autonomic structures, as

introduced above. Baroreceptor afferents synapse in the NTS (28; 47), and tracer techniques and electrophysiological recordings reveal monosynaptic projections of type I and II skeletal muscle afferents to the NTS (34; 39). In addition, horseradish peroxidase tracer studies in rodents have shown retrograde and anterograde projections between the insula and NTS (44), including anterograde tracings to the parasympathetic motor nuclei in the NTS (46). Thus, relays between medullary circuits and higher cortical centers including the insula may be functionally involved in modulating the convergent inputs.

### 4.4.2   Neural Responses

### 4.4.2.1 Lower-body Negative Pressure

The cortical neural responses to LBNP observed in the current study support the baroreceptor-mediated autonomic network established during mild and moderate levels of LBNP including the right superior insula, dorsal ACC, cerebellum, amygdala and prefrontal cortex (25; 26). Experimental studies indicate further that electrical stimulation of the posterior insula increases HR and BP in anesthetized rats (44), and a large predominance of sympatho-excitatory neurons exists in the right posterior insula (36; 56). Lateralization of cardiovascular representation within the insula appears to exist in humans, wherein HR and BP increase upon stimulation of the right insula, and left insular stimulation usually produces depressed cardiac and pressor responses (37). In animal stimulation studies, the superior insula is associated with tachycardia whereas inferior portions produce bradycardia (36). Furthermore, the current finding of enhanced right superior insular activation during LBNP supports these earlier observations of the involvement of this region with sympathetic outflow. The lack of

activation in the insula during LBNP+SS combined with a reduction in the rise in MSNA burst frequency, suggests a sympatho-inhibitory effect of SS and supports the interpretation that this insular region is involved in sympathetic modulation. In addition, decreased activity was observed in the right posterior insula during LBNP+SS, a region that contains sympatho-excitatory neurons as well as neurons responsive to convergent baroreceptor and muscle receptor input (56; 57). The right posterior insula is tonically active (5) and our results suggest that the right posterior insula is involved in basal sympathetic regulation and is inhibited with type I and II muscle afferent input during baroreceptor unloading.

The MPFC is involved in a range of visceromotor autonomic functions (33) including hypotensive (17), sympatho-inhibitory (50) and parasympathetic responses (55). The dorsal ACC is engaged during heightened levels of sympathetic drive during baroreceptor unloading (26), whereas the ventral ACC is implicated in parasympathetic activity/sympatho-inhibition (7; 25; 50) and bradycardia (4). Consistent with increases in MSNA during LBNP, we observed activation in the dorsal ACC, and decreased activity in the subgenual ACC and prefrontal cortex. With concomitant LBNP and SS, dorsal ACC activation was absent while deactivation was maintained in the right subgenual ACC and prefrontal cortex. The lack of dorsal ACC involvement with LBNP+SS may reflect a sympatho-inhibitory effect, whereas the persistent deactivation patterns in the subgenual ACC and prefrontal cortex may be related to a state of overall increased sympathetic activity and/or, as shown in other models (13; 14; 55) decreased parasympathetic activity with LBNP. This latter interpretation is supported by similar changes in HR during LBNP with or without SS. Thus the prefrontal cortex/subgenual

ACC may continue to modulate the HR response to LBNP with and without concurrent somatosensory stimulation.

### 4.4.2.2 Expiratory Apnea

End-expiratory apnea evoked an increase in MSNA that was associated with activity patterns in the anterior insula, dorsal ACC and cerebellar nuclei, similar to patterns evoked by inspiratory apnea reported earlier (29). Increases in BOLD activity in the anterior insula have been reported during respiratory challenges including Valsalva's manoeuvre and loaded breathing (20; 30). In addition, inspiratory loading has been associated with increased signal intensity in the deep cerebellar nuclei (18). The ACC has also been associated with autonomic function in HR and BP control in obstructive sleep apnea as well with an intention role of upper airway muscle control (20).

SS did not change apnea-induced activation in the right anterior insula, right dorsal ACC and left cerebellum. These comparable central responses during Apnea and Apnea+SS combined with similar increases in MSNA suggest that somatosensory stimulation did not impact sympathetic outflow during apnea. Thus, we suggest that integrating somatosensory stimuli during expiratory breath hold does not depress sympathetic autonomic function. The interpretation that somatosensory afferents interact with baroreflex but not chemoreflex pathways is supported by evidence from studies in rats whereby skeletal muscle afferent stimulation attenuated the reflex bradycardia induced by ramp increases in arterial pressure but not during chemoreflex activation (42). In light of this, we observed stronger activation in the right anterior insula during Apnea+SS compared to Apnea, whereas stronger activation in the dorsal

ACC occurred during Apnea compared to Apnea+SS. The time courses of activity were similar between the insula and dorsal ACC; thus, both regions may be involved in the initiation of MSNA with apnea. In addition, the activation patterns present in the anterior insula and dorsal ACC support the conjoint action of these two regions as a system involved in the generation of autonomic responses (31). The functional connectivity of these two regions is supported by structural connections observed between Brodmann area 24 corresponding to the dorsal ACC and the insula (32; 52), as well as the presence of von Economo neurons in the anterior insula and ACC, which appear to form the basis for the connections between these two regions (7).

### 4.4.3   Limitations

In the apnea sessions, prior re-breathing was not performed so that similar basal levels of end tidal $CO_2$ would be achieved between all participants. However, MSNA was increased comparably during Apnea compared to LBNP, with similar increases in burst frequency. Importantly, arterial pressure was not significantly higher than baseline during apnea; thus the effect of afferent BP information to the cortical autonomic regions via the baroreceptors was minimized. The ability to perform 20 s expiratory breath holds was tolerable for the participants. However, as the urge to breathe begins after approximately 10 s (3), we cannot rule out activation patterns related to the emotional and mechanical components in the drive to breathe.

### 4.4.4   Conclusions

In conclusion, we have identified central and autonomic responses to the interactive effects of baroreceptor unloading and type I and II muscle sensory afferent input. The sympatho-inhibition occurring with somatosensory input during

baroreceptor unloading is suggested to be modulated cortically, and appears to be a reflex-specific mechanism as sensory processing during expiratory apnea did not alter the cortical responses to chemoreflex activation. These findings indicate a discrete network of sites involved in convergent baroreceptive and somatosensory processing that modulate autonomic control.

## 4.5     Reference List

1. **Ashburner J and Friston K**. Multimodal image coregistration and partitioning - a unified framework. *NeuroImage* 6: 209-217, 1997.

2. **Bennarroch EE**. Functional anatomy of the central autonomic network. In: Central Autonomic Network: Functional Organization and Clinical Correlations, Armonk, NY: Futura Publishing Company Inc., 1997, p. 29-60.

3. **Bloch-Salisbury E, Binks AP, Banzett RB and Schwartzstein RM**. Mechanical chest-wall compression does not relieve air hunger. *Respiratory Physiology & Neurobiology* 134: 177-190, 2003.

4. **Buchanan S, Thompson RH, Maxwell BL and Powell DA**. Efferent connections of the medial prefrontal cortex in the rabbit. *Experimental Brain Research* 100: 469-483, 1994.

5. **Butcher KS and Cechetto DF**. Autonomic responses of the insular cortex in hypertensive and normotensive rats. *American Journal of Physiology* 268: R214-R222, 1995.

6. **Cechetto DF and Saper CB**. Role of the cerebral cortex in autonomic function. In: Central Regulation of Autonomic Functions, edited by Loewy AD and Spyer KM. New York: Oxford University Press, 1990, p. 208-223.

7. **Craig AD**. How do you feel - now? The anterior insula and human awareness. *Nature ReviewsNeuroscience* 10: 59-70, 2009.

8. **Critchley HD, Mathias CJ, Josephs O, O'Doherty J, Zanini S, Dewar B, Cipolotti L, Shallice T and Dolan RJ**. Human cingulate cortex and autonomic control: converging neuroimaging and clinical evidence. *Brain* 126: 2139-2152, 2003.

8. **Dampney RAL, Coleman MJ, Fontes MAP, Hirooka Y, Horiuchi J, Li YW and Polson JW**. Central mechanisms underlying short- and long-term regulation of the cardiovascular system. *Clinical and Experimental Pharmacology and Physiology* 29: 261-268, 2002.

9. **Delius W, Hagbarth KE, Hongell A and Wallin BG**. General characteristics of sympathetic activity in human muscle nerves. *Acta physiologica Scandinavica* 84: 65-81, 1972.

10. **Donadio V, Kallio M, Karlsson T, Nordin M and Wallin BG**. Inhibition of human muscle sympathetic activity by sensory stimulation. *Journal of Physiology* 544: 285-292, 2002.

11. **Eckberg DL and Orshan CR**. Respiratory and baroreceptor reflex interactions in man. *The Journal of Clinical Investigation* 59: 780-785, 1977.

12. **Fagius J and Sundlof G**. The diving response in man: effects on sympathetic activity in muscle and skin nerve fascicles. *Journal of Physiology* 377: 429-443, 1986.

13. **Gianaros PJ, Van Der Veen FM and Jennings JR**. Regional cerebral blood flow correlates with heart period and high-frequency heart period variability during working-memory tasks: Implications for the cortical and subcortical regulation of cardiac autonomic activity. *Psychophysiology* 41: 521-530, 2004.

14. **Goswami R, Frances MF and Shoemaker JK**. Representation of somatosensory inputs within the cortical autonomic network. *NeuroImage* 54: 1211-1220, 2011.

15. **Gray M, Rylander K, Harrison NA, Wallin BG and Critchley HD**. Following one's heart: cardiac rhythms gate central initiation of sympathetic reflexes. *The Journal of Neuroscience* 29: 1817-1825, 2009.

16. **Hagbarth KE and Vallbo AB**. Pulse and respiratory grouping of sympathetic impulses in human muscle nerves. *Acta physiologica Scandinavica* 74: 96-108, 1968.

17. **Hardy SGP and Holmes DE**. Prefrontal stimulus-produced hypotension in rat. *Experimental Brain Research* 73: 249-255, 1988.

18. **Harper RM, Gozal D, Bandler R, Spriggs D, Lee J and Alger J**. Regional brain activation in humans during respiratory and blood pressure challenges. *Clinical and Experimental Pharmacology and Physiology* 25: 483-486, 1998.

19. **Henderson LA, Richard CA, Macey PM, Runquist ML, Yu PL, Galons J and arper RM**. Functional magnetic resonance signal changes in neural structures to baroreceptor reflex activation. *Journal of Applied Physiology* 96: 693-703, 2004.

20. **Henderson LA, Woo MA, Macey PM, Macey KE, Frysinger RC, Alger JR, Yan-Go F and Harper RM**. Neural responses during Valsalva maneuvers in obstructive sleep apnea syndrome. *Journal of Applied Physiology* 94: 1063-1074, 2003.

21. **Hollman JE and Morgan BJ**. Effect of transcutaneous electrical nerve stimulation on the pressor response to static handgrip exercise. *Physical Therapy* 77: 28-36, 1997.

22. **Kaada B, Flatheim E and Woie L**. Low-frequency transcutaneous nerve stimulation in mild/moderate hypertension. *Clinical Physiology* 11: 161-168, 1991.

23. **Kaada B, Vik-Mo H, Rosland G, Woie L and Opstad PK**. Transcutaneous nerve stimulation in patients with coronary arterial disease: Haemodynamic and biochemical effects. *European Heart Journal* 11: 447-453, 1990.

24. **Kalia M, Mei SS and Kao FF**. Central projections from ergoreceptors (C fibers) in muscle involved in cardiopulmonary responses to static exercise. *Circulation Research* 48: I48-I62, 1981.

25. **Kimmerly DS, O'Leary DD, Menon RS, Gati JS and Shoemaker JK**. Cortical regions associated with autonomic cardiovascular regulation during lower body negative pressure in humans. *Journal of Physiology* 569: 331-345, 2005.

26. **Kimmerly DS, Wong SW, Menon RS and Shoemaker JK**. Forebrain neural patterns associated with sex differences in autonomic and cardiovascular function during baroreceptor unloading. *American Journal of Physiology - Regulatory, Integrative and Comparative Physiology* 292: R715-R722, 2006.

27. **Lancaster JL, Woldorff MG, Parsons LM, Liotti M, Freitas CS, Rainey L, Kochunov PV, Nickerson D, Mikiten SA and Fox PT**. Automated Talairach atlas labels for functional brain mapping. *Human Brain Mapping* 10: 120-131, 2000.

28. **Loewy AD and Spyer KM**. *Central Regulation of Autonomic Functions*. New York: Oxford Univ. Press, 1990.

29. **Macefield VG, Gandevia SC and Henderson LA**. Neural sites involved in the sustained increase in muscle sympathetic nerve activity induced by inspiratory capacity apnea: a fMRI study. *Journal of Applied Physiology* 100: 266-273, 2006.

30. **Macey PM, Macey KE, Henderson LA, Alger JR, Frysinger RC, Woo MA, Yan-Go F and Harper RM**. Functional magnetic resonance imaging responses to expiratory loading in obstructive sleep apnea. *Respiratory Physiology & Neurobiology* 138: 275-290, 2003.

31. **Medford N and Critchley HD**. Conjoint activity of anterior insular and anterior cingulate cortex: awareness and response. *Brain Structure and Function* 214: 535-549, 2010.

32. **Mesulam MM and Mufson EJ**. Insula of the old world monkey. III: Efferent cortical output and comments on function. *The Journal of Comparative Neurology* 212: 38-52, 1982.

33. **Neafsey EJ**. Prefrontal cortical control of the autonomic nervous system: Anatomical and physiological observations. *Progress in Brain Research* 85: 147-165, 1990.

34. **Nyberg G and Blomqvist A**. The central projection of muscle afferent fibres to the lower medulla and upper spinal cord: an anatomical study in the cat with the transganglionic transport method. *The Journal of Comparative Neurology* 230: 99-109, 1984.

35. **Oldfield RC**. The assessment and analysis of handedness: the Edinburgh inventory. *Neuropsychologia* 9: 97-113, 1971.

36. **Oppenheimer SM and Cechetto DF**. Cardiac chronotropic organization of the rat insular cortex. *Brain Research* 533: 66-72, 1990.

37. **Oppenheimer SM, Gelb A, Girvin JP and Hachinski VC**. Cardiovascular effects of human insular cortex stimulation. *Neurology* 42: 1727-1732, 1992.

38. **Owens S, Atkinson ER and Lees DE**. Thermographic evidence of reduced sympathetic tone with transcutaneous nerve stimulation. *Anesthesiology* 50: 62-65, 1979.

39. **Person RJ**. Somatic and vagal afferent convergence on solitary tract neurons in cat: electrophysiological characteristics. *Neuroscience* 30: 283-295, 1989.

40. **Potts JT, Lee SM and Anguelov PI**. Tracing of projection neurons from the cervical dorsal horn to the medulla with the anterograde tracer biotinylated dextran amine1. *Autonomic Neuroscience: Basic and Clinical* 98: 64-69, 2002.

41. **Potts JT and Li J**. Interaction between carotid baroreflex and exercise pressor reflex depends on baroreceptor afferent input. *American Journal of Physiology - Heart and Circulatory Physiology* 43: H1841-H1847, 1998.

42. **Potts JT, Paton JFR, Mitchell JH, Garry MG, Kline G, Anguelov PT and Lee SM**. Contraction-sensitive skeletal muscle muscle afferents inhibit arterial baroreceptor signalling in the nucleus of the solitary tract: role of intrinsic GABA interneurons. *Neuroscience* 119: 201-214, 2003.

43. **Radhakrishnan R and Sluka KA**. Deep tissue afferents, but not cutaneous afferents, mediate transcutaneous electrical nerve stimulation-induced antihyperalgesia. *The Journal of Pain* 6: 673-680, 2005.

44. **Ruggiero DA, Mraovitch S, Granata AR, Anwar M and Reis DJ**. A role of insular cortex in cardiovascular function. *The Journal of Comparative Neurology* 257: 189-207, 1987.

45. **Sanderson JE, Tomlinson B, Lau MSW, So KWH, Cheung AHK, Critchley JAJH and Woo KS**. The effect of transcutaneous electrical nerve stimulation (TENS) on autonomic cardiovascular reflexes. *Clinical Autonomic Research* 5: 81-84, 1995.

46. **Shipley MT**. Insular cortex projection to the nucleus of the solitary tract and brainstem visceromotor regions in the mouse. *Brain Research Bulletin* 8: 139-148, 1982.

47. **Spyer KM**. Central nervous mechanisms contributing to cardiovascular control. *Journal of Physiology* 474: 1-19, 1994.

48. **Steinback CD, Breskovic T, Frances M, Dujic Z and Shoemaker JK**. Ventilatory restraint of sympathetic activity during chemoreflex stress. *American Journal of Physiology - Regulatory, Integrative and Comparative Physiology* 299: 1407-1414, 2010.

49. **Sundlof G and Wallin BG**. Effect of lower body negative pressure on human muscle sympathetic nerve activity. *Journal of Physiology* 278: 525-532, 1978.

50. **Verberne AJ**. Medullary sympathoexcitatory neurons are inhibited by activation of the medial prefrontal cortex in the rat. *The American Journal of Physiology* 270: R713-R719, 1996.

51. **Verberne AJM and Owens NC**. Cortical modulation of the cardiovascular system. *Progress in Neurobiology* 54: 149-168, 1998.

52. **Vogt BA and Pandya DN**. Cingulate cortex of the rhesus monkey: II. Cortical afferents. *The Journal of Comparative Neurology* 262: 271-289, 1987.

53. **Watenpaugh DE, Muenter NK, Wasmund WL, Wasmund SL and Smith ML**. Post-apneic inhalation reverses apnea-induced sympathoexcitation before restoration of blood oxygen levels. *Sleep* 22: 435-440, 1999.

54. **Wesseling KH, Jansen JR, Settels JJ and Schreuder JJ**. Computation of aortic flow from pressure in humans using a nonlinear, three-element model. *Journal of Applied Physiology* 74: 2566-2573, 1993.

55. **Wong SW, Masse N, Kimmerly DS, Menon RS and Shoemaker JK**. Ventral medial prefrontal cortex and cardiovagal control in conscious humans. *NeuroImage* 35: 698-708, 2007.

56. **Zhang ZH, Dougherty PM and Oppenheimer SM**. Characterization of baroreceptor-related neurons in the monkey insular cortex. *Brain Research* 796: 303-306, 1998.

57. **Zhang ZH, Dougherty PM and Oppenheimer SM**. Monkey insular cortex neurons respond to baroreceptive and somatosensory convergent inputs. *Neuroscience* 94: 351-360, 1999.

## Chapter 5 General Discussion and Perspectives

The importance of the cerebral cortex in modulating autonomic regulatory functions including heart rate (HR), blood pressure, sympathetic and parasympathetic activity, gastrointestinal and sudomotor control has been well established.  Various tasks have been utilized to elicit autonomic responses in human neuroimaging studies to characterize the regions involved with cardiovascular function.  However, tasks such as exercise, mental stress and chemoreflex stressors activate multiple neural pathways including central command, baroreflex activity and somatosensory afferents.  Of these neural pathways, the cortical autonomic regions associated with the integration of somatosensory afferents have not been identified.  Previous studies have found linkages between somatosensory stimulation and decreased sympathetic tone and hypotension. Thus, the association between the somatosensory system and the autonomic nervous system required further study on a) the representation of somatosensory afferents within the cortical autonomic regions, and how the regions may operate as a network to regulate autonomic function and somatosensory integration; b) the association between brain regions activated during  somatosensory stimulation and measures of autonomic cardiovascular activity; and c) organization of somatosensory afferents within the cortical autonomic network (CAN) during altered levels of baroreceptor activity.

One novel finding of this research is that somatosensory signals from skeletal muscle are represented in specific regions of the CAN and that they have an impact on increasing vagal outflow to the heart.  This was exemplified by the observation that type I and II afferent stimulation (sub-motor threshold stimulation) is associated with activation in the ventral medial prefrontal cortex (vMPFC) and subgenual anterior

cingulate cortex (ACC), regions implicated with parasympathetic activity. In addition, there was a tendency towards increased heart rate variability during type I and II afferent stimulation, indicative of increased parasympathetic outflow. Motor threshold stimulation to additionally recruit the type III and IV afferents led to increased activity in the left posterior insula but did not impact the vMPFC or subgenual ACC. This is important on two levels. First, this is the first neuroanatomical description of how these afferents are represented in supramedullary sites. Earlier research has indicated their anatomical distribution within the brainstem, and within sensori-motor cortical regions. The anatomical pathways studied in the current study shows how axonal connectivity exists from the thalamus to the insula and from there distributions exist both anteriorly to the subgenual ACC and MPFC, superiorly to the sensory cortex and posteriorly to the posterior cingulate cortex (PCC). These structural connections may underlie the conjoint activity of the anterior insula-ACC in autonomic regulation, and the posterior insula-PCC involvement in sensory processing and environmental monitoring. Second, the new observation that somatosensory stimulation of such a small forearm surface area can have effects on parasympathetic activity points to an interesting feature of the integrative nature of muscle sensory afferents. In particular, whereas the types III and IV afferents raise sympathetic outflow during exercise, the type I and II may impact parasympathetic outflow at rest. How these are integrated into volitional handgrip exercise will have important implications on the concept of descending pathways associated with volitional exercise and the concurrent cardiovascular arousal that occurs with exercise. Also, the finding of somatosensory afferents affecting parasympathetic outflow during sub-motor stimulation levels raises the intriguing possibility that such an

approach could be used as a countermeasure against age-, and disease-related decrements in parasympathetic activity that are so detrimental to cardiac health. The potential for therapeutic use is supported by recent evidence showing the use of vagus nerve stimulation as a treatment for improving mood and cognition in epilepsy, depression and anxiety (1). In addition to the effects of sub-motor threshold stimulation during supine rest with basal levels of baroreceptor loading on parasympathetic control of cardiac function, type I and II afferent stimulation is associated with an inhibitory effect on sympathetic outflow to the vasculature when baroreceptor input to the central nervous system is minimized. Thus, the level of baroreceptor input switches control from a parasympathetic to a sympathetic mechanism during concurrent somatosensory activation. This follows in line with evidence showing baroreceptor activity plays a role in pulmonary modulation of autonomic function and with somatosensory integration of electrical shocks. This will have implications for the integration of sensory inputs during changes in baroreflex activity and central command, which occur during normal physiological fluctuations in HR and during arousal-inducing tasks such as mental stress and exercise.

## 5.1 Reference List

1. **Groves DA and Brown VJ**. Vagal nerve stimulation: a review of its applications and potential mechanisms that mediate its clinical effects. *Neuroscience & Biobehavioral Reviews* 29: 493-500, 2005.

**Appendix A – Supplementary Data Heart Rate Variability**
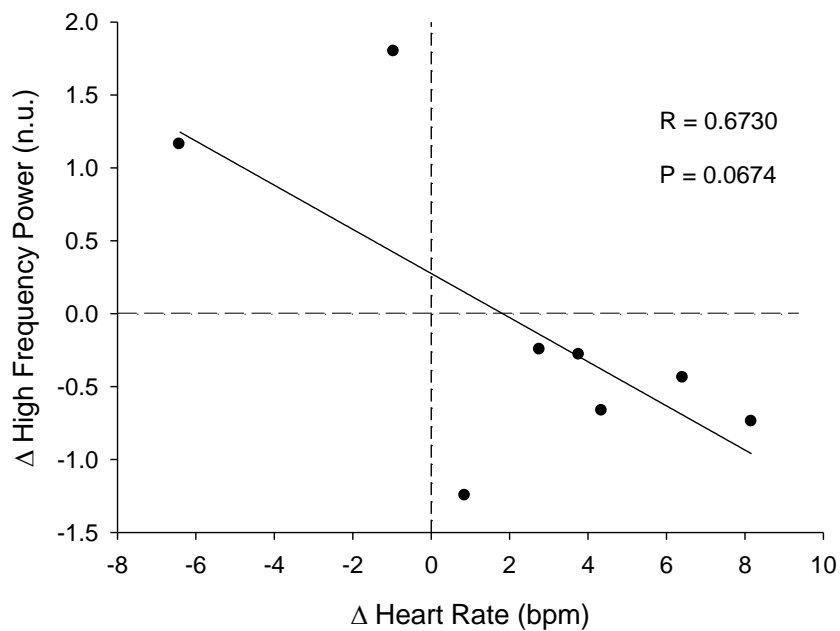


**Figure A.1 -- Change in heart rate for a given change in high frequency power between supine and seated rest. Note two participants with decreased heart rate and increased high frequency power on going from supine to seated rest shown in top left quadrant of origin.**

**Figure A.2 -- Individual data indicating changes in heart rate (top) and high frequency power (bottom) on going from supine rest to seated rest. Bolded lines indicate two participants in whom heart rate decreased and high frequency increased during seated rest.**

# Appendix B -- Ethics Approval

**Office of Research Ethics**

The University of Western Ontario
Room 00045 Dental Sciences Building, London, ON, Canada N6A 5C1
Telephone: (519) 661-3036 Fax: (519) 850-2466 Email: ethics@uwo.ca
Website: www.uwo.ca/research/ethics

**Use of Human Subjects - Ethics Approval Notice**

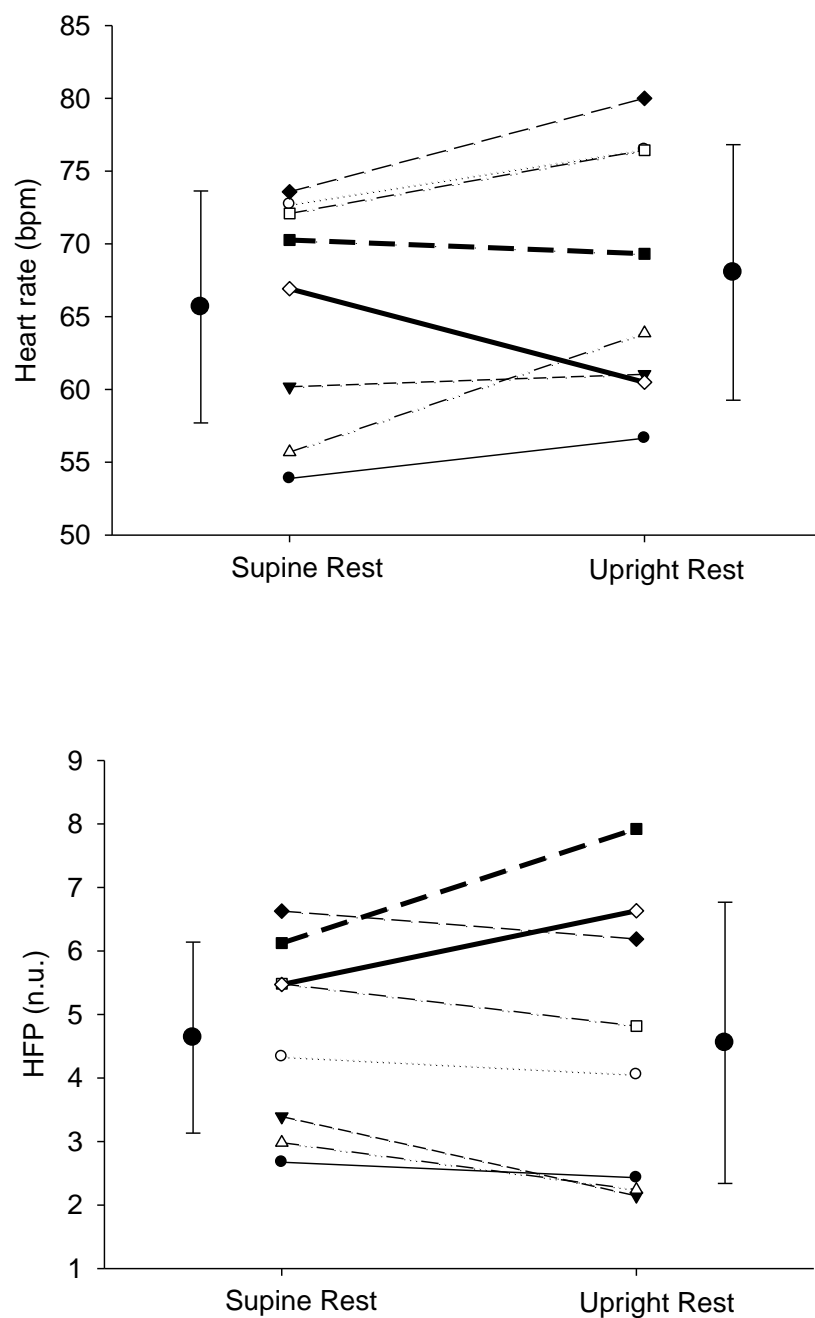| | | | |
|---|---|---|---|
| **Principal Investigator:** | Dr. J.K. Shoemaker | | |
| **Review Number:** | **15059** | **Review Level:** | Full Board |
| **Review Date:** | April 08, 2008 | | |
| **Protocol Title:** | Cortical integration of baroreceptive and somatosensory afferents in humans. | | |
| **Department and Institution:** | Kinesiology, University of Western Ontario | | |
| **Sponsor:** | CANADIAN SPACE AGENCY | | |
| **Ethics Approval Date:** | May 28, 2008 | **Expiry Date:** | December 31, 2010 |
| **Documents Reviewed and Approved:** | UWO Protocol, Letter of information & consent form, and advertisement | | |
| **Documents Received for Information:** | | | |

This is to notify you that The University of Western Ontario Research Ethics Board for Health Sciences Research Involving Human Subjects (HSREB) which is organized and operates according to the Tri-Council Policy Statement: Ethical Conduct of Research Involving Humans and the Health Canada/ICH Good Clinical Practice Practices: Consolidated Guidelines; and the applicable laws and regulations of Ontario has reviewed and granted approval to the above referenced study on the approval date noted above. The membership of this REB also complies with the membership requirements for REB's as defined in Division 5 of the Food and Drug Regulations.

The ethics approval for this study shall remain valid until the expiry date noted above assuming timely and acceptable responses to the HSREB's periodic requests for surveillance and monitoring information. If you require an updated approval notice prior to that time you must request it using the UWO Updated Approval Request Form.

During the course of the research, no deviations from, or changes to, the protocol or consent form may be initiated without prior written approval from the HSREB except when necessary to eliminate immediate hazards to the subject or when the change(s) involve only logistical or administrative aspects of the study (e.g. change of monitor, telephone number). Expedited review of minor change(s) in ongoing studies will be considered. Subjects must receive a copy of the signed information/consent documentation.

Investigators must promptly also report to the HSREB:
    a) changes increasing the risk to the participant(s) and/or affecting significantly the conduct of the study;
    b) all adverse and unexpected experiences or events that are both serious and unexpected;
    c) new information that may adversely affect the safety of the subjects or the conduct of the study.

If these changes/adverse events require a change to the information/consent documentation, and/or recruitment advertisement, the newly revised information/consent documentation, and/or advertisement, must be submitted to this office for approval.

Members of the HSREB who are named as investigators in research studies, or declare a conflict of interest, do not participate in discussion related to nor vote on such studies when they are presented to the HSREB.

Chair of HSREB: Dr. John W. McDonald

| Ethics Officer to Contact for Further Information | | | |
|---|---|---|---|
| ☑ Janice Sutherland (jsutherland@uwo.ca) | ☐ | ☐ Grace Kelly (grace.kelly@uwo.ca) | ☐ Denise Grafton (dgrafton@uwo.ca) |

*This is an official document. Please retain the original in your files.*  cc: ORE File

# Appendix C -- NeuroImage Permission

This is a License Agreement between Ruma Goswami ("You") and Elsevier ("Elsevier"). The license consists of your order details, the terms and conditions provided by Elsevier, and the payment terms and conditions.

| | |
|---|---|
| License Number | 2703080429077 |
| License date | Jul 06, 2011 |
| Licensed content publisher | Elsevier |
| Licensed content publication | NeuroImage |
| Licensed content title | Representation of somatosensory inputs within the cortical autonomic network |
| Licensed content author | Ruma Goswami, Maria Fernanda Frances, J. Kevin Shoemaker |
| Licensed content date | 15 January 2011 |
| Licensed content volume number | 54 |
| Licensed content issue number | 2 |
| Number of pages | 10 |
| Type of Use | reuse in a thesis/dissertation |
| Portion | full article |
| Format | electronic |
| Are you the author of this Elsevier article? | Yes |
| Will you be translating? | No |
| Order reference number | 3000403020 |
| Title of your thesis/dissertation | Representation of somatosensory inputs in the cortical autonomic network |
| Expected completion date | Jul 2011 |
| Estimated size (number of pages) | 200 |
| Elsevier VAT number | GB 494 6272 12 |
| Permissions price | 0.00 USD |

# Appendix D -- Permission for Copyright Figures

## Figure 1.2

---

**Ruma Goswami**                                                      **Tue, Jul 19, 2011 at 11:05 AM**

Hello,
I am writing to request permission to use your Figure 3 showing the anatomical delineations between the anterior and posterior insula on your website: http://prefrontal.org/blog/2009/07/brain-dissection-insula-anatomy/, within my PhD Dissertation.
Thank you very much,
Sincerely,
Ruma Goswami
Ph.D. Candidate
Neurovascular Research Laboratory
The University of Western Ontario
1151 Richmond Street, London, ON, N6A3K7

---

**CB**                                                                    **Tue, Jul 19, 2011 at 6:40 PM**
To: Ruma Goswami

Ruma,

Sure, you can put Figure 3 in your dissertation.

Thanks for checking.

~CB

## Figure 1.6

                                                                          **Mon, Jul 18, 2011 at 12:58 PM**
**Ruma Goswami**

Hello Dr. Vogt,
I am writing to request permission to reuse the figure of the Regional Morphology of the cingulate cortex (taken from: http://www.cingulumneurosciences.org/), in my Ph.D dissertation.
Thank you very much,
Sincerely,
Ruma Goswami
Ph.D. Candidate
Neurovascular Research Laboratory
The University of Western Ontario
1151 Richmond Street, London, ON, N6A 3K7

---

**BV**                                                                    **Mon, Jul 18, 2011 at 3:14 PM**
To: Ruma Goswami

Dear Ruma,
Use it as you please!
Best wishes for your research,

BV
[Quoted text hidden]

## Figure 1.7

This is a License Agreement between Ruma Goswami ("You") and John Wiley and Sons ("John Wiley and Sons") provided by Copyright Clearance Center ("CCC"). The license consists of your order details, the terms and conditions provided by John Wiley and Sons, and the payment terms and conditions.

**All payments must be made in full to CCC. For payment instructions, please see information listed at the bottom of this form.**

| | |
|---|---|
| License Number | 2713120219774 |
| License date | Jul 20, 2011 |
| Licensed content publisher | John Wiley and Sons |
| Licensed content publication | Journal of Magnetic Resonance Imaging |
| Licensed content title | Principles of magnetic resonance assessment of brain function |
| Licensed content author | David G. Norris |
| Licensed content date | Jun 1, 2006 |
| Start page | 794 |
| End page | 807 |
| Type of use | Dissertation/Thesis |
| Requestor type | University/Academic |
| Format | Electronic |
| Portion | Figure/table |
| Number of figures/tables | 1 |
| Number of extracts | |
| Original Wiley figure/table number(s) | Figure 1 |
| Will you be translating? | No |
| Total | 0.00 USD |

**Figure 1.8**

---

**Ruma Goswami**                                                    **Tue, Jul 19, 2011 at 11:19 AM**
To: CV

Dear Dr. van Ravenswaaij-Arts,
I am writing to request permission to use Figure 3 of the heart rate trace and power spectrum in your
paper entitled 'Heart rate variability' in *Annals of Internal Medicine* 118: 436-447 1993, for use in my
Ph.D Dissertation.
Thank you very much,

Sincerely,
Ruma Goswami
Ph.D. Candidate
Neurovascular Research Laboratory
The University of Western Ontario
1151 Richmond Street, London, ON, N6A3K7

---

                                                                   **Tue, Jul 19, 2011 at 11:23 AM**
To: Ruma Goswami


Dear Ruma,
I have no objections as long as you mention the source.

kind regards and success
CV

# CURRICULUM VITAE

## Ruma Goswami
Neurovascular Research Laboratory, School of Kinesiology
The University of Western Ontario, Thames Hall Room 3110, London, ON, N6A 3K7


## EDUCATION:

**September 2006-Present**
**Ph. D. Candidate, School of Kinesiology: Neurovascular Physiology**
The University of Western Ontario
　　Dissertation:  Representation of somatosensory afferents in the cortical autonomic network
　　Advisor: J. Kevin Shoemaker, Ph.D.


**September 2004-August 2006**
**M.Sc., Department of Community Health Sciences: Cardiovascular Physiology**
Brock University
　　Thesis:  Does altering brachial artery tone during lower-body negative pressure and flow-mediated dilation affect arterial stiffness?
　　Advisor: Deborah O'Leary, Ph.D.


**September 1999 – April 2003**
**B.A. (Hons), Community Health Sciences**
Brock University


## AWARDS & EDUCATIONAL ACCOMPLISHMENTS:

| | |
|---|---|
| 2009 - 2010 | Ontario Graduate Scholarships in Science and Technology (Doctoral – $15,000) The University of Western Ontario |
| 2007, 2008, 2010, 2011 | Graduate Thesis Research Award |
| 2004 - 2006 | Heart and Stroke Foundation of Ontario Master's Studentship Award ($18,000/year for 2 years) Brock University |
| 2004 | President's Surgite Award, Brock University |

**PUBLICATIONS:**

Salmanpour A, Brown L, Steinback CD, Usselman CW, **Goswami R**, Shoemaker JK. (In Press). Relationship between size and latency of action potentials in human muscle sympathetic nerve activity. *Journal of Neurophysiology*.

Davenport MH, **Goswami R**, Shoemaker JK, Mottola MF. (In Submission). The influence of hyperglycemia on postpartum arterial stiffness during and after pregnancy. *American Journal of Physiology*.

**Goswami R**, Frances MF, Shoemaker JK. (2011). Representation of somatosensory inputs within the cortical autonomic network. *NeuroImage*, 54(2): 1211-1220.

Zamir M, **Goswami R**, Liu L, Salmanpour A, Shoemaker JK. (2011). Myogenic activity in autoregulation during low frequency oscillations. *Autonomic Neuroscience: Basic and Clinical*, 159(1-2): 104-110.

Zamir M, Norton K, Fleischhauer A, Frances MF, **Goswami R**, Usselman C, Nolan RP, Shoemaker JK. (2009). Dynamic responsiveness of the vascular bed as a regulatory mechanism in vasomotor control. *The Journal of General Physiology*, 134(1): 69-75.

Zamir M, **Goswami R**, Salzer D, Shoemaker JK. (2007). Role of vascular bed compliance in vasomotor control in skeletal muscle. *Experimental Physiology*, 92(5): 841-848.

Sanchez A, Simone B, Yarascavitch ME, **Goswami R**. (2004). Low frequency of neurocysticercosis in patients with epilepsy and seizure disorders in the Niagara Region, Canada: a retrospective study. *Canadian Journal of Infectious Diseases*, 15(3): 179-180.

**PEER REVIEWED CONFERENCE PRESENTATIONS:**

**Goswami R**, Frances MF, Sharma HA, Shoemaker JK. Anatomical connections between brain regions of the autonomic network. Organization of Human Brain Mapping, June 2011, Quebec City, Quebec.

Nielson, CA, Frances, MF, **Goswami, R**, Gimon, TI, Prapavessis, H, Zamir, M, Shoemaker, JK. Impact of smoking, and smoking cessation, on peripheral vascular mechanics on young women. *The FASEB Journal*, 25: 818.1, 2011. Experimental Biology, Washington, DC.

**Goswami R**, Frances MF, Shoemaker JK. Somatosensory inputs inhibit insular activation during baroreceptor unloading. *Clinical Autonomic Research*, 20(5): 314, 2010. American Autonomic Society, Marco Island, Florida.

Norton KN, **Goswami R**, Nolan RP, Shoemaker JK.  Cortical autonomic alterations with hypertension.  *Clinical Autonomic Research*, 20(5): 314, 2010.  American Autonomic Society, Marco Island, Florida.

Nielson CA, Frances MF, **Goswami R**, Gimon TI, Prapavessis H, Shoemaker JK.  Smoking behaviour differentially affects central versus peripheral vascular mechanics in young women.  *Applied Physiology Nutrition and Metabolism*, S78, 2010.  Canadian Society for Exercise Science, Toronto, Ontario.

Shoemaker JK, **Goswami R**, Liu L, Zamir M.  Evidence challenging a sympathetic mechanism for the 0.1 Hz rhythms in blood pressure (Mayer waves).  *Applied Physiology Nutrition and Metabolism,* S94, 2010.  Canadian Society for Exercise Science, Toronto, Ontario.

**Goswami R**, Frances MF, Shoemaker JK.  Cortical activation patterns associated with skeletal muscle afferent stimulation. *Autonomic Neuroscience: Basic and Clinical*, 149(1): 74, 2009.  International Society for Autonomic Neuroscience, Sydney, Australia.

**Goswami R,** Jackson P, Frances MF, Fleischhauer A, Shoemaker JK.  Skeletal muscle sensory afferents affect cardiac regulation in humans. *The FASEB Journal*, 23: 786.1, 2009.  Experimental Biology, New Orleans, Louisiana.

Frances MF, Zamir M, Usselman CW, **Goswami R**, Masse N, Fleischhauer A, Nolan R, Shoemaker JK.  Vasomotor changes in controlled and uncontrolled hypertension. *Applied Physiology Nutrition and Metabolism*, 22: 737.18, 2008.  Canadian Society for Exercise Science, Banff, Alberta.

**Goswami R**, Masse N, Jackson P, Shoemaker JK.  Effect of arm position on reflex-induced changes in the compliance of skeletal muscle vasculature. *Applied Physiology Nutrition and Metabolism*, 32(1): S35, 2007.  Canadian Society for Exercise Science, London, Ontario.

**Goswami R**, Salzer D, Zamir M, Shoemaker JK.  Modeling reflex changes in pulsatile mechanics emphasizes a role for vascular capacitance in forearm vasomotor control. *The FASEB Journal*, 21(5): 612.1, 2007.  Experimental Biology, Washington, DC.

**Goswami R**, Shoemaker JK, Bakker J, O'Leary DD.  Effect of LBNP on peripheral vascular stiffness. *The FASEB Journal*, 20:A1403, 2006.  Experimental Biology, San Diego, California.

**Non-Peer Reviewed Conference Presentations:**

- Ontario Exercise Physiology (OEP) Conference, "*Cortical activation patterns associated with somatosensory input*", Barrie, ON, January 2010.

- Ontario Exercise Physiology (OEP) Conference, "*Assessing conduit vessel tone*", Barrie, ON, January 2005.


## RELEVANT ACTIVITIES:

*Research:*

- **Research Assistant**: September 2004-June 2005, *Developmental Coordination Disorder and Physical Fitness Activity and Movement Research.*
  Supervisor: John Hay, Ph.D., Brock University
- **Researcher ("Identifier")**: April 2004-September 2004, *West Nile Virus Investigative Unit, Mosquito Division*, Department of Biological Sciences, Brock University.
- **Research Assistant**: September 2002-April 2004, *Neurocysticercosis in Epilepsy and Seizure Disorder Patients.*
  Supervisor: Supervisor: Ana Sanchez, Ph.D., Brock University.
- **Research Assistant**: September 2002-July 2003, Dept. of Cardiology, St. Catharines General Hospital.
- **Research Assistant**: September 2001-June 2002, *Youth Gambling Research Initiative*, Supervisor: Kelli-an Lawrance, Ph.D., Brock University.


*Teaching:*

2009        **Guest Lecture**: Graduate course in Regulation of Fuel Metabolism
            Instructor: Sandra Peters, Ph.D., Brock University.

2008        **Teaching Assistant** (Fall), 3rd year Laboratory in Exercise Physiology
            Instructor: John Kowalchuk, Ph.D., The University of Western Ontario.

2007        **Teaching Assistant** (Fall-Winter), 3rd year Ergonomics
            Instructor: Kent Gillin, Ph.D., The University of Western Ontario.

2007        **Teaching Assistant** (Winter), 4th year Training of Exercise Physiology
            Instructor: Don Paterson, Ph.D., The University of Western Ontario.

2006        **Teaching Assistant** (Fall), 4th year Advanced Exercise Physiology
            Instructors: J. Kevin Shoemaker, Ph.D., John Kowalchuk, Ph.D., The
            University of Western Ontario

2007        **Guest Lecture**: Graduate course in Regulation of Fuel Metabolism
            Instructor: Sandra Peters, Ph.D., Brock University.

2005        **Teaching Assistant/Seminar Leader** (Fall): 4th year Pathology
            Instructor: Brian Jeynes, Ph.D., Brock University.

2004  **Teaching Assistant/Seminar Leader** (Fall): 4th year Pathology
    Instructor: Brian Jeynes, Ph.D., Brock University.

2003  **Teaching Assistant** (Fall-Winter): 3rd year Fundamentals of Infectious
    Diseases
    Instructor: Ana Sanchez, Ph.D., Brock University

*Mentoring:*
- Oversee honours project of undergraduate thesis student: January-April 2008. The University of Western Ontario
- High school Mentorship Program Research Mentor: September 2005-March 2006. Brock University
- Scientifically Yours Science and Math Camp Workshop Leader: July 2003, 2005, 2006. Brock University

## PROFESSIONAL SERVICE:

*Committee Involvement:*
- School of Kinesiology Councillor, UWO Society of Graduate Students, July 2008 – July 2009
- Society of Graduate Students Committee Member: Profile Author for The Western Graduate Review, May 2008-present

*Conference Organization:*
- Organizing Committee: Canadian Society for Exercise Physiology 2007 (The University of Western Ontario)
- Organizing Committee: Ontario Exercise Physiology 2006 (The University of Western Ontario)
- Organizing Committee: Ontario Exercise Physiology 2005 (Brock University)

## RELEVANT SKILLS:
- Neuroimaging: Functional MRI experimental set-up and analysis (Matlab, SPM); Diffusion tensor imaging (BrainVoyager)
    - SPM8 Course for Basic and Clinical Investigators – Houston, USA, Dec. 2010
- Cardiovascular: Doppler ultrasound (arterial, stroke volume), Applanation tonometry (Millar).

## PROFESSIONAL MEMBERSHIPS:
- Student member of The Organization of Human Brain Mapping (OHBM)
- Student member of International Society of Autonomic Neuroscience (ISAN)